K^+ CHANNEL'S EQUILIBRIUM PREFERENCE REVEALS THE ORIGIN OF ITS CONDUCTION SELECTIVITY AND THE INACTIVATED STATE OF THE SELECTIVITY FILTER

A Dissertation

by

SHIAN LIU

Submitted to the Office of Graduate and Professional Studies of
Texas A&M University
in partial fulfillment of the requirements for the degree of

DOCTOR OF PHILOSOPHY

Chair of Committee,	Steve W. Lockless
Committee Members,	L. Rene Garcia
	Paul E. Hardin
	Frank M. Raushel
	Hays S. Rye
Head of Department,	Thomas D. McKnight

May 2016

Major Subject: Biology

ABSTRACT

K^+ channels are a class of membrane proteins that rapidly and selectively transport K^+ ions across lipid membranes. K^+ ions are concentrated inside the cell, and its efflux is responsible for the rapid repolarization during action potential. Given that K^+ channels play important roles in cell physiology, their activities are tightly controlled through a variety of features, of which high ion selectivity and gating are the two most common. The work presented in this dissertation will address two fundamental questions about them. First, what is the origin of the ion selectivity during conduction? Second, C-type inactivation is gating mechanism that takes place in the selectivity filter, and how is the C-type inactivated state of the filter differ from other functional states?

Ion selectivity is achieved through a highly conserved region in the channel named the selectivity filter, which is a queue of four binding sites observed in crystal structures of all K^+ channels. These sites are selective for K^+ over another abundant Na^+ ion at equilibrium, so a model based on the equilibrium selectivity was proposed to explain the conduction selectivity in K^+ channels. A recent study showed that eliminating sites from the filter of K^+-selective channels abolished their conduction selectivity, suggesting that these channels may have lost their equilibrium selectivity. To test the hypothesis, we measured the ion binding preference of K^+ channels and non-selective mutant channels. Unexpectedly, my results demonstrated that these channels have strong K^+ selectivity at equilibrium, suggesting that the conduction selectivity is likely derived from a blocking mechanism created by interacting ions inside the filter.

C-type inactivation reduces ion flow through the selectivity filter of K^+ channels following channel opening. Crystal structures of the open KcsA K^+ channel shows a constricted selectivity filter that does not permit ion conduction, which was proposed by others to be the inactivated conformation. However, recent work using a semi-synthetic channel that is unable to adopt the constricted conformation but inactivates like wild-type channels challenges this idea. I measured the equilibrium ion-binding properties of channels in three different conformations to differentiate their apparent binding affinities. My results revealed that the inactivated filter is more similar to the conductive conformation than the constricted conformation from an energetic point of view.

In this dissertation, I primarily applied isothermal titration calorimetry to measure the ion equilibrium preference to the selectivity filter, because it is a mechanism-free approach to detect the states of the channel in an aqueous solution. These data provide further constraints on mechanistic models of ion selectivity and inactivation in K^+ channels, which allowed to propose that the conduction selectivity of K^+ channels derives from ion interaction in the filter and that the inactivated filter resembles the conductive filter of the KcsA K^+ channel.

DEDICATION

The dissertation is dedicated to my parents for their unconditional support. I will be forever grateful for their encouragement and love, which has given me the strength to pursue my dreams.

I would also like to thank all my friends, especially Sarah W. Beagle, for giving me encouragement throughout graduate school.

ACKNOWLEDGEMENTS

I would like to express my great appreciation to my advisor Dr. Steve Lockless for his guidance and support. His patience and humor also made this journey enjoyable for me.

I would like to thank all the committee members, Dr. Rye, Dr. Garcia, Dr. Hardin and Dr. Raushel for their constructive criticisms. Thanks also go to all the lab members for their help, to the Department of Biochemistry and Biophysics and Begley's lab for sharing ITC machines, and to all the collaborators for their support. I also want to extend my gratitude to the Welch Foundation and for TAMU start-up funds for financial support of this work.

NOMENCLATURE

ITC	Isothermal titration calorimetry
Kv channel	Voltage-gated K^+ channel
K2P channel	Two-pore-domain K^+ channel
IRK channel	Inwardly-rectifying K^+ channel
BK channel	Big K^+ channel
CNG channel	Cyclic-nucleotide gated channel
DM	*n*-decyl-β-D-maltopyranoside
NMG	*n*-methyl-D-glucamine
NMR	Nuclear magnetic resonance
EPR	Electron paramagnetic resonance

TABLE OF CONTENTS

Page

LIST OF FIGURES

Page

LIST OF TABLES

Page

CHAPTER I

INTRODUCTION

The smallest living unit of all organisms is the cell, where a lipid membrane creates a boundary to shield cellular components against the outside environment. However, a cell must exchange nutrients, waste and store energy across its membrane to survive and divide that attributes to the cellular signaling. Electrochemical gradient is a form of energy stored across the membrane, which is based on the asymmetric distributions of ions. For instance, the extracellular Na^+ ion concentration is higher than the intracellular side (**Figure 1A**), creating a driving force to facilitate the transport of molecules through many transporter proteins. Conventionally, the membrane potential is defined as the difference in charge on the intracellular side of the membrane compared to the extracellular side, and it stays negative at the resting state of the cell. The negative resting potential plays essential roles in maintaining osmotic homeostasis by keeping a high concentration of K^+ inside the cell.

The electrochemical gradient is utilized in many signaling processes. For example, higher organisms such as vertebrates rely on the transient Na^+-selective influx and K^+-selective efflux across the membrane, termed an action potential (**Figure 1B**), to rapidly propagate electrical signals along axons. Since the lipid membrane contains a hydrophobic layer with a thickness of ~30 Å, the movement of charged ions has to be facilitated by a series of membrane proteins called ion channels, which physically open selective pores on the membrane when activated. K^+ channels are members of a class of

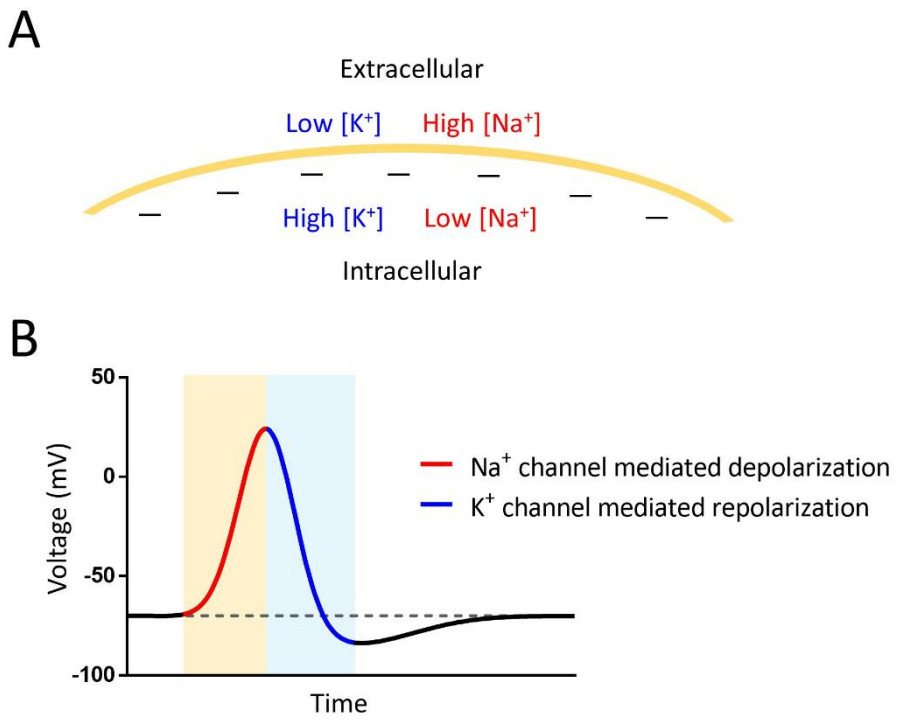

Figure 1. K^+ and Na^+ ions distribution across the cell membrane and action potential. (A) A representation of Na^+ and K^+ distribution across the cell membrane. The membrane potential of cell membrane at resting state is negative, shown as the negative signs on the intracellular side. (B) Illustration of action potential. After activated, Na^+ channels allow a Na^+-selective influx that depolarizes the cell membrane until they are inactivated. The subsequent opening of K^+ channels allow the efflux of K^+ ions to bring the membrane potential down to the negative voltage. The depolarization and repolarization processes are colored in red and blue, respectively.

highly conserved tetrameric ion channels whose activities are determined by several important properties, such as their high selectivity and the C-type inactivation. Despite the importance of K^+-selective conduction to cellular physiology, there is still much unknown about K^+ channels. I will briefly describe the history of K^+ channel research and introduce some of their essential properties, which will assist in understanding the subsequent chapters of my dissertation.

A brief history of K^+ channel research

The requirement for potassium ions in excitable tissues, such as nerves and muscles, has been known for longer than a century. In the late 1800s, Sidney Ringer showed that the ratio of potassium, sodium and calcium ions is essential in the solution used to keep a frog heart beating continuously [1-3]. It had been known that the K^+ ions were enriched inside the cell, while Na^+ ions were mostly found on the extracellular side. Walther Nernst used this observation to develop an electrolyte diffusion theory based on the thermodynamics of ions separated by a membrane [4]. The Nernst equations demonstrated that the chemical potential from an ion gradient across a membrane is equivalent to another form of energy, the electrical potential or the voltage across the same membrane. On this basis, Julius Bernstein proposed a model that, if excited membranes are more permeable for K^+ ions, the membrane potential could become negative [5, 6]. Due to experimental limitations, his model was not tested until Cole & Curtis measured the membrane resistance of a squid's giant axon and detected a decrease of membrane conductance [7]. Bernstein's other prediction was that there must be a small current circuit occurring locally within the axon and that it self-propagates to travel a long distance, which was experimentally validated by Hodgkin [8, 9].

However, Hodgkin noticed that the interior of axons was able to reach a positive potential rather than a negative potential during conduction, which did not fit into Bernstein's model. Driven by this unexpected result, Hodgkin and Huxley started a collaboration and captured the first evidence of the action potential [10]. After a halt of research during World War II, the underlying cause of the positive membrane potential

was finally unveiled to be the influx of sodium ions [11]. They found that a brief Na^+-selective influx though voltage-gated Na^+ channels leads to the positive membrane potential. The subsequent opening of voltage-gated K^+ channels allows K^+ ions to efflux, which repolarizes the membrane potential back to the negative value (**Figure 1**). Thereafter, the principle of action potential was widely accepted.

With the growing interest in ion channels, there was a high demand to understand the biophysical properties of single ion channels. In 1976, Erwin Neher and Bert Sakmann invented the patch clamp technique that enhanced the signal-to-noise of electrophysiology recordings, and thereby enabled researchers to observe single channel current with a glass tip of 1-3 microns [12-17]. The ion conduction through single channel typically dwells at two different current levels, one representing the open and the other closed state. This behavior allows researchers to calculate the conductance, or the conducting capability, of any single channel simply using the applied voltage and the current. (See next section 'The fundamental properties of K^+ channels' for more details)

However, biochemical characterizations on K^+ channels had been impeded, because these proteins are not abundant in any types of cells or tissues, meaning extracting and purifying them from natural sources was impractical. In the 1980s, a mutation in Drosophila's genome was found to cause the fly to shake its legs when anesthetized with ether [18]. Analyzing the excitability of the fly's tissues revealed that a K^+ selective current was affected [19-21]. The putative gene encoding a voltage-dependent K^+ channel, named the *shaker* channel, was cloned soon after a Drosophila cDNA library was available [22, 23]. Combined with a technique to express functional

ion channels in *Xenopus* oocytes by injecting exogenous mRNA [24, 25], the cloning of *shaker* allowed researchers to characterize the activity of wild-type and mutant K^+ channels more easily through patch clamping techniques [26, 27]. This paved the way to discover and characterize a large number of ion channels over the past three decades.

The explosion of sequencing technology in the 1990s led to an era of many genome projects. This included the completion of sequencing the *C.elegans* genome and the Drosophila genome, in which 76 and 27 K^+ channel genes were found, respectively [28, 29]. Based on their functional properties and secondary structures, K^+ channels from higher organisms are generally divided into four classes [30] (**Figure 2**). The first class is the voltage-gated K^+ channel (Kv channel) with six transmembrane helices (TM), including a 4 TM voltage sensing domain. The second class is the inwardly rectifying K^+ channel (IRK channel) with only 2 TM. The third class, the Ca^{2+}-activated K^+ channel, such as BK channels, has 6 or 7 TM including a 4 or 5 TM voltage sensing domain. These three classes of K^+ channels all form tetrameric complexes [31]. A common feature of all three classes of K^+ channels is the pore domain is composed of 2 TMs from each subunit that is able to create an ion permeating pathway [32-34]. The fourth class is unique since it encodes two tandem pore domains which come together as a dimer to form a functional channel; this class was, therefore, named the 2-P-domain K^+ channel or K2P channel [35]. Among all the K^+ channels, the P-loop connecting two pore TMs is conserved, which builds the selectivity filter with a highly conserved amino acid sequence, TVGYG [36, 37].

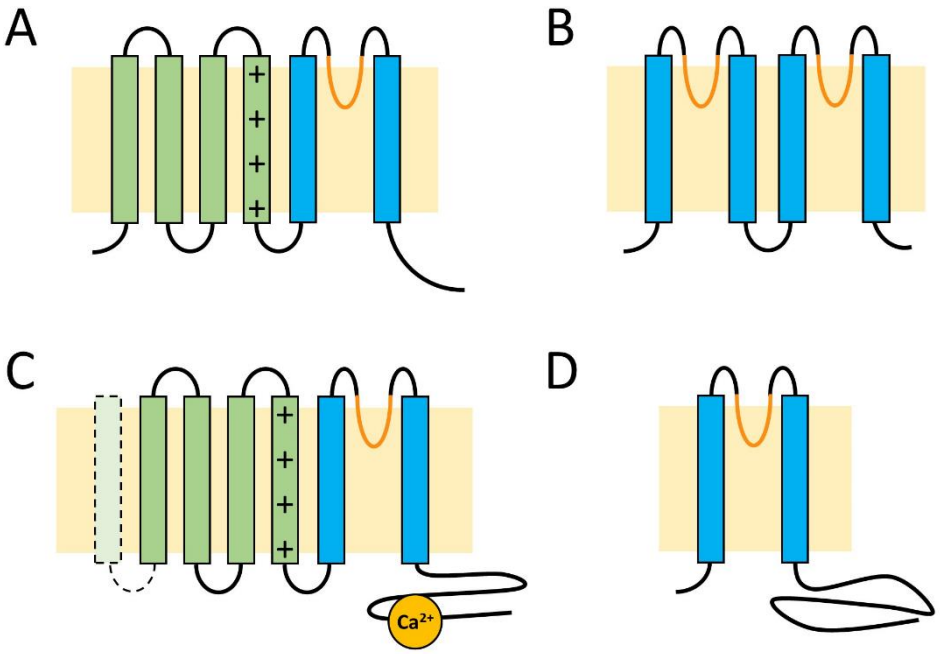

Figure 2. K^+ channels are classified and compared according to the architecture of the transmembrane helices and their function. (A) Kv channel, (B) K2P channel, (C) BK channel, and (D) IRK channel are modeled in the same orientation in the membrane. The voltage sensing domains and pore domains are in green and blue, respectively. The calcium binding site of BK channel is displayed in a yellow sphere. The conserved P-loop region is colored in orange.

Due to the high conservation of the signature sequence in all classes of K^+ channels, understanding its role was a main research focus in the 1990s. Initially, it was found that P-loop carries the permeation properties in experiments using chimeric channels with swapped P-loops [33, 38]. Mutagenesis studies not only confirmed the importance of the P-loop to ion conduction, but also showed that the signature sequence (TVGYG) determines the ion selectivity [37, 39]. Toxins extracted from venoms could target specific K^+ channels and, therefore, were used to map the spatial architecture of the P-loop from the protein surface [40-42]. All of these findings led to one conclusion:

the signature sequence is K^+ channel's selectivity filter [42, 43]. However, the research on the selectivity filter was largely constrained to measuring the ion current due to the difficulties of isolating enough protein for biochemical studies. The situation was improved in 1995 with the discovery of a K^+ channel gene in a Gram-positive bacterium, *Streptomyces lividans* [44]. This channel, later named KcsA, can be highly expressed in *E.coli*, and functions as a canonical tetrameric K^+ channel in lipid bilayers [44-50].

Given the ease of expressing and purifying the KcsA K^+ channel, the crystal structure of its pore domain was solved by MacKinnon and colleagues in 1998 [51]. Although the resolution was only 3.2 Å, it was the first snapshot of how ions pass

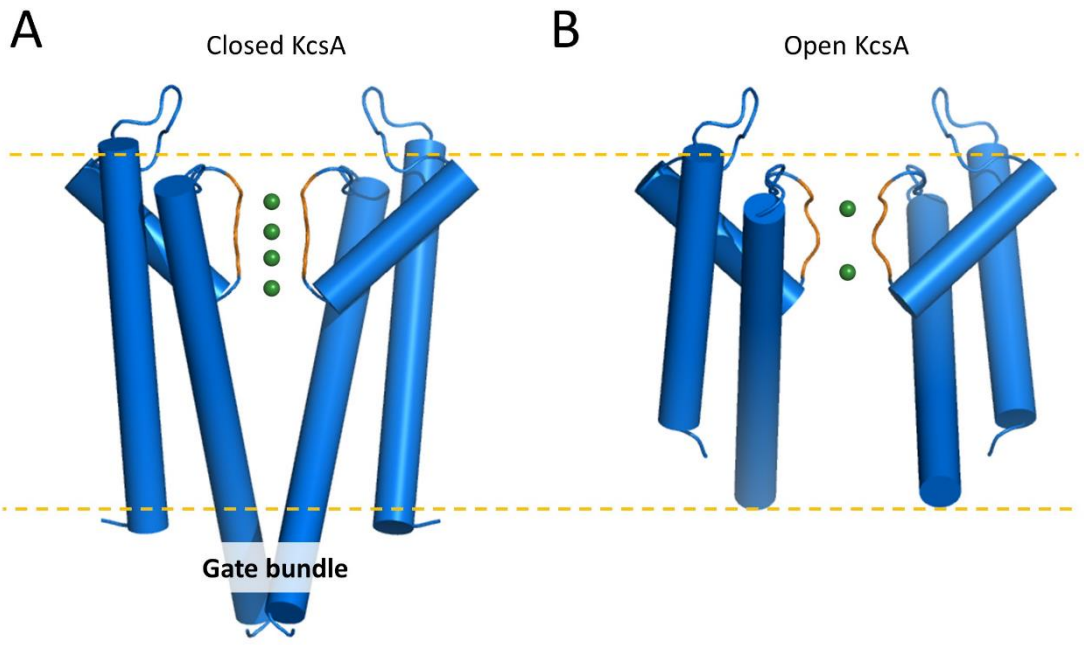

Figure 3. Gating of the KcsA K^+ channel. Cartoon representations of the closed (A, PDB: 1K4C) and the open (B, PDB: 3F7V) KcsA structures are shown. The front and back subunits are excluded for clarity. The selectivity filter regions are in orange, and the potassium binding sites are in green spheres.

through a K^+ channel (**Figure 3**). As predicted by functional studies, the pore domain of KcsA is formed by four identical subunits, each of which contains two hydrophobic helices spanning the membrane. The center of the tetramer is an ion permeation pathway. The selectivity filter containing the signature sequence is located near the extracellular side, whereas a helix bundle on the intracellular side controls the opening and closing of the gate. Initially, due to the structure's resolution, substitute ions with higher electron density such as Rb^+, Cs^+ or Ba^{2+} were used to verify ion binding sites in the selectivity filter based on their anomalous difference maps [51, 52].

In 2001, two additional KcsA structures bound with a specific monoclonal antibody were solved at 2.0 Å [53]. These two structures with high or low potassium concentration showed two distinct conformations in the selectivity filter (**Figure 4**). In high K^+ concentration, a queue of four K^+ binding sites is formed by the carbonyl groups from the protein backbone and hydroxyl groups from the threonine side chains. However, in a low K^+ solution, the filter adopts a different conformation where the middle sites are destroyed leaving only the outer sites (**Figure 4**). This conformational change may underlie how the selectivity filter responses to different physiological K^+ concentrations [49]. The structural information guided the studies on ion conductance and ion selectivity with more advanced mathematical models [54-56]. Crystal structures from all classes of K^+ channels including Kv channels [57-59], BK channels [60, 61], IRK channels [62-66] and K2P channels [67-69] have now been solved, yet how they select ions remains to be determined.

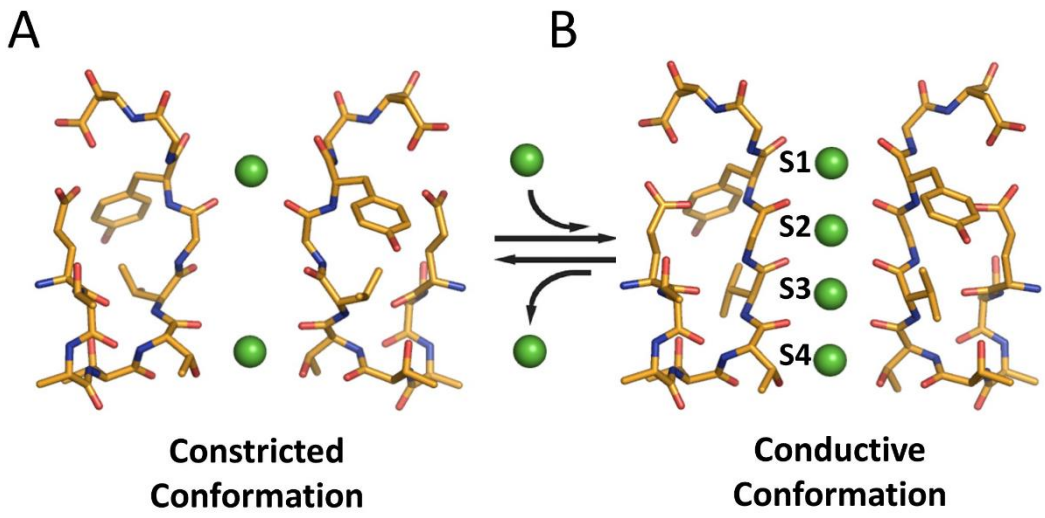

Figure 4. Two states of the selectivity filter of the KcsA channel. The stick models of the constricted conformation in the low K^+ concentration or Na-only solution (A) and the conductive conformation in the high K^+ concentration (B) are shown. The K^+ ions are modeled as green spheres with four binding sites in a queue in the conductive conformation. The arrows indicate that two states of the filter are interchangeable.

The fundamental properties of K^+ channels

The goal of the work presented in this dissertation is to study two fundamental properties of K^+ channels, the ion selectivity and C-type inactivation. Since K^+ channel's activity is mainly manifested in the ion current, understanding these two properties requires dissecting how ions travel through K^+ channels. In this section, I will introduce some physical properties of ion current and how to interpret them in order to assist the understanding of subsequent chapters.

To begin, considering an ion channel as a conductor such that the movement of positively charged ions is simply driven by the voltage applied to the membrane. Therefore, the conduction follows Ohm's law:

$$I = \gamma \cdot V$$

where I is the current, V is the applied voltage, and γ is the conductance that shows the conducting capability of the channel in units of Siemens (1 S = 1A/V). Conduction can be also observed by creating an ion gradient across the membrane in the absence of the applied voltage. For example, ions move from the high concentration to the low concentration side of the membrane, where the movement tendency is described as the equilibrium potential. Based on the Boltzmann equation of statistical mechanics, Walther Nernst derived the relationship between equilibrium potential and ion concentrations. For instance, in the case of an open K^+ channel in a lipid membrane with symmetric K^+ solutions on both sides of the membrane, this relation is given as:

$$E_S = \frac{RT}{zF} ln \frac{[S]_o}{[S]_i}$$

where R is the ideal gas constant, T is the temperature in Kelvin, z is the charge of ion species, F is the Faraday's constant, $[S]$ is the ion activity from the outside and the inside of the membrane, and E_S is the Nernst potential of the ion species in units of volts [4]. For simplicity, $[S]$ is treated as the ion concentration, so it yields:

$$E_K = \frac{RT}{F} ln \frac{[K^+]_o}{[K^+]_i}$$

where E_K is the Nernst potential of K^+ ions. As shown in the Nernst equation, chemical potential and electrical potential are both able to drive ion conduction.

In studying K^+ channel's properties, three important aspects of conduction need to be under scrutiny, conductance, ion selectivity and gating. The conductance (γ) shows ion's conducting rate. The ion selectivity captures how preferably an ion goes through a

K^+ channel. The gating process controls how often ions are able to enter the channel. All three aspects together shape the number of ions that cross a lipid membrane within a given time course. These three aspects are discussed individually below.

Conductance

The rate at which some K^+ channels can conduct ions is remarkably fast, and approaches the theoretical limitation of ion conduction. If a K^+ channel is modeled as a cylindrical tunnel that has a diameter to allow only one ion to pass through, once an ion hits the channel, it is able to move through the tunnel as if there is no barrier inside. Hille performed a series of calculations with several simple assumptions, and predicted that a maximum conductance of ~500 pS can be reached according to either Ohm's law based on conduction or Fick's law based on diffusion [70, 71]. For all the K^+ channels that have been characterized thus far, their conductance falls within two orders of magnitude below this theoretical ceiling. The fastest channels are BK channels, or Big K^+ channels, which can reach 400 pS under certain conditions. The high conductance nature of some K^+ channels makes their signals detectable at the single molecule level relatively compared to the thermal noise of lipid bilayers, whereas ion transporters and carriers are too slow for such measurements.

One potential barrier to rapid ion flux is the dehydration rate of the ion. Since ions get dehydrated before entering the selectivity filter, the high conductance of K^+ channels implies that the ion dehydration rate is not rate-limiting in this process. Indeed,

most permeant ions to K^+ channels are found in the first group of metal elements in the periodic table, whose water substitution rates are as fast as the rate of diffusion [72].

The high conductance also implies that the electrostatic barrier must not be high inside the pore. According to the Born equation, there is a huge energy barrier to transfer charged ions from bulk water ($\varepsilon = 80$) into lipid membrane ($\varepsilon = 2$). Atomic resolution structures of KcsA give some hints of how this energy barrier is overcome in K^+ channels. First of all, the length of the selectivity filter is much shorter than the membrane allowing an ion to reach the hydrophobic interior of a lipid membrane by minimizing negative electrostatic interactions [51]. Additionally, the ion binding sites are coordinated by the oxygen atoms from the carbonyl groups of the backbone and hydroxyl groups from the threonine residues that mimic a water-like environment [53].

Interestingly, K^+ conductance does not always saturate over the measured range for a given channels (**Figure 5**). For example, in a condition with same K^+ concentration on both sides of the membrane, the conductance of the barrier-less BK channels increases hyperbolically as a function of K^+ concentration [73]. Without invoking more complicated models, the saturation behavior can be explained by Hodgkin and Huxley's independence principle that claims ions travel through the pore individually [74]. In this case, ion conduction is a two-step flux reaction, meaning the overall flux rate must reach a plateau with respect to K^+ concentration. In other cases, conductance does not saturate even at high K^+ concentrations [54]. It was after a careful examination of the influx/efflux ratio from a delayed rectifying K^+ channel that Hodgkin and Keynes found their results did not obey the one-ion flux model [75, 76]. They thereafter proposed a

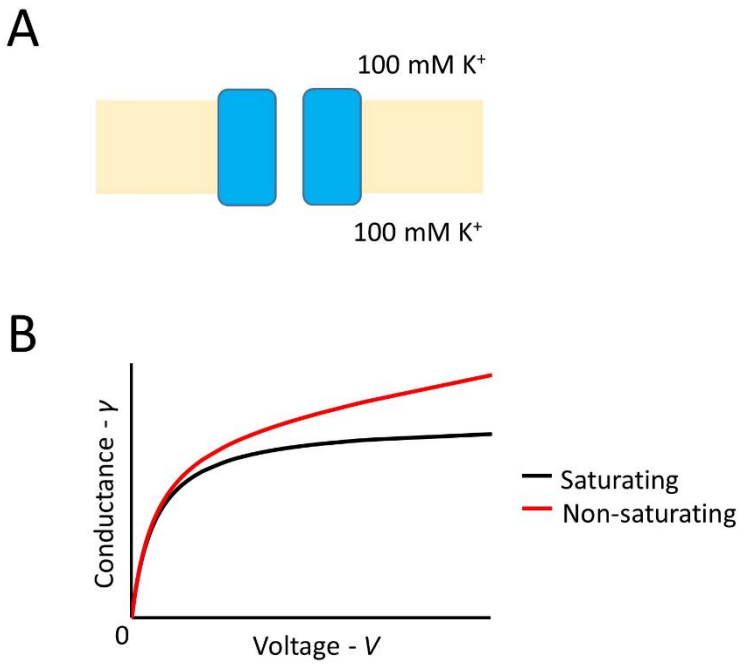

Figure 5. Illustration of the conductance – voltage relation. (A) The measurement of K^+ conductance is usually carried out with a single channel (Blue) in a K-only solution, such as 100 mM K^+ on both sides of the membrane. (B) The conductance value is plotted as a function of the voltage. At high voltage, the conductance of K^+ channels may (black) or may not (red) reach plateau over measured range.

flux-coupling mechanism, suggesting that some K^+ channels must have a queue of multi-ion binding sites in their pores [75], which was proven by several mathematical [77-81] and experimental studies [82-84].

In another test to multiple ions interact inside the channel, with a mixture of two permeant ions in the solution, the ion conductance of K^+ channels was found to vary non-monotonically as a function of the mole fraction of the ion concentrations [85-91] (**Figure 6**). This so-called anomalous mole-fraction effect (or dependence) suggests that there are at least two competing ions moving in a single-file pore, which results in an

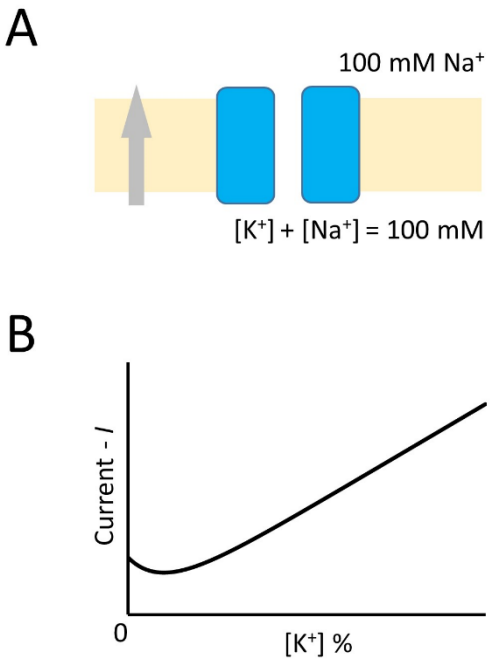

Figure 6. Illustration of the anomalous mole fraction effect. (A) The measurement of the anomalous mole fraction is usually carried out in a lipid membrane with a constant voltage across the membrane. One side of the membrane is a Na-only solution, while the other side is a mixture of K^+ ions and Na^+ ions. (B) The current from the side of ion mixture is plotted as a mole fraction of K^+ ion concentration. The fall and rise of the trend line indicates that ions interact with one another in the pore during conduction.

impeded conduction. This effect was mathematically modeled and explained that the outer ions block the inner sites to allow selective conduction to occur based on two ions' equilibrium preference. Later, the crystal structures of KcsA K^+ channel revealed a physical picture of the K^+ binding sites that confirmed the existence of multi-ion binding sites in a queue [51, 53]. Furthermore, it was calculated that only two or three K^+ ions reside in the KcsA's filter during conduction [92], and the remaining sites are likely occupied by water molecules.

In summary, the high conductance of K^+ channels revealed that ion conduction is almost barrier-less with a queue of K^+ ions interacting inside the selectivity filter.

Selectivity

K^+ channels have a high selectivity for K^+ over Na^+ during ion conduction. In all eukaryotic cells, the selectivity of K^+ channels modulates the membrane potential, which affects insulin secretion, cell volume control, electrolyte transport and plays a critical role in the repolarization of the cell membrane during action potential [11]. Due to the essential roles of ion selectivity in cell physiology, mutations that cause the loss of selectivity are often lethal at the early stage of development or lead to disease. For example, patients who were diagnosed with long-QT syndrome have mutations in the selectivity filter of K^+ channels, which leads to a delayed repolarization in the heartbeat [93, 94]. In knock-out mice, after knocking out this gene, a severe heart development defect was observed, manifesting in a combination of symptoms such as depolarization of the resting potential and prolonged action potentiation [95]. Another example is a missense mutation in IRK3.2 that was identified from mice with a weaver gait [96-99], which alters the resting potential and the excitability of granule cells in the central nervous system. This eventually leads to a progressive neural degeneration [98-103]. Recently, it was found that mutations that cause KCHJ5 to lose K^+ ion selectivity are linked to adrenal aldosterone-producing adenomas and hereditary hypertension [104-107]. Therefore, studying how K^+ channels achieve selective conduction could help us understand many aspects of cell physiology.

A prerequisite of studying selectivity in K^+ channels is quantifying the number of ions passing through the protein, which the most common measurement is to detect the reversal potential of two competing ions. The reversal potential is how much voltage must be applied to the membrane in order to reach a zero net conduction, and is dependent of two parameters, the permeability ratio and ion concentrations. The empirical definition of selectivity dates back when Nernst mathematically derived how the equilibrium potential could result from a chemical gradient at equilibrium. The reversal potential applied to stop the current from electrolytes is the equilibrium potential [4]. However, in a biological system, cells contain and are surrounded by a mixture of cations and anions. Based on a few simple assumptions of diffusion, Goldman [108] and Hodgkin and Katz [11] extended this idea by taking all major physiologically relevant ions into consideration. Here, if we only focus on two permeant ions, K^+ and X^+, their formula can be given by:

$$E_{rev} = \frac{RT}{F} ln \frac{P_{K^+} \cdot [K^+]_o + P_{X^+} \cdot [X^+]_o}{P_{K^+} \cdot [K^+]_i + P_{X^+} \cdot [X^+]_i}$$

where E_{rev} is the reversal potential or zero-current potential (**Figure 7**), and P_{K^+} and P_{X^+} are the permeability of K^+ and X^+ ions, respectively. The ratio of the two values is therefore named the permeability ratio, indicative of the ion selectivity during conduction. As the expression shows, the Goldman-Hodgkin-Katz (GHK) voltage equation captures a steady-state diffusion process, and the permeability ratio can be easily calculated from the reversal potential at desired conditions. In a simple bi-ionic condition with the Na^+ solution on one side and the K^+ solution on the other at identical

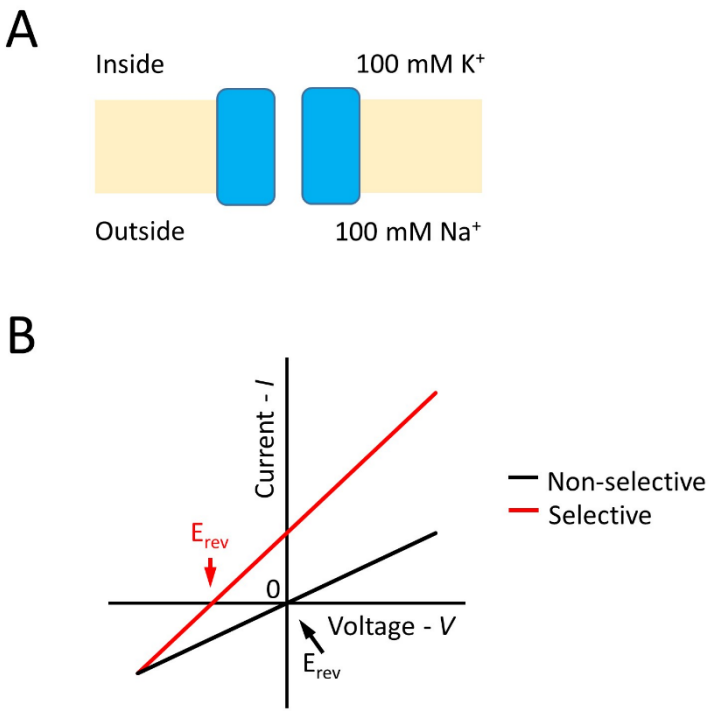

Figure 7. Illustration of the reversal potential. (A) The measurement of the reversal potential is usually carried out in a bi-ionic condition with equal Na and K^+ concentration on both sides of the membrane. (B) The current is plotted as a function of voltage, called the I-V curve. The voltage corresponding to zero current is the reversal potential of a given channel. A reversal potential of zero suggests a non-selective channel (black), while a large reversal potential indicates a high K^+/Na^+ selectivity (red).

concentration, the GHK voltage equation can be further simplified to:

$$E_{rev} = -\frac{RT}{F} ln \frac{P_{K^+}}{P_{Na^+}}$$

The bi-ionic condition is commonly employed to determine the permeability ratio of K^+ channels.

Several models have been proposed to explain the origin of the selectivity of K^+ channels. One early hypothesis focused on comparing the sizes of permeant monovalent

ions, including K^+, Rb^+, Cs^+ and NH_4^+. The selectivity filter acted as a molecular sieve that only passes dehydrated ions smaller than 3.4 Å in diameter, whereas larger ions, such as TEA^+, will be precluded [109, 110]. The crystal structures of KcsA provided a physical confirmation of such hypothesis [53, 55, 111].

Although these structural data seem quite explanatory, the molecular sieve model fails to reconcile the reason why smaller monovalent cations such as Na^+ and Li^+ are less permeant than K^+. Particularly, Na^+ ions are highly abundant cations in higher organisms that constantly compete with, as well as are similar to, K^+ ions. Therefore, one of the focuses in the past decade was to decipher the strategy of K^+/Na^+ selectivity through obtaining high resolution structures. Interestingly, these structures did not yield a unified conclusion. On one hand, Na^+ bound KcsA showed a collapsed conformation at the selectivity filter [111], which created a hydrophobic barrier to prohibit the traveling of Na^+ ions [49] (**Figure 4**). On the other hand, the collapsed filter was not adopted by the MthK K^+ channel from *M. thermoautotrophicum* even in pure Na^+ solutions [90], yet the channel selected against Na^+ ions. Since the conformational change cannot satisfactorily explain the ion selectivity in all types of K^+ channels, a more universal mechanism is in demand to answer the difference between P_{K^+} and P_{Na^+}.

A prevailing hypothesis is that the permeability preference stems from the inherent affinity difference of ions to the multi-ion pore. In other words, when ions are associated with the selectivity filter and move across the membrane, the energy landscape and ion concentrations together determine ions' equilibrium preference [81, 112-119]. Many studies have demonstrated K^+ channels are selective at equilibrium. For

example, the electron densities of K^+ ions from X-ray crystallography showed they outcompete Na^+ ions [53, 54, 90]. A similar permeant ion, Tl^+, is also able to displace Na^+ in a crystallographic titration [55]. Both solid-state and solution NMR titrations of K^+ channels displayed several chemical shifts from residues in the selectivity filter that are consistent with X-ray crystallography titrations [120-123]. The heat change from titrating K^+ ions into Na^+-bound KcsA also suggested a high equilibrium preference for K^+ ions [111]. In addition, calculations and simulations were applied to explain and show: that K^+ ions are preferred in the selectivity filter with regard to 1) their solvation energy [124-127], 2) the coordination number or topology [128-130], and 3) interactions between fluctuating ligand dipoles [127-131]. Using the less permeant Ba^{2+} or non-permeant TEA^+ ions, electrophysiology titrations were designed to determine the ion affinities under near-equilibrium conditions [132-136]. Since Ba^{2+} preferentially sits at site 4 [52, 111] and stays in the filter for longer time, the affinity of ions to other binding sites can, therefore, be calculated using these near-equilibrium titrations.

Another hypothesis emphasizes that a larger energy barrier exists for less permeant ions to enter the selectivity filter. For example, recent MD simulations invoked the significance of how fast ions enter the filter on deciding their conduction selectivity, whereas dissociation rates are not as essential [125, 137-139]. Their conclusion was based on evidence that Na^+ and Li^+ ions could preferentially reside in the oxygen plane rather than oxygen cage formed by the selectivity filter [90, 140-142]. The oxygen cage then becomes a large energy barrier to moving Na^+ ions, for instance, to overcome during conduction, and may give rise to K^+ channels' high selectivity [143]. One

prediction of their model is that the reversal potential would be different from two sides of the channel, because only one planar site has been discovered on the far end of the selectivity filter for either KcsA or MthK. However, thus far, no experimental evidence has shown channel-orientation dependent E_{rev} in the bi-ionic condition. Additionally, there has been no evidence that could show Na^+ blocks K^+ channels from the extracellular side despite an active search [109, 144-147].

Recent work on protein engineering has provided a new platform for studying the selectivity of ion channels. Cyclic nucleotide-gated (CNG) channels are tetrameric non-selective ion channels that have similar transmembrane architecture as K^+ channels, but their structural information was not available. Since a bacterial non-selective channel, NaK channel, was crystalized [148, 149], it has been used as a template to create CNG mimic channels, which showed only three K^+ binding sites in the filter. Due to several advantages of this system, NaK derivative channels with different numbers of K^+-binding sites were created [150, 151]. Interestingly, a four binding site mutant, NaK2K, preferentially conducts K^+ over Na^+ like a natural K^+ channel, whereas destroying either site 1 or site 4 renders loss of the conduction selectivity [150, 151]. Therefore, a strong correlation between the number of ion binding sites and the capability of selecting K^+ during conduction was proposed [150, 152]. Calculations determined that only two or three K^+ ions can reside in a K^+ channel's filter at any given time, so this correlation is reminiscent of the multi-ion model based on the anomalous mole fraction effect. Surprisingly, some other K^+ channels only experienced a partial loss of selectivity upon

eliminating site 1 or site 4 [37, 152], suggesting other factors could also attribute to the K^+/Na^+ selectivity of K^+ channels.

In summary, reversal potential is used to report the ion selectivity during conduction, and it is still unclear how the number of ion binding sites underlies the conduction selectivity of K^+ channels.

Inactivation

Inactivation is a process that allows K^+ channels to attenuate their activities even in the presence of external stimulus. For a single-channel recording, its signal is usually captured between two levels, designated as the open state and the closed state (**Figure 8A**), where two states typically have already reached an equilibrium during the course of recording. In other words, the open probability of a K^+ channel is always the same during a given time course. However, some K^+ channels are able to reduce their open probability immediately after activation. In an ensemble of K^+ channels, this phenomenon is manifested in a simultaneous decay of macroscopic current [153] (**Figure 8B**). Several studies have shown that the gate of activated channels twist open to allow ions to have access for conduction [57, 154-157], so inactivation has also been considered as the second "gate." The most studied forms of inactivation are N-type and C-type inactivations (**Figure 8C**). The two types of inactivation were distinguished from early studies of the *shaker* channel. After removing *shaker*'s N-terminus, a residual slow inactivation was found, and the rate of the decay depended on the C-terminal variants [158], so this residual trace was named the C-type inactivation. Neither type of

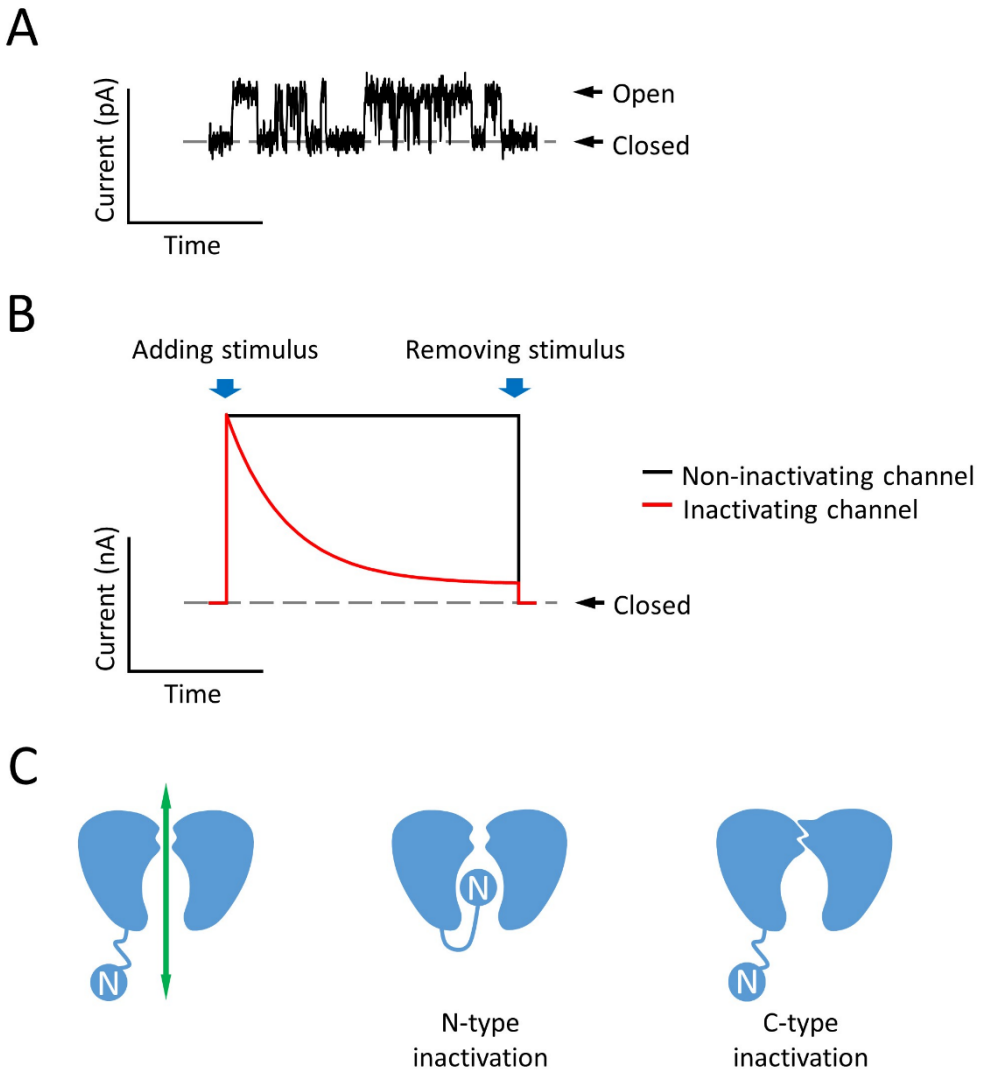

Figure 8. Illustration of electrophysiology recordings and two types of inactivation. The current from single-channel recording (A) and macroscopic recording (B) are plotted as a function of time. (A) The signal from a single channel shifts between an open state and a closed state after activation. (B) In the macroscopic recording, a burst of ion current is followed by either a constant conduction (black) or a decay of conduction (red) until the stimulus is removed. (C) A model of a conducting K^+ channel (left) allows K^+ ions to pass through, shown as a green arrow, but it can be inactivated in two ways. A N-terminal peptide plugs into the pore to block the pathway (middle) is named the N-type inactivation. A conformational change at the selectivity filter (right) that ceases ion conduction is named the C-type inactivation.

inactivations originates from the closing of the intracellular gate. The N-type inactivation has been shown as the "ball-and-chain" mechanism in which the N-terminus of the channel occupies the pore to block the intracellular entry [158-160], while the C-type inactivation involves a conformational change from the extracellular mouth of the pore [161, 162].

The origin of C-type inactivation was mapped onto the selectivity filter, since the rate of C-type inactivation can be altered by several factors, such as the extracellular K^+ concentration [158, 163-168] and mutations to the extracellular side of the pore [163-165]. A few studies showed that Kv1.4 and Kv1.5 are sensitive to the extracellular pH through a histidine residue that is located in the outer pore [169-171]. Other studies revealed that trapped ions in the cavity of the *shaker* channel modulate its C-type inactivation [172-174], which may also underlie the desensitization process of MthK in a similar manner [175, 176]. Different ions are also used to perturb C-type inactivation. For example, Na^+, as a less permeant ion, can accelerate the inactivation rate, but it is inhibited by the presence of K^+ [86, 89, 177-180]. As a similar permeant ion to K^+, Rb^+ conduction showed longer residence time and therefore reduced the inactivation rate [49, 153, 164, 181-184]. Furthermore, the K^+/Na^+ permeability ratio was altered during inactivation in several K^+ channels [177, 185]. Collectively, these findings suggest that the C-type inactivation may occur through a conformational change of the selectivity filter [186-188].

The discovery of KcsA propelled the study of inactivation at a molecular level. Before high-resolution structures were available, simulations already suggested that the

selectivity filter adopts another conformation at low K^+ concentration [189, 190]. The low K^+ concentration structure of closed KcsA clearly showed the selectivity filter collapses in the middle, where K^+ electron density was found primarily at site 1 and site 4 [53]. Since KcsA is a pH-activated K^+ channel [47-49, 155, 191, 192], its macroscopic current was found to decay like the inactivation of a voltage-gated K^+ channel when the channel was activated by a rapid decrease in intracellular pH [193].

Owing to the availability of both the structural and electrophysiological tools, several studies sought to unveil the physical mechanism underlying channel inactivation. Alanine scanning experiments revealed the E71 residue near the selectivity filter is critical in modulating KcsA's inactivation rate [194]. A subsequent examination of E71 mutations surrounding the selectivity filter suggested that a hydrogen network acts as a "spring" in control of the structural dynamics [195-197]. Importantly, the amino acids involved in the hydrogen bound network of KcsA also play essential roles in regulating the inactivation rates of voltage-gate K^+ channels [164, 198, 199], so this local interaction was inferred as a molecular "timer" mechanism [200].

Several experimental studies point to the constricted conformation being the inactivated structure. As mentioned earlier, C-type inactivation is an ion-concentration and ion-identity dependent process [201]. The closed KcsA structures showed in pure Na^+ or low K^+ solutions its selectivity filter pinches in to form a constricted conformation [53, 55, 111] (**Figure 4**). Since under the same conditions the rate of inactivation is faster than in pure K^+ solutions, the constricted conformation was proposed to be the inactivated state of KcsA [202, 203]. However, inactivation occurs

following activation, meaning the inactivated conformation must be revealed when the channel is open. In 2010, a series of deep-truncated open KcsA structures were published, where parts of the intracellular gate was removed [204, 205]. As the gate opens wider and wider, the filter of KcsA shifts from the conductive conformation to a two-K^+-binding-site conformation, which is reminiscent of the constricted conformation captured from the closed KcsA (**Figure 3**). The authors, therefore, concluded that the constricted conformation is the inactivated conformation [205].

This conclusion is inconsistent with several other observations. First, all the open KcsA structures were solved with Fab antibody bound, which has been shown to inhibit inactivation [194]. Second, the structure of a voltage-gated K^+ channel chimera Kv1.2/2.1 stays in the conductive conformation, while under the same condition in electrophysiology it should be inactivated [59, 206]. Third, a recent study using semisynthetic KcsA channel demonstrated that the mutant is unable to adopt the constricted conformation, but inactivates indistinguishably from WT KcsA [207]. Perhaps, the constricted conformation is a deep-inactivated state of KcsA [207]. Contrary to the constriction model, Hoshi and Armstrong proposed that the inactivation could be derived from the transient dilation at the filter [208]. The existing evidence seems to agree with their novel hypothesis, but confirming a dilated selectivity filter will be extremely challenging with the techniques that are currently available.

Overview

In my dissertation I aim to investigate two important properties of K^+ channels:

the high K^+/Na^+ selectivity and the inactivated state of K^+ channels. Since both properties are associated with ion binding to the selectivity filter, finding the best approach to capture the binding reactions became the key objective at the beginning of this research. An obstacle to studying ion binding to K^+ channels is that the conformational change is minute, which most spectroscopic methods are not sensitive to capture the small conformational change; moreover, applying nuclear magnetic resonance spectroscopy requires labeling proteins with isotopic atoms so that producing low expressing protein becomes very costly. To avoid this obstacle, isothermal titration calorimetry (ITC) was applied to measure the enthalpy difference from K^+/Na^+ ion exchange that does not directly report changes of the structure.

In the second chapter, I show how we developed an extended method to obtain the K^+ and Na^+ affinities of empty channels, and the ion selectivity at equilibrium is therefore the ratio of two affinities. Using this method, each of the following chapter or appendix addresses one specific question. In the third chapter, I examine the correlation between the conduction selectivity and the equilibrium selectivity. In the fourth chapter, I test the hypothesis that the constricted conformation is not the inactivated state of the KcsA K^+ channel. The first appendix investigates the ion binding properties of NaK channel, while the second appendix characterizes the kinetics of K^+ binding to KcsA. The third appendix briefly introduces Isothermal Titration Calorimetry with derivations of one-site binding function and two-site sequential binding function, which will be helpful to understand all relevant studies. Overall, two significant conclusions were made in this work. First, equilibrium selectivity alone is insufficient to determine the

conduction selectivity. Second, the thermodynamic properties of the inactivated state are like those found in the conductive state in the KcsA K^+ channel.

CHAPTER II

PREFERENTIAL BINDING OF K^+ IONS IN THE SELECTIVITY FILTER AT EQUILIBRIUM EXPLAINS HIGH SELECTIVITY OF K^+ CHANNELS*

Introduction

Potassium (K^+) channels mediate the near diffusion-limited flow of K^+ ions across cellular membranes [209]. The exquisite selectivity for K^+ over Na^+ is necessary to maintain cellular resting potential and to repolarize cells during an action potential. Mutagenesis experiments, nuclear magnetic resonance spectroscopy and crystal structures of K^+ channels show that a region within the channel, called the selectivity filter, is responsible for the high selectivity [37, 49, 51, 53, 90, 120, 150] (**Figure 9A**). This region of the channel is lined with backbone carbonyl atoms and hydroxyl side chains to create a queue of four K^+ ion-binding sites that distinguish between K^+ ions (r = 1.33 Å) and Na^+ ions (r = 0.95 Å) [51, 55]. In the filter, two K^+ ions can distribute across these four sites spaced with water molecules between them in the so-called 1,3- and 2,4-configurations [54, 55] (**Figure 9B**). During K^+ ion conduction, the near equipotent nature of these configurations was suggested to create a virtually barrier-less passage for K^+ ions through the membrane [54, 210].

---

* Reprinted with permission from "Preferential binding of K^+ ions in the selectivity filter at equilibrium explains high selectivity of K^+ channels", by Shian Liu, Xuelin Bian and Steve W. Locklesss, 2012, *Journal of General Physiology*, 140:671-9, copyright [2012] by Liu et al. My role in the work of this chapter included experimental design to determine the ion selectivity of KcsA and MthK, performing the isothermal titrations of KcsA binding to K^+ ions in different Na^+ concentrations, and data analysis.

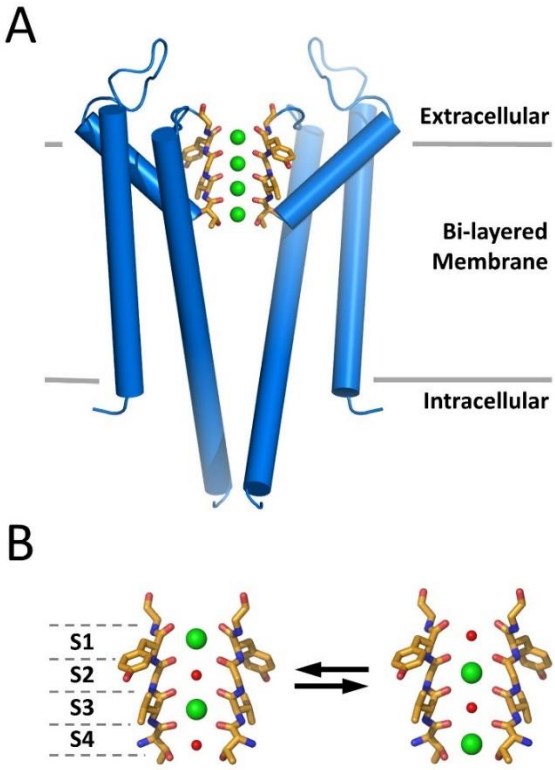

Figure 9. K^+ ion-binding sites within the KcsA K^+ channel. (A) A cartoon representation of KcsA with two of the four subunits shown; the subunits closest to and furthest from the viewer are removed for clarity. The selectivity filter is shown as a stick representation, with the four K^+ ion-binding sites indicated with green spheres. (B) The two K^+ ions within the selectivity filter are separated by water molecules in either a 1,3 or 2,4 configuration, where the number indicates the sites occupied by K^+ ions (S1-S4). Exchange between these two most populated states is thought to create a barrier-less passage for K^+ ions through the membrane.

The selectivity filter creates a more hostile environment for Na^+ ions and practically precludes their transport across the membrane. Two general mechanisms have been proposed to explain how K^+ channels accomplish this task [211]. In the first, a K^+ channel is selective for K^+ over Na^+ ions at equilibrium, meaning that the energy wells would be deeper for K^+ than Na^+ ions. The strongest experimental support for this

model comes from barium block experiments using electrophysiology, from crystal structures of the K^+ channels and from thermal stability measurements on KcsA [51, 53, 86, 133-135, 187, 212, 213]. The second model postulates that K^+ selectivity arises from a kinetic preference for K^+ ions entering the selectivity filter over Na^+ ions. This would be observed as different k_{on} rates of the ions binding to the selectivity filter. Recent experimental support for this hypothesis comes from Na^+- and Li^+-block experiments, X-ray crystal structures and molecular dynamic simulations [140, 143]. Which of these two models best explains the selectivity observed in K^+ channels?

In this study, I measured the affinity of K^+ ions interacting within the selectivity filter of K^+ channels and determined that K^+ channels are selective for K^+ over Na^+ ions at equilibrium. The disassociation constants determined in this study provide a direct link between crystal structures and channel-ion interactions, and are qualitatively consistent with other studies measuring ion binding to K^+ channels [120, 133-135]. The measured selectivity for K^+ over Na^+ ions is on the order found during ion conduction, suggesting that selectivity during ion conduction likely arises from an equilibrium preference for K^+ ions within the selectivity filter. I hypothesize that K^+ selectivity at equilibrium arises from the intrinsic selectivity of each K^+ ion-binding site and the need to satisfy multiple-linked ion binding sites simultaneously within the filter.

Materials and methods

KcsA purification and preparation

Wild-type KcsA in pET28a expression vector was expressed in *Escherichia coli*

BL21(DE3) cells. Cell pellets were re-suspended and sonicated in 50 mM Tris, pH 7.8, 100 mM KCl, 10 µg/ml DNase and 50 µg/ml Lysozyme. DM (*n*-decyl-β-D-maltopyranoside, Affymetrix) was added to 40 mM and KcsA was extracted for 3 hours at room temperature. The soluble cell lysate was loaded onto Ni-NTA resin (QIAGEN), eluted, concentrated to 5-10 mg/ml and dialyzed to remove imidazole. KcsA was cleaved with chymotrypsin (Sigma-Aldrich) for 2 hours at room temperature and purified on a Superdex 200 column (GE Healthcare) equilibrated with 50mM Tris, pH 7.5, 20 mM KCl, 100 mM NaCl and 5 mM DM. The purified pore domain was concentrated to 100µM and dialyzed against solutions containing the desired concentration of NaCl with 50 mM Tris, pH 7.8, 10 mM DM. The concentration of protein for the isothermal titration calorimetry (ITC) experiments was determined by absorbance at 280 nm.

MthK purification and preparation

MthK was expressed and purified as described previously [214]. In brief, the channels were expressed in *E. coli* M15 cells by induction (at $OD_{600} \approx 0.8$) with 0.4 mM IPTG at 37 ^{0}C for 5 hours. Expressed protein was extracted from cell lysate using 40 mM DM and purified on a Talon Co^{2+} affinity column (Takara Bio Inc.). The protein was cleaved with trypsin (Sigma-Aldrich) at room temperature for 5 hours and was terminated using trypsin inhibitor from bovine pancreas (Sigma-Aldrich). The tetrameric pore was purified over a Superdex 200 column equilibrated with 50 mM Tris, pH 8.0, 10 mM KCl, 100 mM NaCl, and 5 mM DM. The purified protein was concentrated to 1

mg/ml and dialyzed against the desired buffer for the ITC experiments. Protein concentrations were determined by absorbance at 280 nm.

ITC measurement and fitting

Measurements of the heat exchange associated with K^+ binding to both channels were acquired using a microcalorimeter (VP-ITC; GE Healthcare). All experiments were performed at a constant temperature of 25 ^{0}C. All solutions were filtered and degassed before each experiment. For KcsA, the sample cell (1.3959 ml) was filled with protein solutions including 100-500 mM NaCl, 50 mM Tris (pH 7.8) and 10 mM DM, whereas the injector contained the same sodium buffer with 40 mM KCl. 25-30 injections were performed with 3µl of ligand injected into sample cell each time. For MthK, the sample cell was filled with a solution containing 50 mM Tris, pH 7.8, 50-250 mM NaCl, 10 mM DM and 10-20 µM MthK. The injection syringe was filled with a ligand solution containing 50 mM Tris, pH 7.8, 50-250 mM NaCl, 3-20 mM KCl and 10 mM DM. 25-75 injections of 3 µl of ligand solution were titrated into the MthK protein solution. The data was fit to a one-site or two-site sequential binding model in the Origin program. The affinities were reported as K_D (or 1/K) in the text and figures. In the one-site model (used for KcsA), n was set to 1 and enthalpy (H) and association constant (K) were fit. In the two-site sequential mode (used for MthK), the enthalpy (H1 and H2) and association constant (K1 and K2) were fit. Binding isotherms with two identical ligands can sometimes have multiple solutions to the fraction-bound equations because of linked parameters and local or shallow minima. The isotherms were fit with different initial

parameters and converged to values within 10% of each other, suggesting a single optimum within the searched parameter space; the parameters yielding the lowest χ^2 were used in subsequent data analyses. The landscape around the optimal solution was explored with two types of perturbation analysis. In the first, one parameter was fixed and the remaining parameters refit such that χ^2 was never > 5% of the optimal value. This approach yielded variation of 1-23% from the optimal values. The second perturbation approach used a covariance matrix to extract the uncertainty of each fitted parameter and yielded a variance of 9-18% [215, 216]. Collectively, these approaches demonstrate that the solutions obtained for MthK are sufficiently constrained by the experimental data. KcsA was also constrained by its experimental data – different initial parameters yielded exactly the same solutions, and both perturbation approaches yielded errors < 3%.

Fitting the K^+/Na^+ competition ITC data

The apparent affinities (K_D) for each K^+ ion-binding event was fit individually to the following equation:

$$1/K_D = \frac{1/K_D^{K^+}}{1 + [Na^+]^n \cdot 1/K_D^{Na^+}}$$

where $K_D^{K^+}$ and $K_D^{Na^+}$ are the dissociation constants of the channel for K^+ and Na^+ binding to empty channels respectively, and *n* is the Hill coefficient associated with Na^+ binding. In effect, this equation describes the ITC-derived association constant K (because $K=1/K_D$) as a function of $[Na^+]$. The fit values and their standard errors were

determined using Prism (GraphPad Software). A perturbation approach was used to examine the landscape around the solution by fixing individual parameters and refitting the remaining variables. This yielded a variation of 2-6% and 0-6% for MthK (K1 and K2, respectively) and < 1% variation for KcsA when χ^2 was not allowed to vary by > 5%. The equilibrium selectivity is $K_D^{Na^+} / K_D^{K^+}$.

Results

The goal of this study is to measure the affinities of K^+ channels' selectivity filter for K^+ and Na^+ ions. Isothermal titration calorimetry (ITC) is ideally suited to this purpose because of the ability to measure equilibrium ligand binding without the need to label the protein or ligand, and the measurement does not rely on ion conductance, which is required for electrophysiology-based experiments. I measure the net enthalpy associated with K^+ ions binding to two different channels. These data are used to determine both the affinity of each binding event and its associated selectivity. Because the equilibrium constants are thermodynamic parameters, no information regarding the physical mechanism or the location of the binding sites in the selectivity filter can be obtained directly from these measurements. However, these results are used to constrain the possible physical mechanisms of selectivity derived from high-resolution protein structures and models.

K^+ ion affinity of the KcsA K^+ channel

ITC was used to monitor K^+ ion binding to the *Streptomyces lividans* K^+ channel

KcsA (**Figure 10A**). The thermogram (**Figure 10B**) shows the heat exchanged after equal injections of a KCl solution into a reaction cell containing the channel. The heat evolved is from the net enthalpy associated with K^+ ions binding within the KcsA channel and from the enthalpy of diluting the concentrated KCl solution. The heat of dilution is constant throughout the experiment because in each case the same amount of KCl is injected and the change in volume is small. The asymptotic nature of curve suggests that the final injections contain little to no K^+ ion binding and that the heat observed at that point is primarily from diluting the concentrated KCl solution (**Figure 10C**).

In the analysis of this ITC data an important assumption is made: ions bind in the selectivity filter and not elsewhere in the channel. Several experimental observations justify this assumption. First, high-resolution x-ray crystal structures show ordered K^+ ions within the selectivity filter and in the central cavity, limiting the number of likely places that ions would specifically interact [53, 90]. Chemical shifts observed in both solution and solid-state nuclear magnetic resonance spectroscopy show changes in the chemical environment around atoms in the selectivity filter when K^+ ions are titrated into the sample, suggesting that the highest affinity sites are within the selectivity filter and not the cavity [120, 217]. Finally, previous ITC experiments with KcsA show that heat is only observed for ions known to conduct through the channel (K^+, Rb^+, Cs^+ and Ba^{2+}) and not with ions that do not readily conduct but can bind in the cavity (Li^+, Na^+, Mg^{2+} and Ca^{2+}) demonstrating specificity for the interaction [111].

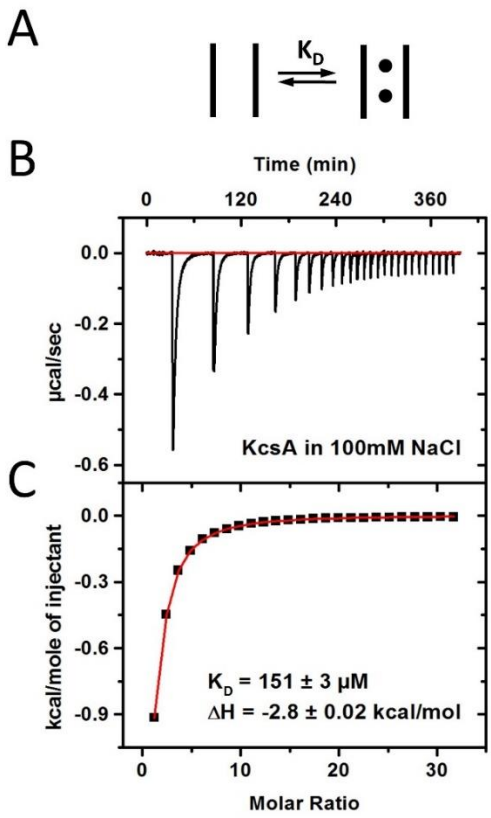

Figure 10. K^+ ion binding to the KcsA K^+ channel using ITC. (A) A generic model showing K^+ ions binding to the channel. (B) Thermogram showing the heat exchange associated with K^+ binding to KcsA in 100 mM NaCl. (C) The ITC data were integrated and fit to a one-site binding model to determine the affinity and enthalpy. The values shown are the parameters describing this experiment.

The data in **Figure 10C** are fit to a one-site binding model, as attempts to fit the data to more complicated models did not significantly improve the fit but added more parameters. The calculated affinity is 150 µM, which is similar to the 430 µM affinity I observed previously at a different temperature (20 ^{0}C instead of 25 ^{0}C here) and in the A98G KcsA mutant channel instead of the wild-type channel used in this study [111].

KcsA ion selectivity at equilibrium

A goal of this study is to measure the affinity and selectivity of the KcsA channel for K^+ and Na^+ ions. The K^+ affinity obtained from the data in **Figure 10** is an apparent affinity because K^+ ions are competing with 100 mM Na^+ ions in the buffer solution (**Figure 11A**). NaCl in the ITC buffer solution is necessary because the channel is unstable when small cations (such as Na^+ or K^+) are replaced by large organic cations (such as *N*-methyl-D-glucamine or glucosamine). Even if the channel were stable in the absence of K^+ or Na^+, the structural state of this or any K^+ channel is not known, which could lead to erroneous interpretations of the data. Equally important, it is unclear how these measurements should be compared with permeability measurements that

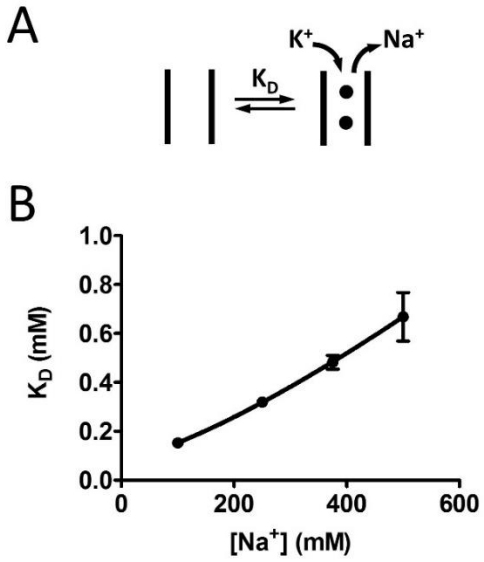

Figure 11. K^+ ions compete with Na^+ ions within the KcsA selectivity filter. (A) A model of K^+ ions displacing Na^+ ions bound within the selectivity filter. (B) The apparent K_Ds vary as a function of [Na^+] in the ITC chamber. The data are fit to a competition model to determine the affinity of K^+ and Na^+ ions. Each data point is determined from three or more independent experiments.

these measurements should be compared with permeability measurements that rely on a mixed Na^+/K^+ ion solution to determine ion channel selectivity.

The equilibrium K^+ and Na^+ ion-binding affinities were determined by measuring the change of K^+-binding affinity (K_D) as a function of [Na^+] in the ITC buffer (**Figure 11B**). These data were fit to a competition model to determine $K_D^{K^+}$, $K_D^{Na^+}$ and *n* (see Methods for details). KcsA is highly selective for K^+ over Na^+ with a $K_D^{K^+}$ of 80 ± 2 µM and a $K_D^{Na^+}$ of 60,000 ± 800 µM, for an equilibrium selectivity of 750 (K^+: Na^+). The affinity for K^+ is very similar to the 30 µM affinity obtained through Ba^{2+} block experiments of the KcsA channel [135]. The Hill coefficient for Na^+ ion displacement was *n* = 1.3, indicating a near-simple exchange of Na^+ with K^+ ions (**Table 1**).

[Na^+] (mM)	K_D (mM)	ΔH (kcal mol^{-1})
100	153 ± 5	-3.2 ± 0.6
250	320 ± 12	-2.5 ± 0.3
375	483 ± 18	-2.2 ± 0.1
500	668 ± 99	-2.3 ± 0.4

Table 1. Thermodynamic parameters for K^+ binding to KcsA in different [Na^+]. K_D and ΔH were obtained by fitting a single binding isotherm. Each value represents the mean and standard deviation of three or more independent ITC experiments.

Ion binding to the MthK K^+ channel

Although KcsA is a structural model for understanding ion selectivity in K^+ channels, a linked conformational change associated with ion binding complicates the interpretation of the selectivity measurements. Crystal structures determined in Na^+ or

low concentration of K^+ show the selectivity filter in a so-called collapsed conformation that cannot conduct ions [53, 55, 111, 205]. Upon raising the concentration of K^+, the channel adopts the conductive conformation that is thought to mediate the flow of ions across the membrane and is observed in all K^+ channel structures solved in high K^+ solutions to date [53, 57, 59, 63, 66, 68, 69, 90, 214, 218]. This conformational change is proposed to contribute to the large selectivity observed in KcsA and could be the

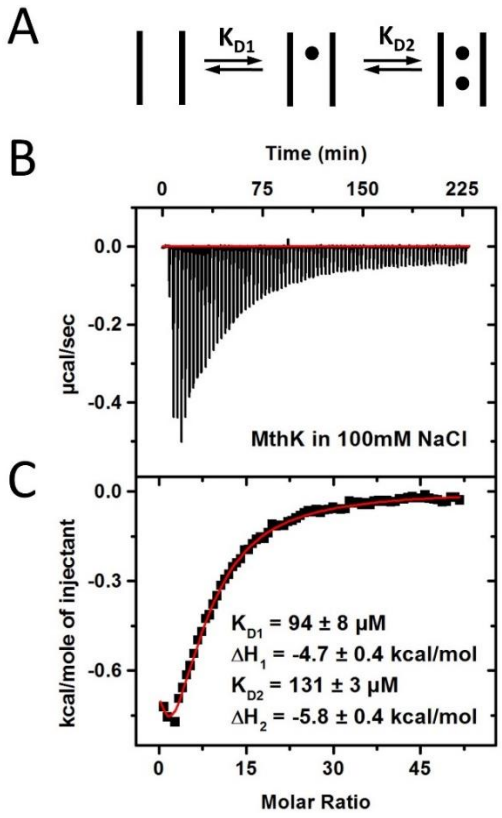

Figure 12. K^+ ion binding to MthK K^+ channel using ITC. (A) A generic model showing two K^+ ions binding to the channel. (B) Thermogram showing the heat exchange associated with K^+ binding to MthK in 100 mM NaCl. (C) The ITC data were integrated and fit to a two-ion binding model to determine the affinities and enthalpies for each K^+ ion-binding event. The values shown are the parameters describing this experiment.

physical basis for the ion selectivity observed in my ITC experiments [55, 219]. Is the conformational change necessary for KcsA's high K^+ ion selectivity? To test this, I measured the selectivity of the MthK channel from *Methanobacterium thermoautotrophicum*, whose selectivity filter is chemically identical to the conductive conformation of KcsA and remains in the same conformation with either K^+ or Na^+ in the filter [90] (**Figure 12**).

The integrated heat changes upon K^+ ion binding to MthK were initially fit to a one-site binding model, but an inspection of the residuals to the fit suggested that a more complicated model is needed to account for the binding isotherm (**Figure 13A&D**). The addition of a second K^+ ion-binding event with different affinities and enthalpies gave a significantly better fit both qualitatively and quantitatively (**Figure 13C&F**; $p < 10\text{-}4$, RSS=72347 for one-site vs. RSS=2193 for two-site models). Note that two K^+ ions binding with identical affinities and enthalpies did not fit the data (**Figure 13B&E**), which is consistent with the "hook" observed at the beginning of the trace (**Figure 12C**); the non-monotonic nature of the binding isotherm is indicative of multiple ligands binding with different binding constants [220, 221]. Measuring two K^+ ion-binding events is not surprising. Both X-ray crystallography and molecular dynamics simulations suggest that two to three K^+ ions bind within the conductive conformation of the KcsA selectivity filter and the same would be expected for MthK whose K^+ ion binding ligands are identical to that of KcsA [53, 55, 92, 143, 210, 222]. These ITC data alone cannot reveal which sites are occupied by each ion, but structural experiments suggest that K^+ ions distribute nearly equally across all four sites of the filter, which are

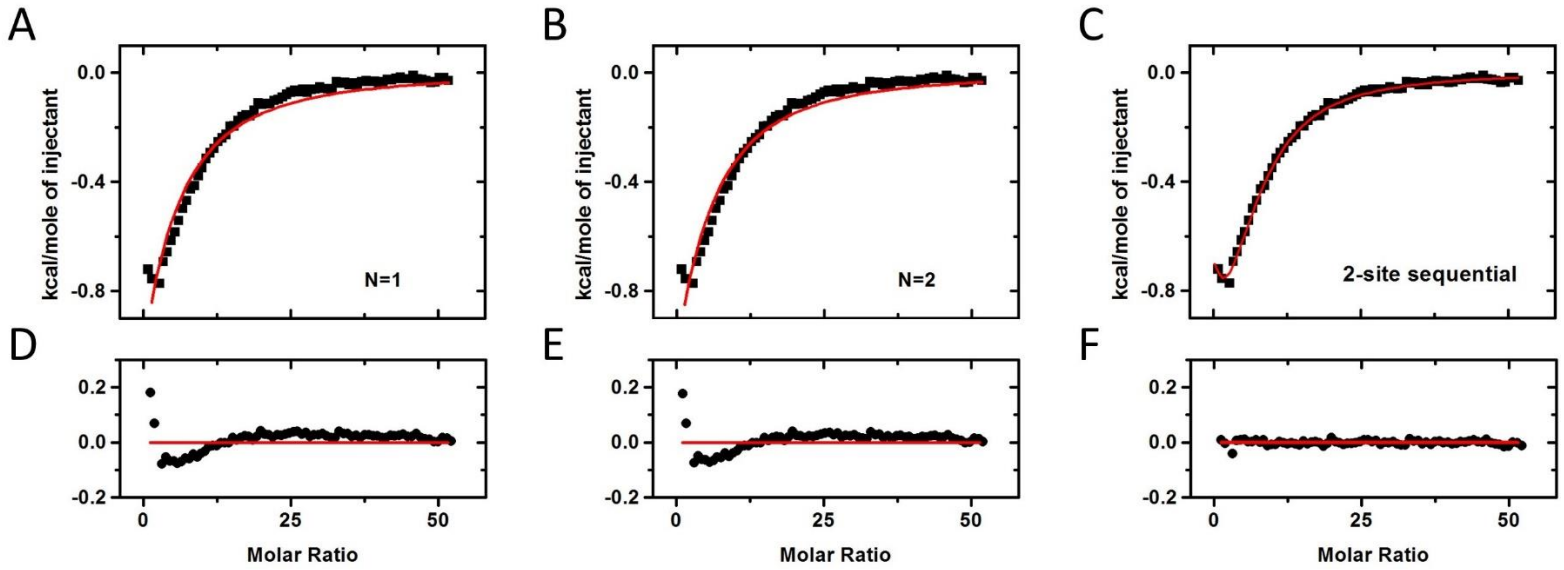

Figure 13. MthK-binding isotherm from **Figure 12C** fit to three different binding models. (A) A one-site model, (B) a two-site model with identical affinity and enthalpies, and (C) a two-site model with different affinities and enthalpies. (D-F) The difference between the model and experimental data is shown for the three models.

likely in rapid equilibrium with each other [53, 55, 90].

The apparent affinity of K^+ was measured in the presence of different Na^+ ion concentrations to obtain the K^+ and Na^+ ion-binding dissociation constants (**Figure 14**). The selectivity of the first ion-binding event is 200 ($K_D^{K^+}$ = 10 µM, $K_D^{Na^+}$ = 2,000 µM) and the second is approximately 110 ($K_D^{K^+}$ = 80 µM, $K_D^{Na^+}$ = 9,000 µM) (**Table 2**). The lack of a ligand-linked conformational change in this channel demonstrates that the conductive conformation of K^+ channels can be selective for K^+ ions at equilibrium. Additionally, the difference in affinity of the first and second K^+ ion binding suggests interactions between ions in the filter, which I discuss in the next section.

The Na^+ dependence of K^+ ion binding reveals a Hill coefficient of 2, but the physical meaning of this observation is unclear. The occupancy of Na^+ ions in the selectivity filter is not known. Additionally, how Na^+ is displaced by K^+ ions is complicated because Na^+ ions seem to prefer interacting in the plane of the oxygen atoms that typically form the oxygen cage around K^+ ions, whereas K^+ ions prefer

[Na^+] (mM)	K_{D1} (mM)	ΔH_1 (kcal mol^{-1})	K_{D2} (mM)	ΔH_2 (kcal mol^{-1})
50	28 ± 5	-3.5 ± 0.7	97 ± 24	-5.7 ± 0.9
100	75 ± 22	-4.4 ± 0.5	143 ± 14	-6.0 ± 0.8
175	211 ± 31	-5.5 ± 0.7	329 ± 45	-4.6 ± 0.6
250	360 ± 27	-5.9 ± 0.4	473 ± 40	-4.8 ± 0.1

Table 2. Thermodynamic parameters for K^+ binding to MthK in different [Na^+]. All parameters were obtained by fitting a 2-site sequential binding isotherm, where K_{D1} and ΔH_2 represent the first K^+ ion binding to the channel and K_{D2} and ΔH_2 represent the second ion. Each value represents the mean and standard deviation of three or more independent ITC experiments.

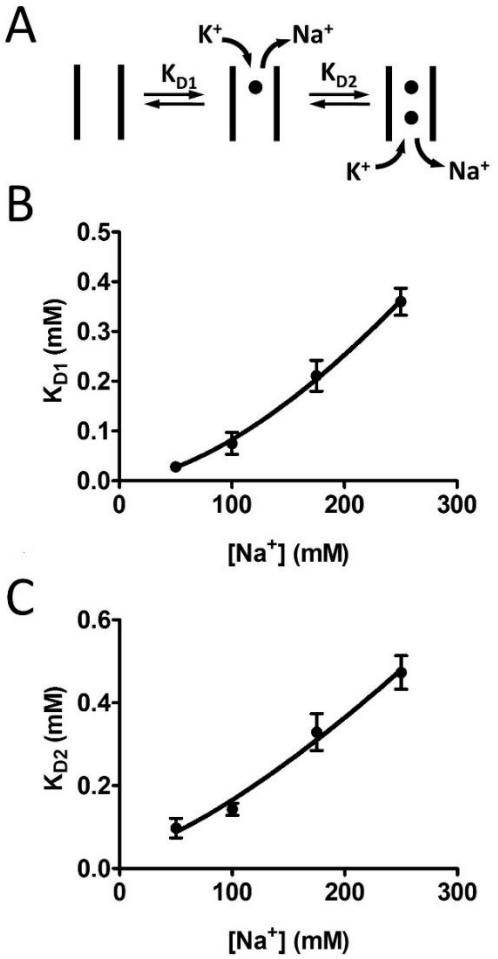

Figure 14. K^+ ions compete with Na^+ ions within the MthK selectivity filter. (A) A model of K^+ ions displacing Na^+ ions bound within the selectivity filter. (B) The apparent K_Ds (K_{D1} and K_{D2}) vary as a function of [Na^+] in the ITC chamber. The data are fit to a competition model to determine the affinity of K^+ and Na^+ for each binding event. Each data point is determined from three or more independent experiments.

residing within the cage itself [53, 90, 140]. The simplest explanation for a Hill coefficient of 2 is that two (or more) Na^+ ions dissociate for each K^+ ion binding. However, this leads to the implausible conclusion that four total Na^+ ions are bound to

the filter when no K^+ ions are present; only two to three positive charges are supported within the selectivity filter based on X-ray crystallography and Ba^{2+} block experiments [55, 133-135]. An alternative explanation for my result is that the increased ionic strength of the solution reduces the apparent affinity for K^+ ions by screening negative charges. A more complete model of K^+ displacing Na^+ from the selectivity filter will require correlating these ITC results with additional structural information on the occupancy and location of Na^+ ions bound to MthK with different numbers of K^+ ions in the selectivity filter.

Discussion

In this study, I measure the affinity of K^+ and Na^+ ions binding within the selectivity filter of two different K^+ channels. My main experimental observation is that both KcsA and MthK K^+ channels have high equilibrium selectivity for K^+ over Na^+ ions. Although not entirely unexpected given the known selectivity of these K^+ channels during ion conduction [49, 90, 135], it does provide a direct link between ion-binding experiments and crystal structures that allows us to propose a hypothesis relating to the physical origins of K^+ channel selectivity at equilibrium.

Interactions between ions in the selectivity filter

The first K^+ ion binds to the MthK channel with a greater affinity than the second (**Table 1**). Different ligand affinities can sometimes arise from a conformational change associated with ligand binding, such as is observed in KcsA, but MthK has the same

conformation with either K^+ or Na^+ ions bound [53, 55, 90]. The close proximity (3-10 Å) of K^+ ions in the selectivity filter of MthK leads us to speculate that the difference in affinities is from electrostatic repulsion between nearby ions within the filter. If so, then the interaction energy and the average distance between ions can be used to calculate the effective dielectric constant (ε_{sf}) encountered by the ions within the selectivity filter using Coulomb's Law. Given the interaction energy of $\Delta\Delta G = RT\ ln\ (80\ \mu M/10\ \mu M) = 1.2 \pm 0.2$ kcal/mol and spacing of 6.6 Ångstroms so that one water molecule separates two monovalent cations, the effective dielectric within the filter is $\varepsilon_{sf} = 40 \pm 7$. This number must be tempered by the usual caveats that thermodynamic values do not reveal the actual mechanism of the process, and that it is possible that the protein itself has a role in mediating ion-ion interactions. However, the relatively high dielectric value suggests that the environment within the selectivity filter could be more like an aqueous solution ($\varepsilon_w = 80$) than a hydrocarbon one such as the lipid membrane ($\varepsilon_m = 2$). The large dielectric constant is not surprising – ion channels rapidly conduct ions across the membrane and could minimize energetic barriers to membrane crossing by making the internal protein environment encountered by the ion as similar to a hydrated ion as possible, both in terms of spacing between oxygen atoms and the dielectric environment [51, 53, 223].

K^+ channels achieve the arduous task of conducting K^+ ions at rates approaching $10^8\ s^{-1}$ while maintaining 10^2 - 10^3 selectivity for K^+ over Na^+ ions. High ion selectivity suggests tight binding to the channel and long residence times. The rate of ions dissociating from channels (k_{off}) set an upper limit on the conductance of ions. In the

case of a 100-μM K^+ affinity, similar to that observed for the second ion binding to MthK, k_{off} would be 10^5 s^{-1} ($K_D = k_{off}/k_{on}$; k_{on} is likely near diffusion limited at 10^9 M^{-1} s^{-1}). This k_{off} rate is too small to fully account for the high ion conductance of many K^+ channels. However, a rate approaching ion conductance can be obtained if a third ion is added to the selectivity filter during ion conduction, which undoubtedly happens at least some of the time. The third K^+ ion would occupy a site adjacent to another K^+ ion with a distance of 3.3 Å between the centers of each ion, and would feel larger charge-charge repulsion than the ions separated by water molecules (6.6 Å apart). The interaction between the ions would be ~2.5 kcal/mol assuming a dielectric of 40, which puts the affinity of this third ion at ~10 mM. The k_{off} rate would then be ~10^7 s^{-1} and within an order of magnitude of that expected for a 10-pA channel.

Equilibrium selectivity versus selective ion conduction

A channel that selectively conducts an ion does not need to selectively bind that same ion at equilibrium. For example, a proposed mechanism by which a non-selective channel at equilibrium could selectively conduct ions is when the k_{on} rates of the competing ions are different [109]. The ions (say X^+ and Y^+) would selectively conduct through the channel at a selective ratio proportional to their k_{on} rates and concentrations ($k_{on}^{X^+}[X^+]/k_{on}^{Y^+}[Y^+]$), but only if the channel binds one ion at a time. This mechanism is not what I observe for K^+ channels. KcsA is approximately 750-fold selective for K^+ over Na^+ ions at equilibrium, which is in line with the minimum 250-fold K^+ over Na^+ selectivity calculated from permeability studies [49, 135]. We measure an ~100-fold

selectivity of the second K^+ ion binding to the MthK channel, which is also close to the 60-fold permeability of K^+ over Na^+ ions [90]. Additionally, crystal structures of KcsA and MthK provide qualitative support that the channel is selective for K^+ over Na^+ at equilibrium [53, 54, 90]. These results demonstrate that K^+ channels are both selective at equilibrium and during ion conduction.

The similarity between values for the equilibrium selectivity and K^+ permeability determined from reversal potentials suggest that K^+ channel selectivity can arise from equilibrium ion selectivity alone. A multi-ion mechanism such as that originally proposed by Hille and Schwarz (1987) suggests a straightforward way to convert an equilibrium preference for K^+ ions into K^+ selective conductance [81]. The interactions between ions in the filter lead to the so-called anomalous mole fraction effect, whereby the total conductance of a channel in mixed ions is not determined solely by the ratio of the two ions in solution and their individual ion conductance. In the case where the ions have very different affinities, such as I observe in this study, the higher affinity K^+ ion effectively blocks conductance of the lower affinity Na^+ ion by allowing the other sites in the channel to equilibrate before the "blocking" K^+ ion dissociates into solution. This mechanism is built upon the assumption that multiple ions selectively bind within the selectivity filter, which has been observed using electrophysiology, crystal structures and now ITC [53-55, 84, 86, 133, 177, 224, 225].

Proposed role of the ion queue for equilibrium selectivity

The selectivity filter within K^+ channels is formed by oxygen atoms, which are

typical direct ligands for both Na^+ and K^+ ions in proteins [56, 226]. Extensive studies on synthetic K^+ selective small molecules have demonstrated that one straightforward mechanism to achieve equilibrium cation selectivity is to build an oxygen-lined cavity that matches the size of the desired cation [227]. This design principle presumably mimics the hydrated ion, thus creating a favorable environment for the ion to partition into. A Na^+ ion-selective site would need a cavity with a radius of 0.95 Å, while the larger K^+ ion would have a cavity closer to 1.33 Å. An inspection of a K^+ binding site in K^+ channels reveals optimal distances between oxygen and K^+ ions in the center of the site and an optimal distance between oxygen and Na^+ ions on the edge of the site (in the plane of the oxygen atoms). Consistent with this, crystal structures show that both K^+ and Na^+ ions are able to bind within the selectivity filter at different overlapping sites [53, 90, 111].

The ITC-based selectivity measurements from this study show a high selectivity for K^+ ions over Na^+ ions at equilibrium. I propose that equilibrium selectivity arises not only from the interactions within individual ion-binding sites but also from the need to satisfy multiple binding sites simultaneously within the selectivity filter. Crystal structures of K^+ channels bound to K^+ ions show that ions distribute to the same sites that would be predicted from the synthetic small molecule studies [53, 90]. This creates a densely packed selectivity filter with oxygen, water and K^+ ions forming an inter-connected set of optimally spaced contacts. By the same chemical logic, the optimal site for any one Na^+ ion would be predicted within the plane of oxygen atoms to form its close packing contacts with the oxygen atoms. However, the crystal structure of Na^+ ions

bound to K^+ channels reveals a different arrangement of the ions. A Na^+ ion is observed at the upper-most site of the selectivity filter as would be predicted, but the density in the remaining sites is more consistent with that of water (r = 1.4 Å) or Na^+ ions bound sub-optimally to K^+-selective sites, which would likely result in a less favorable free energy of the overall system [90]. Computational studies have also proposed that the oxygen cages within the selectivity filter create an unfavorable environment for Na^+ ions [131, 140, 143, 228, 229]. Collectively, these results support the "snug-fit" model where the selectivity filter mimics the chemical properties and spacing of queued hydrated K^+ ions to create an isoenergetic diffusion pathway through the channel [51, 54, 111].

Conclusion

In this study, I show that the KcsA and MthK K^+ channels have a preference for K^+ ions over Na^+ ions in their selectivity filter at equilibrium. Although both ions can bind within the selectivity filter at different overlapping sites, the filter creates the most favorable sites for the larger K^+ ions. In addition to the selectivity filter facilitating ion-ion repulsion between adjacent ions in the queue, I propose that the linked nature of the ion-binding sites sets the register of the bound ions within it, preferring multiple K^+ ions over multiple Na^+ ions in the lowest free energy state of the system.

CHAPTER III

EQUILIBRIUM SELECTIVITY ALONE DOES NOT CREATE K^+-SELECTIVE ION CONDUCTION IN K^+ CHANNELS*

Introduction

Ion channels are essential to maintain ionic homeostasis in cells and to support rapid cellular signaling. Tetrameric cation channels facilitate the flow of Na^+, K^+, and Ca^{2+} ions across cellular membranes. These channels have two essential functional properties – they selectively conduct specific ions and they gate open/closed in response to stimuli [209]. Although channel selectivity has been studied for decades, fundamental questions remain about how a K^+ channel is able to conduct K^+ ions (r=1.33Å) rapidly while selecting against the slightly smaller Na^+ ion (r=0.98Å). For example, is a difference between the affinities for K^+ ions over Na^+ ions sufficient to explain K^+ selectivity during conduction as some models suggest [211]? Because affinity is a thermodynamic parameter, it captures many different physical-chemical determinants of ion selectivity in one quantitative term. If an equilibrium preference is insufficient to explain selectivity, then what kinetic barriers are needed [211]?

---

* Reprinted with permission from "Equilibrium selectivity alone does not create K^+-selective ion conduction in K^+ channels", by Shian Liu and Steve W. Locklesss, 2013, *Nature Communications*, 4:2746, copyright [2013] by Liu et al. My role in the work of this chapter included experimental design to determine the ion selectivity at equilibrium and during conduction, performing the isothermal titrations and electrophysiology as well as data analysis.

A variety of experimental techniques all support the conclusion that different K^+ channels have a preference for K^+ ions over Na^+ ions at equilibrium [53-55, 86, 90, 111, 120, 121, 131-133, 135, 143, 187, 230-234]. The simplest mechanism to explain ion selectivity is that the equilibrium preference of a channel determines its selectivity during ion conduction. The recent crystal structures and functional data on the non-selective *Bacillus cereus* NaK channel and its mutants provide a unique opportunity to test this hypothesis [150, 151]. The NaK channel has the same overall architecture as K^+ channels but has a selectivity filter formed from the sequence TVGDG instead of the canonical TVGYG sequence found in most K^+ channels [148, 149] (**Figure 15**). The K^+ channels contain four contiguous K^+ ion-binding sites in their selectivity filter, but in the NaK filter the two outermost sites (S1 and S2 of K^+ channels) are replaced with a water-containing vestibule. As a result, only the contiguous S3 and S4 sites remain of the filter. Mutations in the selectivity filter of the NaK channel transform it into a channel with two, three or four contiguous sites [150, 151] (**Figure 15**). Remarkably, the channel with four contiguous sites selectively conducts K^+ ions, whereas channels with two- or three-sites remain non-selective.

Is the equilibrium selectivity sufficient to explain ion selectivity during conduction? Here, I address this question by employing isothermal titration calorimetry (ITC) to measure the equilibrium properties of non-selective and K^+-selective mutant NaK channels. I use electrophysiology to characterize the selectivity properties of mutant NaK channels during ion conduction. Previous ITC-based experiments on the KcsA and MthK K^+ channels revealed a strong preference for K^+ ions over Na^+ ions at

equilibrium [111, 234]. If equilibrium selectivity alone is sufficient to explain selective ion permeation of a channel, then the four-site mutant NaK channel should also have a

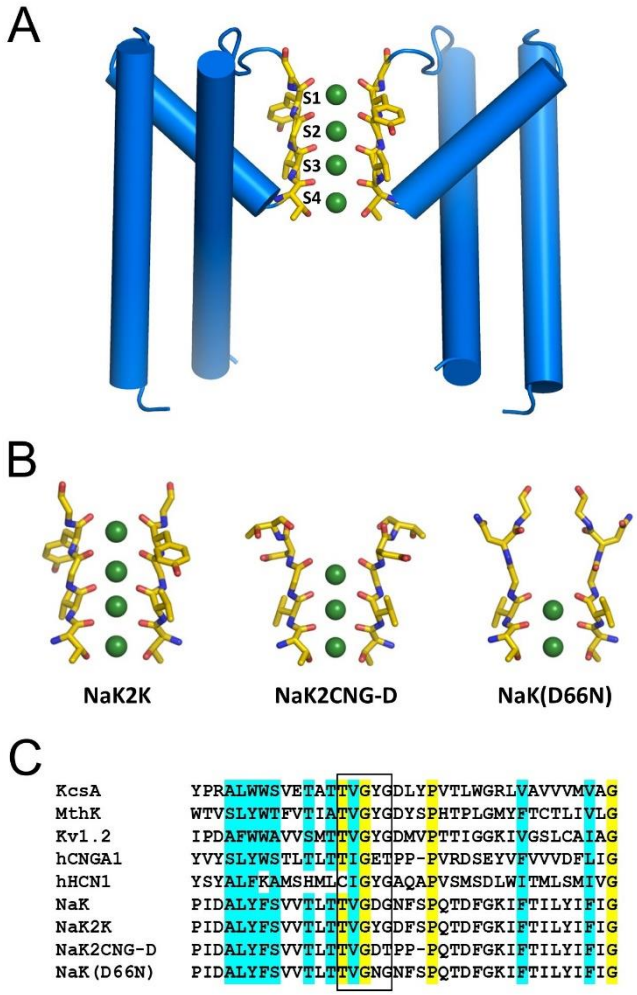

Figure 15. Structure of MthK K^+ channel and filters from NaK channel's mutants. (A) A cartoon diagram of MthK (pdb 2LDC) showing two of the four subunits in blue. (B) A comparison of the number of K^+ binding sites in the filter from NaK2K, NaK2CNG-D and NaK(D66N). Their selectivity filters are yellow sticks and K^+ ion binding sites are indicated with a green sphere. (C) A sequence alignment of the selectivity filter region of various tetrameric cation and NaK mutant channels used in this study. The box indicates the selectivity filter of K^+ channels.

K^+ preference at equilibrium, whereas the two- and three-site mutant NaK channels should be non-selective at equilibrium. I found that channels do not conduct selectively are all highly selective for K^+ over Na^+ ions at equilibrium, demonstrating that equilibrium selectivity alone cannot explain ion conduction selectivity. I conclude that the selectivity of K^+ channels is based on a mechanism that requires multiple K^+ ions to bind selectively and simultaneously in the channel's filter, whereas this mechanism is disrupted in the non-selective channels.

Materials and methods

Protein expression and purification

All mutant NaK channels are cloned into pQE60 expression vector without the first 19 amino acids. Plasmids were chemically transformed into M15[pREP4] *Escherichia coli* competent cells and grown on LB agar plates containing 100 μg/ml ampicillin and 50 μg/ml kanamycin. The freshly grown colonies were used to inoculate LB media and the cultures grown at 37 °C to an OD_{600} = 0.8. Protein expression was induced with 0.4 mM IPTG (isopropyl β-D-1-thiogalactopyranoside) at 25 °C. Cells were harvested after 18 hours of expression, spun down at 4,500 rpm using JA-10 rotor (Beckman Coulter) and stored at -80 °C. For purification, cells were re-suspended in 50mM Tris (pH 8.0), 150 mM KCl, 1 mM PMSF, 2 μg/ml DNase, 10 μg/ml lysozyme and 2 μg/ml leupeptin and lysed by sonication. *n*-Decyl-β-D-maltoside (DM) was added to the lysate to a final concentration of 40 mM and the mixture was incubated at room temperature for 3 hours. The membrane-solubilized lysate was spun at 12,000 rpm in a

JA-20 rotor (Beckman Coulter) for 20 min to clarify the solution. The supernatant was applied to Co^{2+} resin (Clontech) equilibrated in 50 mM Tris (pH 8.0), 150 mM KCl, 5 mM DM, washed with buffer containing 15 mM imidazole and eluted in 300 mM imidazole. Thrombin was added to the elution (0.5 U/mg mutant NaK protein) and incubated for 5 hours at room temperature to remove the His_6 tag. The digestion was stopped with 1 mM PMSF and the tetramer purified through a Superdex 200 (GE Healthcare) size exclusion column.

Measuring ion-binding affinity using ITC

Purified mutant NaK channels were concentrated to 25-150 μM depending on the enthalpy and affinity of each specific reaction. The protein was dialyzed against 50 mM Tris (pH 8.0), 50-400 mM NaCl, 5 mM DM immediately before use. ITC thermograms were collected on an iTC200 (GE Healthcare) at 25 °C with a spinning speed of 1,000 rpm. The sample chamber was filled with protein in the desired concentration of Na^+ and the injector syringe contained the same buffer with the addition of 5-60 mM KCl; the concentration of KCl was increased with higher NaCl concentrations since more K^+ was needed to saturate the channel. In the thermogram, the area under each downward deflection is the heat change of the system upon injecting a KCl solution into a chamber containing the channel. There are two primary sources of heat, the first is the heat of diluting the concentrated KCl solution into the chamber and the second is ion binding to the channel. The corresponding binding isotherm is generated from the integrated heat of each injection. The enthalpy (*H*) and apparent association constant (*K*) were fit in Origin

(GE Healthcare) to a one-binding site model with the number of sites fixed to 1. The apparent dissociation constant K_D (1/*K*) is reported in the text. As both Na^+ and K^+ ions compete within the channel's selectivity filter, I determined the affinity of the empty channel for K^+ and Na^+ ions using the following competition equation:

$$1/K_D = \frac{1/K_D^{K^+}}{1 + [Na^+]^n \cdot 1/K_D^{Na^+}}$$

where K_D is the fit apparent dissociation constant, $K_D^{K^+}$ and $K_D^{Na^+}$ are dissociation constants for K^+ and Na^+ to the empty channel, and n is a Hill coefficient. $K_D^{K^+}$, $K_D^{Na^+}$ and n were fit using Prism (GraphPad Software). The equilibrium selectivity of the channel is the ratio $K_D^{Na^+} / K_D^{K^+}$.

Channel reconstitution and electrophysiology

For reconstitution and electrophysiology, F92A was also mutated in the channels to increase their open probability [150]. A lipid mixture containing a 3:1 ratio of 1-palmitoyl-2-oleoyl-phophatidylethanolamine (Avanti Polar Lipids) and 1-palmitoyl-2-oleoyl-phophatidylglycerol (Avanti Polar Lipids) was dried and then re-suspended in reconstitution buffer containing 10 mM HEPES (pH 7.4), 450 mM KCl and 4 mM *N*-methyl-D-glucamine to a final concentration of 10 mg/ml. The lipid mixture were sonicated and solubilized in 10 mM DM for 1 hour. Protein was added to to a concentration of 0.1 mg protein per mg lipid with an additional 10 mM DM. The lipid-protein-detergent mixture was incubated overnight at room temperature before being dialyzed for 4-5 days to remove the detergent. Vesicles were flash frozen and stored at -

80 °C. The activity of the NaK(D66N) channel was measured using a vertical lipid-bilayer set-up with 10 mM HEPES (pH 7.4), 1 mM EGTA and 200 mM NaCl in the cup (outside) and with 10 mM HEPES (pH 7.4), 1mM EGTA, 100 mM NaCl and 100 mM KCl in the chamber (inside). The activity of NaK2K and NaK2CNG-D channels were measured with 200 mM KCl in the cup and 50 mM KCl and 150 mM NaCl in the chamber. Membrane voltage was controlled using a BC-535 Amplifier (Warner Instruments) with a Digidata 1440A analogue-to-digital converter (Molecular Devices). The currents were low-pass filtered at 1 kHz and were sampled at 20 kHz. Subsequent analyses were done using pClamp 10 (Molecular Devices). The lack of K^+ selectivity in NaK(D66N) was observed from three different channels in three independent experiments. The reversal potential for NaK2K was determined from six different channels while the reversal potential for NaK2CNG-D was determined from three different channels.

Results

Ion selectivity in the four-site NaK2K channel

I used mutant NaK channels to understand the ion selectivity properties of K^+ channels. It was therefore essential to determine whether mutant NaK channels can have the physical and functional properties of natural K^+ channels. A central feature of all K^+ channels is that they selectively conduct K^+ ions through a selectivity filter that contains four contiguous ion-binding sites, with adjacent sites sharing ligand-binding oxygen atoms [53, 54, 57, 59, 63, 218] (**Figure 15A**). The NaK2K mutant channel, which

contains four ion-binding sites, was previously shown in a high-resolution crystal structure to have a selectivity filter indistinguishable from other K^+ channels [150] (**Figure 15B**). I measured the ion permeability ratio in mixed-ion conditions using purified NaK2K channels reconstituted into liposomes to allow Na^+ and K^+ ions to directly compete for binding to the selectivity filter (**Figure 16A**). Single channel recordings using a vertical bilayer system were obtained with 50 mM KCl and 150 mM NaCl in the cup and 200 mM KCl in the chamber. In these conditions, NaK2K has a reversal potential of -32±3 mV (average ± s.d., *n*=6), which corresponds to a permeability ratio of 21 (K^+:Na^+); a non-selective channel would reverse near 0 mV and a perfectly K^+-selective channel would reverse at -35 mV. A similar permeability ratio of ~25 was obtained using bi-ionic conditions in giant liposome patches [150]. NaK2K, like natural K^+ channels, is selective for K^+ over Na^+ during ion conduction.

Affinity measurements of the KcsA and MthK K^+ channels revealed that they are selective for K^+ during ion conduction and bind K^+ ions selectively at equilibrium [234]. It was therefore of interest to determine whether the NaK2K channel also selectively binds K^+ over Na^+ ions at equilibrium. Isothermal titration calorimetry (ITC) quantifies the heat change upon ligand binding to a protein, and is used to measure the equilibrium binding affinities between ions and transport proteins [111, 235]. A thermogram of K^+ binding to NaK2K solubilized in detergent is shown in Figure 16B. The data are fit to a one-site binding model to give the total enthalpy of the reaction and the binding affinity (**Figure 16B**). Although K^+ channels have more than one ion in their selectivity filter during ion conduction, the data fits well to either a one or two ion-binding model. It is

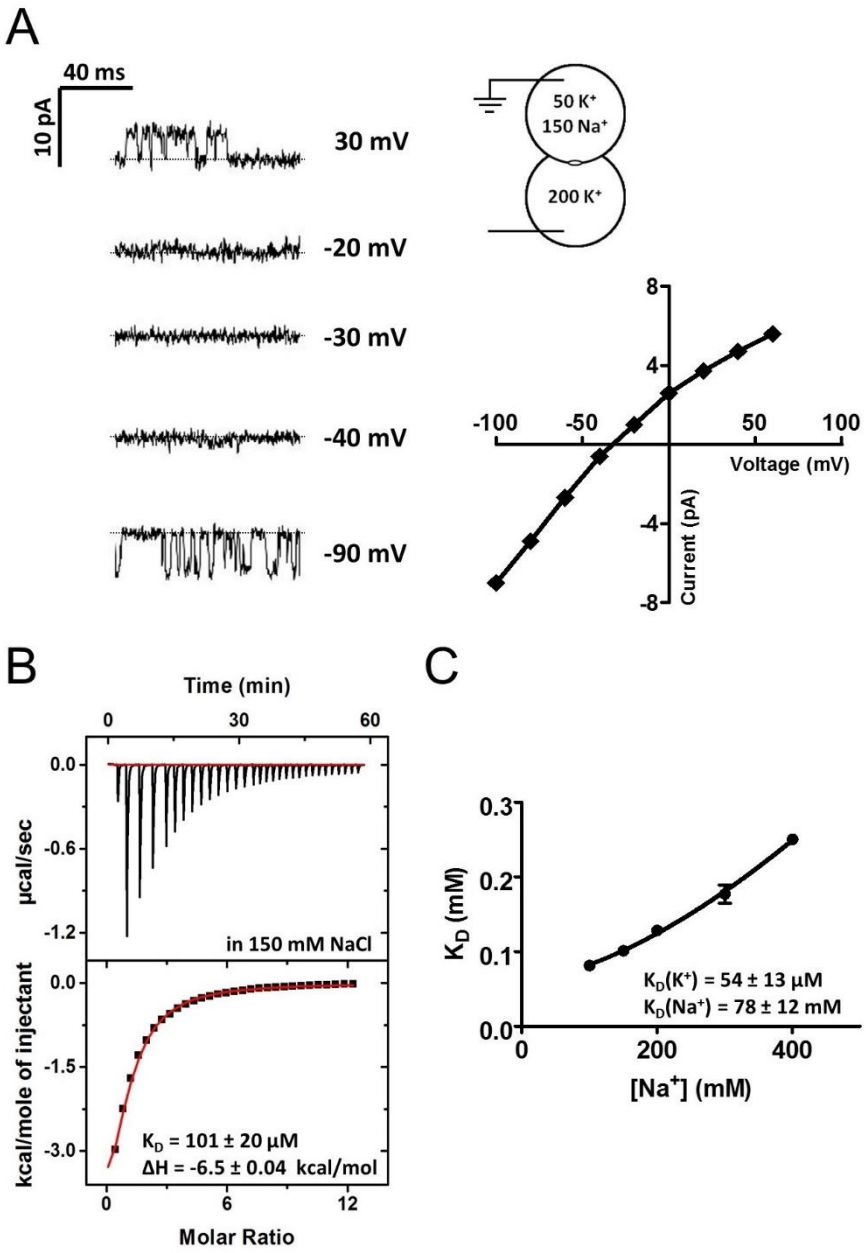

Figure 16. Ion binding and conduction of NaK2K channel. (A) Single channel traces at different membrane potentials (left) and the I-V curve (right). Currents are recorded with 150 mM NaCl + 50mM KCl in the cup (outside) and 200 mM KCl in the chamber (inside). The dotted lines mark the closed, zero current level. (B) Thermogram of K^+ binding to NaK2K in the presence of 150 mM NaCl (top). The integrated heat exchange from each injection is fit to a binding isotherm to obtain the relevant thermodynamic parameters (bottom). (C) The apparent affinity of K^+ ions for NaK2K as a function of NaCl concentration in solution. The line shows the fit to a competition binding equation described in the methods to obtain $K_D(K^+)$ and $K_D(Na^+)$; the average of 3 or more experiments and their s.e.m are plotted.

unclear why I do not observe two distinct ion-binding events, but a possible explanation is that both ions bind with similar affinity and enthalpy. This would make the individual binding events inseparable at the resolution of these experiments and the measured affinity would represent a combination of the individual ion-binding events.

As expected based on the similar physical and functional characteristics of the NaK2K channel and other K^+ channels, NaK2K is selective for K^+ at equilibrium. The affinity for K^+ ions is in line with the observed values for other K^+ channels [111, 234]. The results suggest that NaK2K is selective for K^+ at equilibrium because K^+ ions are able to outcompete the much more abundant Na^+ ions in the buffer. The ion selectivity at equilibrium was determined by measuring the apparent K^+ affinity in the presence of different concentrations of Na^+. This competition mimics the competition encountered within the channel during ion conduction, when ion selectivity is calculated by measuring the reversal potential of mixed-ion conditions. **Figure 16C** is a plot of the apparent affinity of K^+ as a function of Na^+ ion concentration, and those data are fit to the competition model described in the Materials and Methods. The affinity of NaK2K for K^+ is 54 μM and that of Na^+ is 78 mM, which is a ~1,500-fold selectivity of K^+ over Na^+ at equilibrium (**Table 3**). A Hill coefficient (n) of 1.4±0.3 is calculated that may originate from interactions between ions within the filter. In addition, K^+ ions prefer to reside within the oxygen cage of the selectivity filter whereas Na^+ ions are found both within the oxygen cage and in the plane of the atoms forming the cage [53, 90, 111, 140]. This difference in binding-site preferences within the selectivity filter could result in a non-stoichiometric displacement of Na^+ for K^+ ions, which was also seen in KcsA

and MthK channels. Collectively, these results mean that the K^+-selective NaK2K channel retains the same basic equilibrium selectivity properties found in K^+ channels studied to date, demonstrating that the mutant NaK channels can be profitably used to study K^+ channel selectivity.

Channel	K_D^{K+} (μM)	K_D^{Na+} (μM)	n	Selectivity
NaK2K	54 ± 13	78,000 ± 12,000	1.4 ± 0.3	1500 ± 420
NaK2CNGD	28 ± 11	11,000 ± 2,000	1.4 ± 0.2	390 ± 170
NaK(D66N)	56 ± 22	18,000 ± 5,000	1.0 ± 0.1	320 ± 160

Table 3. Thermodynamic parameters for Na^+ and K^+ ions binding to NaK mutant channels

Ion selectivity in the three-site NaK2CNG-D channel

I next examined the NaK2CNG-D mutant of NaK, which was originally constructed to mimic the selectivity filter of the cyclic-nucleotide gated (CNG) channels [151]. Its selectivity filter is comprised of three contiguous ion-binding sites that are very similar to the S2-S4 K^+ binding sites in K^+ channels (**Figure 15B**). Like CNG channels, NaK2CNG-D is non-selective for K^+ and Na^+ during ion conduction when measured in either mixed ion or bi-ionic conditions. A permeability ratio of 1.4±0.2 (K^+:Na^+; average ± s.d., n=3) in mixed ion condition was measured (**Figure 17A**), confirming the lack of selectivity observed in bi-ionic conditions [150]. If equilibrium ion selectivity is a major determinant of selectivity during ion conduction, then NaK2CNG-D should be non-selective at equilibrium.

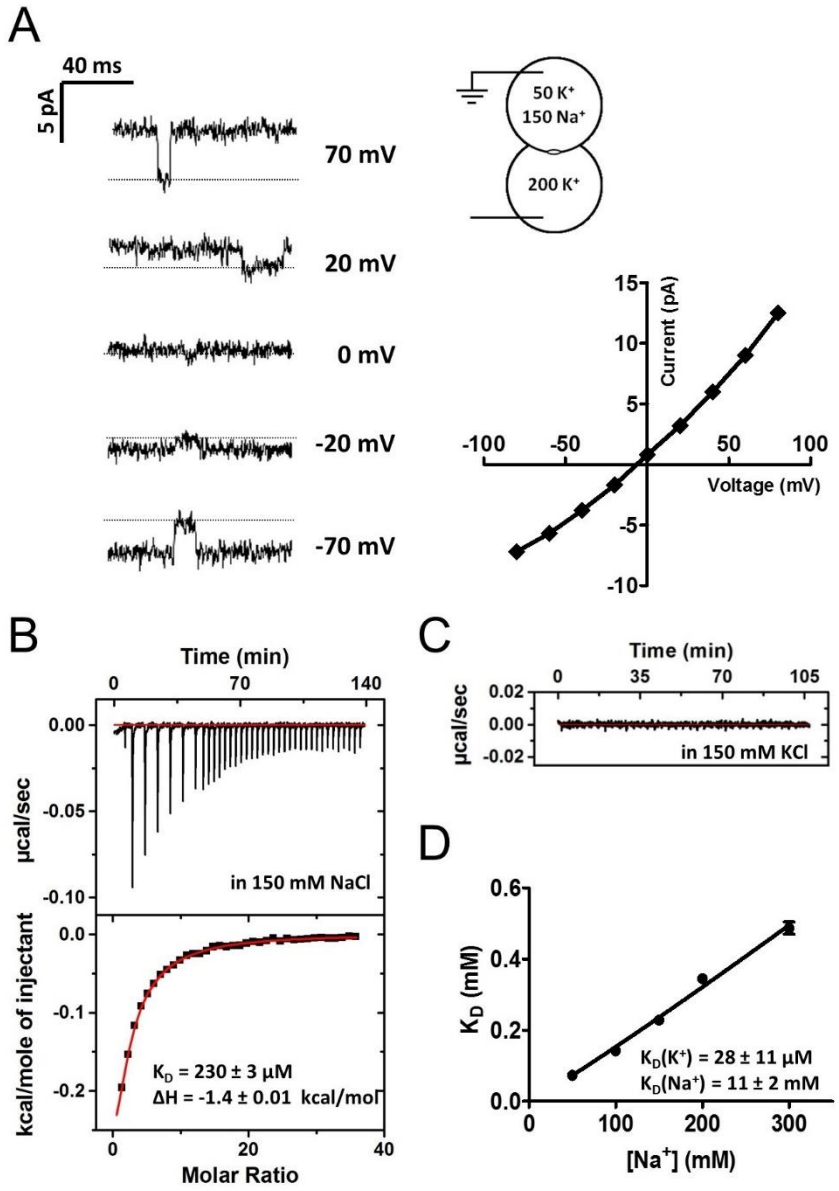

Figure 17. Ion binding and conduction of NaK2CNG-D. (A) Single channel traces at different membrane potentials (left) and the I-V curve (right). Currents are recorded with 150 mM NaCl + 50mM KCl in the cup (outside) and 200 mM KCl in the chamber (inside). The dotted lines mark the closed, zero current level. (B) Thermogram of K^+ binding to NaK2CNG-D in the presence of 150 mM NaCl (top). The integrated heat exchange from each injection is fit to a binding isotherm to obtain the relevant thermodynamic parameters (bottom). (C) Thermogram of Na^+ binding to NaK2CNG-D in the presence of 150 mM KCl. (D) The apparent affinity of K^+ ions for NaK2CNG-D as a function of NaCl concentration in solution. The line shows the fit to a competition binding equation described in the methods to obtain $K_D(K^+)$ and $K_D(Na^+)$; the average of 3 or more experiments and their s.e.m are plotted.

To test the equilibrium ion selectivity of the NaK2CNG-D channel, I measured both Na^+ binding in the presence of competing K^+ ions and K^+ binding in the presence of competing Na^+ ions. As expected for a non-selective channel, I observed no measurable Na^+ binding in the presence of competing K^+ ions (**Figure 17C**). However, I observed K^+ binding in the presence of Na^+ ions (**Figure 17B**), which suggests that NaK2CNG-D is selective for K^+ at equilibrium; if the channel were non-selective, no heat from K^+ ion binding would have been observed, as the 150 mM Na^+ ions in the reaction chamber would outcompete the sub-millimolar K^+ ions injected from the syringe. The equilibrium selectivity of NaK2CNG-D for K^+ was quantified by measuring the apparent K^+ affinity as a function of Na^+ concentration as described for the NaK2K channel (**Figure 17D**). A fit to the experimental data revealed a K^+ affinity of 28 μM and a Na^+ affinity of 11 mM (**Table 3**).

The fact that its individual ion-binding sites are so similar to those in K^+ channels likely explains the ~400-fold selectivity of the NaK2CNG-D channel for K^+ at equilibrium. Further support for this observation comes from the recent crystal structures of NaK2CNG-D channels determined at different ratios of Na^+ and K^+ ions. These structures show an increased K^+ occupancy in site 3 of the channel relative to the adjacent sites 2 and 4 in the presence of competing Na^+ ions [236]. Therefore, site 3 of NaK2CNG-D is likely more K^+ selective than the other two sites in the selectivity filter.

Ion selectivity in the two-site NaK(D66N) channel

Does further reducing the number of ion-binding sites alter the equilibrium

selectivity? The two-site mutant NaK channel, D66N, has two of the canonical four ion binding sites found in K^+ channels (**Figure 15B**), but lacks the additional ion-binding sites found in the K^+ channels [148, 237] (**Figure 15A**). I first determined the affinity and selectivity of this channel for K^+ and Na^+ at equilibrium using ITC. As with NaK2CNG-D, I observed no Na^+ binding to NaK(D66N) in the presence of high concentration of K^+ ions (**Figure 18B**). In the presence of competing Na^+ ions, I observe K^+ binding demonstrating that NaK(D66N) is also selective for K^+ over Na^+ at equilibrium (**Figure 18A**). By varying the concentration of Na^+ ions, the selectivity of this channel was determined to be 56 uM for K^+ and 18 mM for Na^+ giving an equilibrium selectivity of ~300 (**Figure 18C** and **Table 3**). Ion binding to NaK(D66N) has a Hill coefficient (*n*) of 1.0±0.1, suggesting a stoichiometric exchange of K^+ and Na^+ ions within the selectivity filter.

I then determined the selectivity during ion conduction by measuring ion permeation using purified NaK(D66N) channels reconstituted into liposomes. Single-channel recordings using a vertical bilayer system were obtained with 200 mM NaCl on the outside and 100 mM KCl and 100 mM NaCl on the inside. These recordings show the channel conducts both K^+ and Na^+ ions, but Na^+ seems to conduct through the channel faster than K^+ ions (**Figure 18D).** The membrane potential was varied from 200 mV to -100 mV to determine whether the channel is K^+ selective based on its ion permeability ratio. In these conditions, a non-selective channel would reverse at zero millivolt and a K^+-selective channel would reverse at a membrane potential much less than zero. As shown in **Figure 18D**, NaK(D66N) is not K^+ selective during conduction

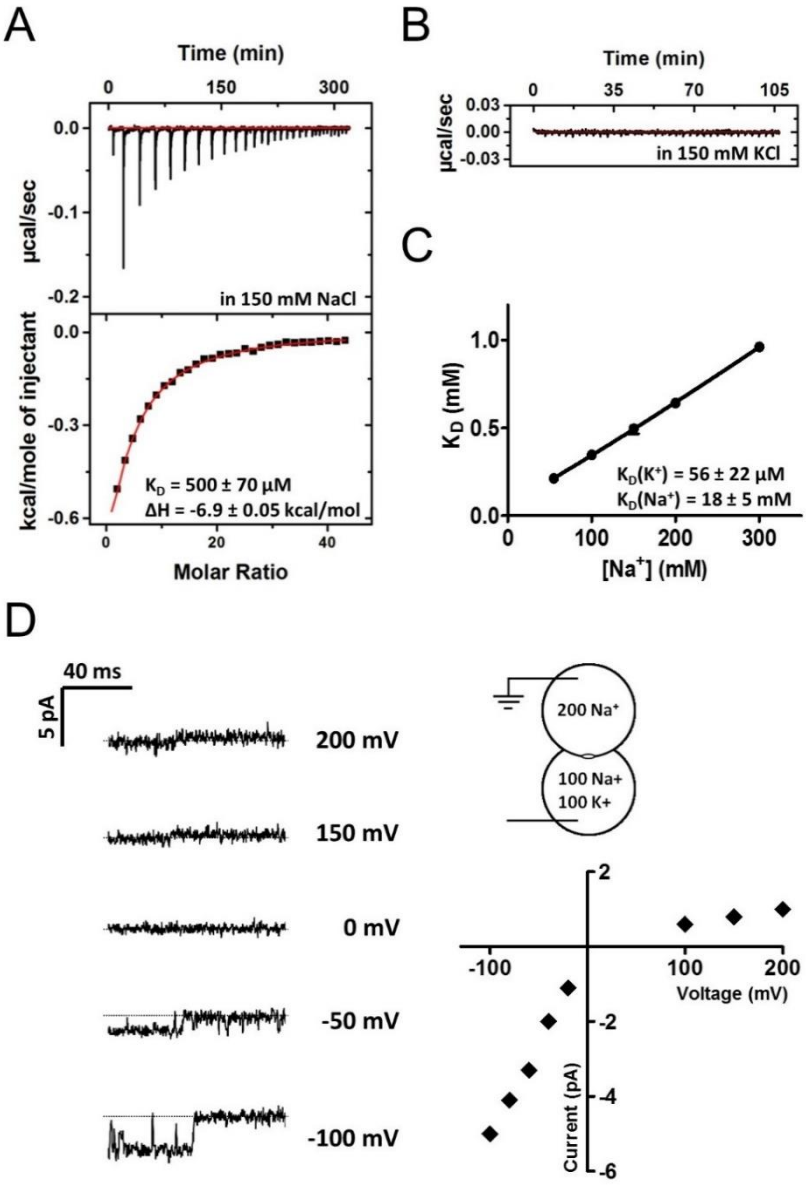

Figure 18. Ion binding and conduction of NaK(D66N) channel. (A) Thermogram of K^+ binding to NaK(D66N) in the presence of 150 mM NaCl (top). The integrated heat exchange from each injection is fit to a binding isotherm to obtain the relevant thermodynamic parameters (bottom). (B) Thermogram of Na^+ binding to NaK(D66N) in the presence of 150 mM KCl. (C) The apparent affinity of K^+ ions for NaK(D66N) as a function of NaCl concentration in solution. The line shows the fit to a competition binding equation described in the methods to obtain $K_D(K^+)$ and $K_D(Na^+)$; the average of 3 or more experiments and their s.e.m are plotted. (D) Single channel traces at different membrane potentials (left) and the I-V curve (right). Currents are recorded with 200 mM NaCl in the cup (outside) and 100 mM NaCl + 100 mM KCl in the chamber (inside). The dotted lines mark the closed, zero current level.

despite a strong K^+ selectivity at equilibrium. The small currents observed in K^+ or mixed Na^+/K^+ limit my ability to determine whether NaK(D66N) is indeed non-selective, although both sides of the I-V curve could be seen as approaching 0 mV or a positive mV. NaK(D66N) shares the same two contiguous ion binding sites as the wild-type non-selective NaK channel, suggesting that this channel is likely non-selective during ion conduction [150].

Discussion

In this study, I asked whether the selectivity of a tetrameric cation channel is mirrored in its selectivity for binding ions at equilibrium. My data show that K^+-selective and non-selective channels select K^+ over Na^+ at equilibrium, demonstrating that equilibrium selectivity is insufficient to determine the selectivity of ion permeation. The preference for K^+ in both types of channel likely originates from their nearly identical individual ion binding sites, which are known to bind K^+ ions better than Na^+ ions [56, 227]. One fundamental difference between the non-selective and K^+-selective channels is that the latter bind two or more K^+ ions, whereas the non-selective channels bind fewer ions in their filters. I hypothesize that although an equilibrium preference for K^+ is essential and is observed in all K^+-selective channels, having multiple K^+ ions bound simultaneously is required for selective K^+ conduction in K^+ channels (**Figure 19**).

What mechanism can explain the large equilibrium preference of NaK2CNGD and NaK(D66N) channels for K^+ ions while displaying non-selective ion conduction?

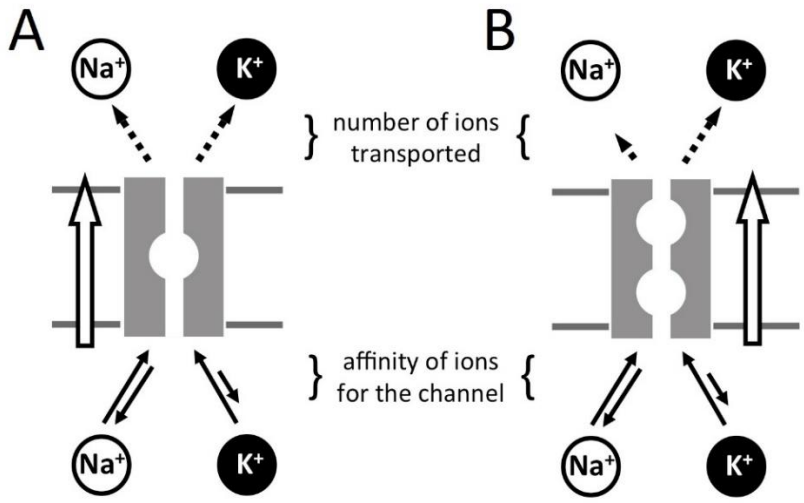

Figure 19. Schematic summary of key observations. A representation of the (A) one ion- and (B) two ion-binding models for a channel. The circles within the channel represent the ion binding sites. A membrane potential drives ions across the membrane from the inside to the outside (hollow arrows). Solid arrows indicate the rates of ion association and dissociation from the channel, which together determine the affinity (K_D). The dashed arrows are proportional to the net number of ions that cross the membrane, the ratio of which determines the selectivity during ion conduction.

The model that is most consistent with the data presented here is that non-selective conductance of the NaK(D66N) channel arises from the similar rates at which Na^+ and K^+ bind, and the equal probability that a bound ion will dissociate on the other side of the membrane. If their concentrations are equal, then the probability that Na^+ and K^+ will bind the channel is determined by their k_{on} rates; when the ion concentrations are different, the probability is determined by $k_{on}[X^+]$. A small membrane potential will bias either ion to dissociate on one side of the membrane. The different k_{off} rates for Na^+ and K^+ primarily alter how quickly an ion dissociates from the channel, not which side it will dissociate. So if the two ions have similar association rates and minimal barriers to ion

transport, the conductance ratio will be the same as the ratio of ion binding and the channel would be non-selective for K^+/Na^+ ions. The ion conduction selectivity of the NaK(D66N) channel can thus be explained simply by its high rate of conductance and the fact that it is occupied by a single ion at a time (the selective exclusion mechanism) [109].

The mechanism of K^+-channel conduction selectivity is still under debate, but it is likely the result of both equilibrium and kinetic parameters [131, 133, 140, 143, 187, 211, 231, 234, 238]. The thermodynamic nature of the studies reported here prevents us from comparing these results directly to those of kinetic experiments. In addition, these ITC-based ion-binding experiments yield no information on the specific sites that the ions interact with in the selectivity filter or on the total number of ions bound in the filter. However, electrophysiology and crystallography experiments utilizing other K^+ channels show that at least two ions interact within the selectivity filter of K^+ channels during ion conduction, suggesting that two ions likely bind within the NaK2K channel [55, 75, 81, 133]. An important difference between the non-selective and K^+-selective mutant NaK channels is their number of ion-binding sites, which determines the number of ions that simultaneously occupy the channels during ion conduction. Multi-ion queues lead to the anomalous mole-fraction effect where the higher-affinity K^+ ions effectively block the conduction of lower-affinity Na^+ ions [81, 112, 114, 239]. This phenomenon allows the sites to equilibrate to their ion preference. In K^+ channels, K^+ ions would then primarily occupy the available sites in the filter, which leads to selective ion conduction under a variety of conditions [75, 81, 82, 84-86, 133, 224]. I propose that the reduction

in the number of K^+ ions bound in the two- and three-site channels effectively destroys the multi-ion selectivity mechanism utilized by K^+ channels.

Three categories of K^+ transport systems (channels, transporters, and carriers) likely achieve their selectivity against Na^+ by slowing down the transport process such that Na^+ is able to dissociate back into solution before ion transport takes place. In ion carriers, such as K^+-selective nonactin or valinomycin, the time it takes to diffuse and enter the membrane is long enough to allow the ion-binding sites to equilibrate. In transporters, the requirement for a global conformational change slows transport rates to allow near-equilibration of the sites. The mechanism for K^+ channels is a multi-ion queue as discussed above. One possible evolutionary route from a K^+ transporter to a high-conductance K^+ channel is through mutations that allow a second K^+ ion to bind within the ion transport pathway. This simple process would retain selectivity although increasing the rate of conductance. By contrast, losing K^+-binding sites without reducing the transport rate would lead to non-selective ion conduction. This is potentially the situation with the mutant KCNJ human K^+ channel that causes severe hypertension because of its loss of K^+-selective ion binding sites [104].

CHAPTER IV

ION BINDING PROPERTIES OF A K^+ CHANNEL SELECTIVITY FILTER IN DIFFERENT CONFORMATIONS*

Introduction

K^+ channels are found in all three domains of life where they selectively conduct K^+ ions across cell membranes. Specific stimuli trigger the activation of K^+ channels, which results in a hinged movement of the inner helix bundle [51, 53, 58, 192, 214, 218, 240]. This opening on the intracellular side of the membrane initiates ion conduction across the membrane by allowing ions to enter into the channel. After a period of time, many channels spontaneously inactivate to attenuate the response [158, 168, 180, 187, 195, 204, 205, 241-243]. The inactivation process is a timer that terminates the flow of ions in the presence of an activator to help shape the response of the system. Two dominant types of inactivation have been characterized in voltage-dependent channels, N-type and C-type [244]. N-type inactivation is fast and involves an N-terminal positively charged 'ball' physically plugging the pore of the channel when the membrane is depolarized. C-type inactivation, on the other hand, is a slower process

* Reprinted with permission from "Ion binding properties of a K^+ channel selectivity filter in different conformations", by Shian Liu, Paul J. Focke, Kimberly Matulef, Xuelin Bian, Pierre Moënne-Loccoz, Francis I. Valiyaveetil and Steve W. Lockless, 2015, *Proceedings of the National Academy of Sciences*, 112:15096-15100, copyright [2015] by Liu et al. My role in the work of this chapter included experimental design, making mutants of the KcsA K^+ channel, performing ITC analysis and data analysis.

involving a conformational change in the selectivity filter that is initiated by a functional link between the intracellular gate and the selectivity filter [205, 208].

Several experimental observations indicate a role for the selectivity filter in C-type inactivation. First, mutations in and around the selectivity filter can alter the kinetics of inactivation [161, 164, 194, 245]. Second, increasing concentrations of extracellular K^+ ions decrease the rate of inactivation, as if the ions are stabilizing the conductive conformation of the channel to prevent a conformational change in the selectivity filter [164, 168, 180, 187]. Finally, a loss of selectivity of K^+ over Na^+ has been observed during the inactivation process in Shaker channels, suggesting a role for the selectivity filter [177, 246]. Together, these data indicate that channels in their inactivated and conductive conformations interact with K^+ ions differently, and suggest that C-type inactivation involves a conformational change in the selectivity filter. Although several structures of K^+ channels in their conductive state have been solved using X-ray crystallography, there is at present no universally accepted model for the C-type inactivated channel [51, 53, 59, 62, 204, 207, 208, 214, 218] (**Figure 20B**).

Inactivation in the KcsA K^+ channel has many of the same functional properties of C-type inactivation, which has made it a model to understand its structural features [194]. KcsA channels transition from their closed to open gate upon changing the intracellular pH from high to low (**Figure 20A**). The rapid flux of ions through the channel is then attenuated by channel inactivation, where most open wild-type channels are not conducting suggesting that crystal structures of open KcsA channels would reveal the inactivated channel. In some crystal structures of truncated wild type KcsA

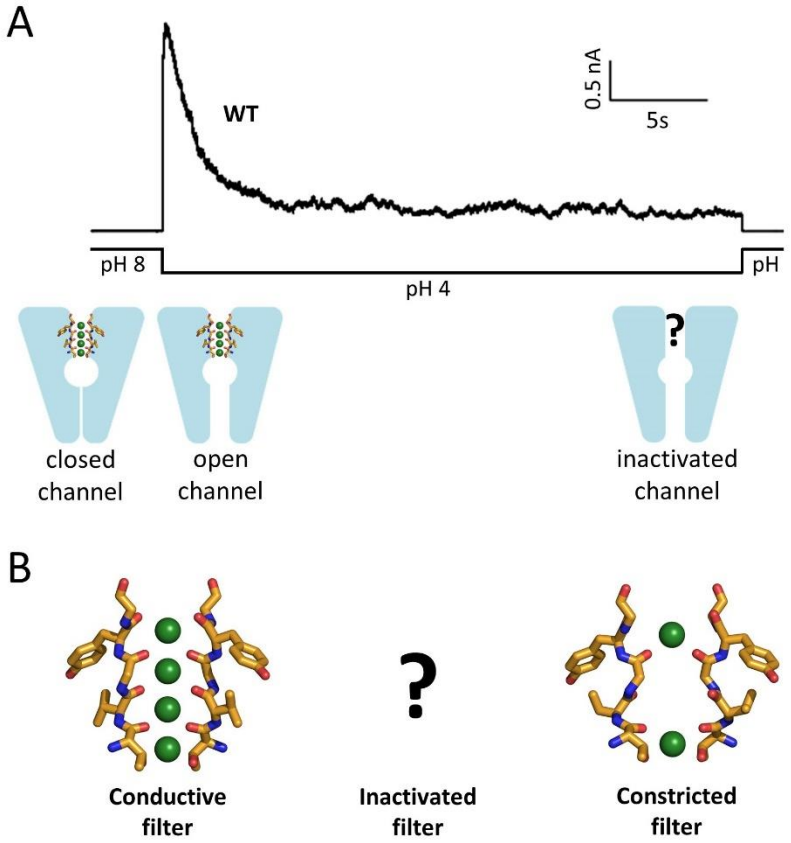

Figure 20. Macroscopic recording and structural models of KcsA K^+ channel. (A) Macroscopic currents of wild-type KcsA obtained by a pH jump from pH 8 to 4 reveals channel inactivation. Two models representing the conformation of the channel are shown below. (B) The selectivity filter of the conductive (left, pdb1K4C) and the constricted (right, pdb1K4D) conformations of the selectivity filter are shown as sticks and the ion binding sites are indicated with green spheres. The thermodynamic properties of the conductive, constricted and inactivated (middle) conformations are the subject of this study.

solved with an open gate, the selectivity filter appears in the constricted conformation, similar to the conformation observed in structures of the KcsA channel determined in the presence of only Na^+ ions or low concentrations of K^+ ions [53, 55, 111, 205] (**Figure 20B**). Solid-state and solution NMR also indicate that the selectivity filter of the KcsA

channel is in the constricted conformation when the cytoplasmic gate is open [121, 122, 247].

However, a recently published study shows that even when the constricted conformation of KcsA's selectivity filter is prevented by a non-natural amino acid substitution, the channel inactivates like wild-type channels, suggesting the constricted filter does not correspond to the functionally observed inactivation in KcsA [207]. In this study, I use isothermal titration calorimetry (ITC) to quantify the ion-binding properties of wild type and mutant KcsA K^+ channels with their selectivity filters in different conformations, and electron paramagnetic resonance (EPR) spectroscopy to determine the conformation of the channels' intracellular gates. A comparison of these ion-binding properties lead us to conclude that the conductive and inactivated filters are energetically more similar to each other than the constricted and inactivated filters.

Materials and methods

KcsA expression and purification for ITC

Wild-type and mutant KcsA channels were expressed from a pET28 vector chemically transformed into *Escherichia coli* BL21 (DE3) cells. Cultures were grown in LB media with 50 µg/ml kanamycin at 37 °C to an OD_{600} = 0.8. Protein expression was induced with 0.5 mM ITPG (isopropyl β-D-1-thiogalactopyranoside) and grown for an additional 3 hours at 37 °C. Cells were harvested at 5,000 rpm for 15 min using JA-10 rotor (Beckman Coulter) at 4 °C and then stored at -80 °C. KcsA was purified by resuspending the cell pellet in buffer containing 50 mM Tris, pH 8.0, 150 mM KCl, 10

μg/ml DNase, 50 μg/ml lysozyme and 1 mM PMSF (phenylmethylsulfonyl fluoride) followed by sonication to lyse the cells. Channels were extracted by incubating the lysate with 40 mM n-decyl-β-D-maltopyranoside (DM; Anatrace) for 3 hours at room temperature. The clarified lysate was loaded onto Ni-NTA resin (QIAGEN), washed and eluted using 400 mM imidazole.

To obtain full-length KcsA channels, the His-tag was cleaved with thrombin (Sigma-Aldrich) at 0.8 U/mg of KcsA for 4-5 hours at room temperature. The pore region of the protein (including KcsA-ΔC, OM1, OM2, E71C used for ITC and M96V) was generated by incubating the channels with chymotrypsin (Sigma-Aldrich) at 0.3 mg/mg of KcsA for 2 hours at room temperature. Protein was further purified on a Superdex 200 column (GE Healthcare) pre-equilibrated with buffer containing 50 mM Tris, pH 8.0, 5 mM DM and the appropriate concentrations of NaCl and KCl. The protein concentration was determined by absorbance at 280 nm prior to experiments.

Isothermal titration calorimetry and data analysis

ITC experiments were performed and the data analyzed as previously described [234, 248]. Briefly, the reported ion binding reactions were performed using a MicroCal iTC_{200} (Malvern Instruments) at 25 °C with a string speed of 700 rpm in the high gain mode. The ITC chamber was filled with concentrated KcsA protein (37-260 μM, depending on the experiment) in buffer with 50 mM Tris (pH 8.0) and 5 mM DM with desired concentration of NaCl and/or NMG (N-methyl-D-glucamine; Sigma-Aldrich). The injector syringe was loaded with a buffer matching the chamber plus either KCl or

RbCl as the ligand. Following data collection, the resulting thermograms were analyzed by integrating the heat exchange after ligand injection into the chamber, and the background heat of dilution was determined. Because the heat change is from both ligand dilution and binding, control experiments without protein were done to ensure the heat of dilution was constant in the range of NaCl concentrations used. The heat of dilution was subtracted from each injection from an experiment.

The resulting isotherm was fit in Origin (Malvern Instruments) to a one-site binding model to obtain the enthalpy (H) and apparent association constant (K) with N fixed to 1; note that the apparent K_D reported throughout the main text is obtained by the relationship $K_D = 1 / K$. Although K^+ channels bind to multiple ions in the selectivity filter at a time, I fit the ion-binding thermograms to a model that assumes one ion binds to the channel because more complicated models did not statistically improve the fit to the experimental data [234, 248]. Three plausible scenarios could explain this observation: (i) the ion-binding sites have nearly equal binding constants (within 10-fold of each other) with very little electrostatic repulsion between them; (ii) with no K^+ ions bound in the filter, the sites have nearly equal binding constants and binding of the first ion increases the K_D of subsequent binding events enough to not be detectable using ITC; or (iii) one ion binds to a specific site and the other sites are not discernable in our studies (a K_D in the middle millimolar range). I suspect that the second scenario is the most likely, based on crystallographic data on KcsA, MthK, and NaK2K that show an increase of electron density is observed in multiple sites within the filter as the concentration of K^+ (or Tl^+) ions is increased [55, 90, 236], yet channels are able to

conduct ions at rates approaching the diffusion limit, which implies weak ion binding in a fully occupied selectivity filter. Additionally, in cases where the K_D values are greater than ~10 μM, only the binding constant can be reliably fit because there is an inherent correlation between ΔH and N that results from the lack of unique features in the binding isotherm [249]. I chose to fix N to 1 so that ΔH would represent the enthalpy change of the whole reaction.

All isotherms were fit to minimize $\chi 2$, which has no comparative value between experiments because the number of data points for each isotherm is no necessarily the same. Only one set of parameters was found for ΔH and K_D when the fitting process was initialized with different values. The errors of the parameters were < 7% for K and < 3% for ΔH for all experiments, demonstrating that the experimental data are well constrained by the binding isotherms.

The ion binding affinity in the absence of competing ions was determined by measuring the apparent K_D at different NaCl concentrations and then fitting those values in Prism (GraphPad Software) to the following competition function:

$$1/K_D = \frac{1/K_D^{X+}}{1 + [Na^+]^n \cdot 1/K_D^{Na+}}$$

where K_D is the experimentally determined apparent dissociation constant, K_D^{X+} (where $X^+ = K^+$ or Rb^+) and K_D^{Na+} are the dissociation constants for the ligand with no competing ligand, and *n* is the Hill coefficient. The errors of the fits are reported in Table 4.

Reconstitution and electrophysiology measurements

KcsA channels were purified and reconstituted into vesicles composed of soybean polar lipids as described [250]. For the reconstitution, the lipids in chloroform were dried under argon, desiccated to remove residual chloroform and then resuspended at 5 mg/mL in rehydration buffer [200 mM KCl, 5 mM MOPS pH 7.0, 2 mM tris-(2-carboxyethyl)-phosphine (TCEP)]. After 30 min at room temperature, lipids were subjected to 10 freeze-thaw cycles, followed by sonication in a bath sonicator. The lipid vesicles were solubilized by the addition of n-dodecyl β-D-maltoside (DDM) to 4 mM and gentle rotation at room temperature for 30 minutes. Purified KcsA was added at protein: lipid ratios varying from 1:40 to 1:200 and incubated at room temperature for 1-4 hours. The detergent was then removed using Bio-Beads SM2 (Biorad). Following detergent removal, the vesicles obtained were collected by centrifugation, resuspended in reconstitution buffer at ~50 mg/mL of lipid and flash-frozen in aliquots.

For patch clamp recordings, the frozen vesicles were dried onto a clean glass coverslip for 12-36 hrs at 4 °C. The dried vesicles were rehydrated in 200 mM KCl, 10 mM MOPS pH 7.0 for either 2 hours at room temperature or overnight at 18 °C. Blisters were formed by adding rehydrated vesicles into bath solution containing 200 mM KCl, 40 mM $MgCl_2$, 0.5 mM $CaCl_2$, 10 mM MOPS pH 7.0. KcsA channel currents were measured using inside-out patches with 200 mM KCl, 10 mM MOPS, 0.5 mM CaCl2 pH 7.0 in the pipette. KcsA channel currents were elicited by a pH jump of the bath solution from pH 8.0 to pH 4.0 using an RSC-160 rapid solution exchanger (Biologic). The pH 4.0 and 8.0 solutions contained 10 mM MOPS, 200 mM KCl.

EPR spectroscopy

KcsA channels with the G116C substitution were labeled with the spin probe (1-oxyl-2,2,5,5-tetramethylpyrrolidin-3-yl) methyl methanethiosulfonate (Toronto Research) at a 20: 1 probe to channel ratio, overnight at 4 °C. Following labeling, the unreacted spin probe was removed using size exclusion chromatography on a Superdex S200 column in 20 mM HEPES-KOH, 150 mM KCl, 0.25% (w/v) n-decyl β-D-maltoside (DM). For measurements in lipid vesicles, the spin-labeled channels were reconstituted into soybean polar lipids vesicles at a protein to lipid ratio of 1:500 by dialysis as previously described [251].

Continuous wave EPR spectra was obtained at room temperature on a Bruker E500 X band spectrometer equipped with a dielectric resonator using the following parameters: microwave frequency 9.82 GHz, modulation frequency 100 kHz, incident power 2 mW and modulation amplitude 1 G. EPR spectra were collected at pH 7.5 in 20 mM HEPES-KOH, 150 mM KCl and at pH 3.5 in 15 mM citrate-phosphate, 150 mM KCl.

Results

Ion binding to open KcsA channels

Electrophysiology experiments demonstrate that KcsA is closed at pH 8 and that shifting the intracellular pH to 4 opens intracellular gate of the channel [48, 146]. These open channels then inactivate reaching a current level that is ≤10% of the maximum, suggesting that most channels with an open intracellular gate are inactivated at

equilibrium [194] (**Figure 20A&B**). To measure the ion-binding properties of open channels, I initially examined two C-terminally truncated KcsA channels containing

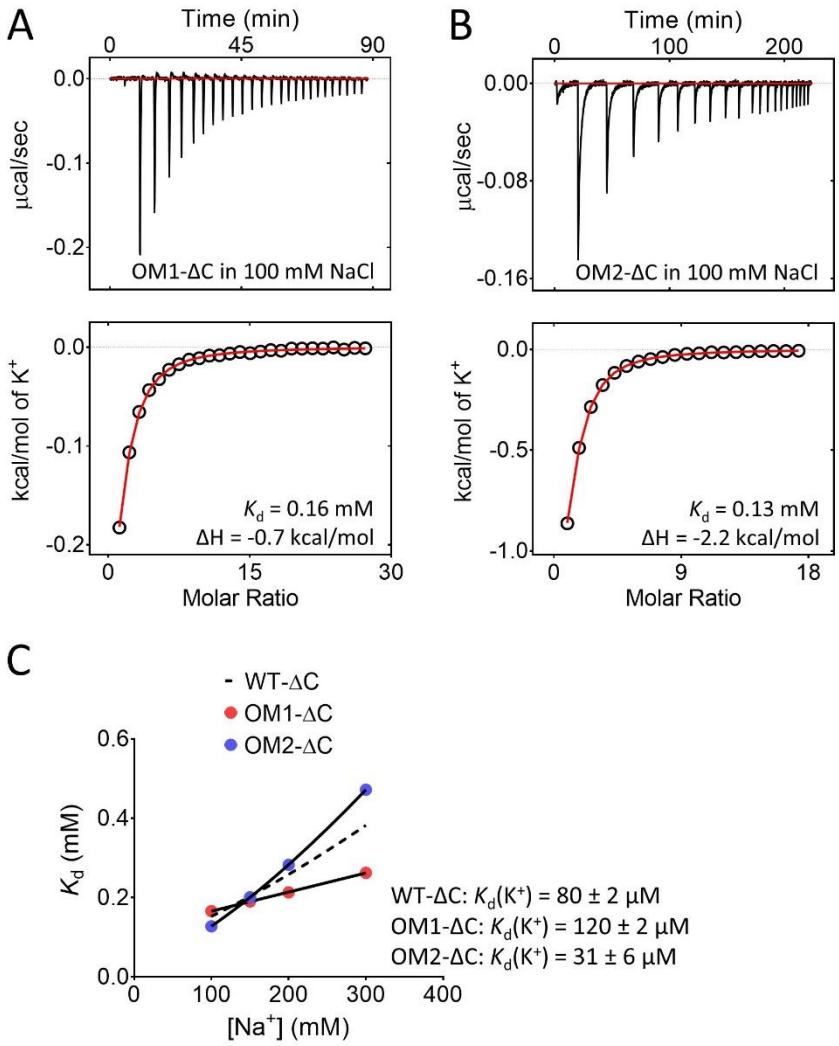

Figure 21. Ion binding to wild type and mutant KcsA channels measured at pH 8. (A and B) (top) Thermograms of OM1 (H25R-E118A-E120A) (A) and OM2 (H25Q-E118+) (B) titrated with KCl in the presence of 100mM NaCl. (bottom) The integrated heat from each injection is fit to a single ion-binding function to obtain the apparent binding affinity. (C) The apparent K^+ affinities are plotted as a function of Na^+ concentration in the ITC chamber, which are fit to a competition function to obtain $K_D(K^+)$. The mean and s.d. of three or more experiments are shown.

mutations H25R-E118A-E120A (OM1-ΔC) or H25Q-E118+ (OM2-ΔC) that are open at pH 8 in the lipid bilayer [252, 253]. The ITC experiment consisted of titrating a solution containing K^+ ions into an ITC chamber with appropriate KcsA channels solubilized in *n*-decyl-β-D-maltopyranoside (DM) micelles and 100 mM NaCl at pH 8 (**Figure 21A&B**). The integrated heat change from each injection was fit to a binding isotherm to reveal apparent K_D values of 0.16 mM and 0.13 mM for OM1-ΔC and OM2-ΔC, respectively, which is similar to the apparent K_D for WT-ΔC of 0.15 mM [234]. Since these apparent K_D values reflect the competition between Na^+ and K^+ in the chamber, I varied the concentration of Na^+ ions in the chamber to obtain the K^+ ion affinity in the absence of Na^+ ions [111, 234, 248]. The apparent K_D values were then fit to a competition equation to obtain $K_D(K^+)$ (**Figure 21C)**, which are similar for the three channels (**Table 4**). This was unexpected since the cytoplasmic gate in the OM1-ΔC and OM2-ΔC channels is presumably open at pH 8, which presumably puts their selectivity filters in the inactivated conformation while the cytoplasmic gate in the WT-ΔC channels is presumably closed with their selectivity filters in the conductive

channel	pH	$K_D(X^+)$ (μM)		$K_D(Na^+)$ (mM)	n
WT-ΔC	4	Rb^+	51 ± 2	14 ± 4	1
OM1 (H25R-E118A-E120A) -ΔC	8	K^+	120 ± 2	250 ± 10	1
OM2 (H25Q-E118+)-ΔC	8	K^+	31 ± 6	13 ± 2	1.4 ± 0.03
E71C-ΔC	8	K^+	83 ± 5	13 ± 1	2.6 ± 0.1
M96V-ΔC	8	K^+	350 ± 40	0.48 ± 0.16	1.6 ± 0.1
R64A-ΔC	8	K^+	54 ± 9	17 ± 2	1.4 ± 0.1
WT-FL	8	K^+	67 ± 4	9 ± 1	1

Table 4. Thermodynamic parameters for ion competition in KcsA channels

channels is presumably closed with their selectivity filters in the conductive conformation. The similar $K_D(K^+)$s for these channels suggests that ITC is insensitive to changes in the inactivated and conductive filter conformations or that the intracellular gates are in different conformations in the electrophysiological studies (in lipid bilayers) and ITC measurements (in detergent).

Different conformations of KcsA's intracellular gate in detergent and lipid bilayers

I used EPR spectroscopy to determine the state of the intracellular gate of wild type and mutant KcsA channels under the conditions of the ITC experiment. The KcsA channels were labeled with a spin probe near the bottom of TM2 (using a Cys substitution at G116) that has been previously used to determine the state of the intracellular gate [154, 155, 194] (**Figure 22A**). The resulting spectra show that full-length wild type KcsA (WT-FL) is closed in liposomes at pH 7.5 and open at pH 3.5, consistent with previously published experiments (**Figure 22A**) [192]. Similar to full-length KcsA, WT-ΔC in liposomes is also closed at pH 7.5 and open at pH 3.5 (**Figure 22B**). Unexpectedly I found that WT-ΔC in DM detergent at pH 7.5 showed an EPR spectrum closer to an open rather than a closed intracellular gate (**Figure 22C**); replacing the lipid membrane around WT-ΔC channels with DM detergent appears to shift the equilibrium of the intracellular gate to favor the open conformation. Not surprisingly, the EPR spectra of the OM1-ΔC and OM2-ΔC channels both show that the intracellular gate is open in DM detergent at pH 7.5 (**Figure 22C**). The similar

conformation of the intracellular gate of the WT-ΔC, OM1-ΔC, and OM2-ΔC channels can explain the similar behavior of these channels in ion-binding experiments.

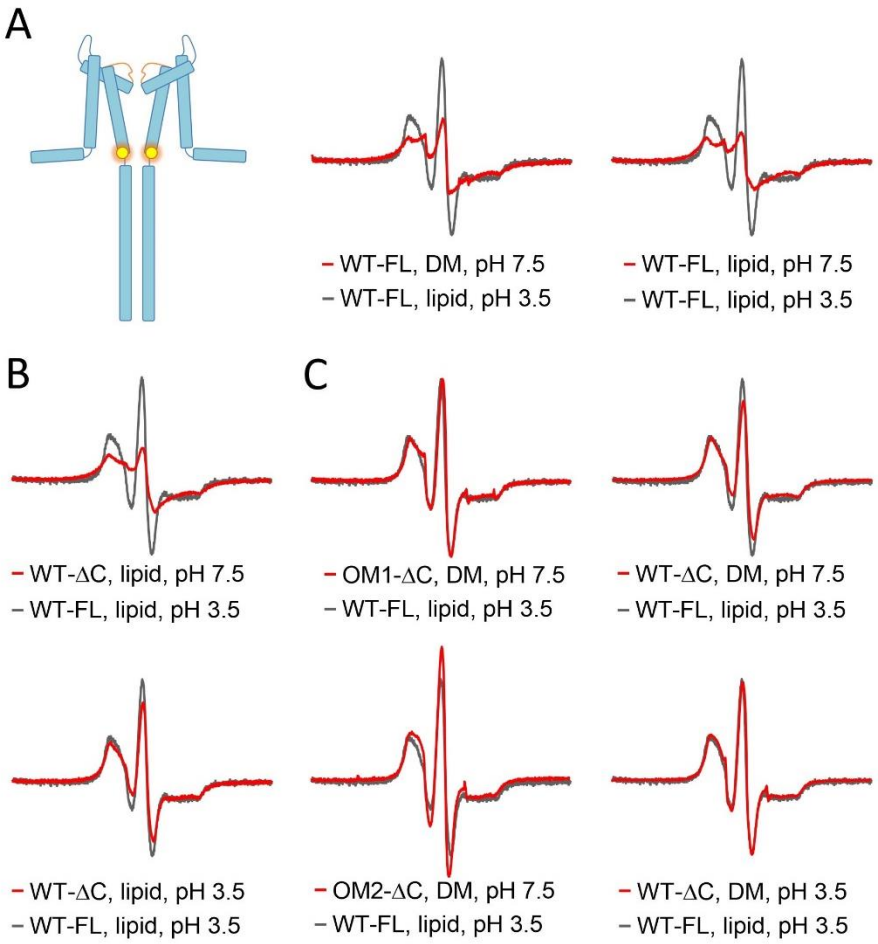

Figure 22. CW-EPR spectra of KcsA channels. Spin-labeled spectra of KcsA-ΔC (A), OM1 (B) and OM2 (C) obtained in DM detergent at pH 7.5 are compared to full-length wild-type channel in lipids at pH 7.5 and 3.5. (D) Spin-labeled spectra of KcsA-ΔC in lipid vesicles is compared at between pH 3.5 and pH 7.5. Spin labels were attached to the gating-sensitive G116 position of the channels.

Ion binding to KcsA channels with conductive or partially conductive selectivity filters

I used two different approaches to measure ion binding to KcsA channels with selectivity filters in the conductive or partially conductive conformations. First, as was shown previously, both E71C-FL and R64A-FL channels have reduced inactivation in electrophysiology experiments (**Figure 23A&F** and **Table 5**), and therefore, their selectivity filters are in a mixture of conductive and inactivated conformations when the intracellular gate is open [194, 195]. Because C-terminally truncated KcsA channels are open in detergent at pH 8 (**Figure 22**), I expect ITC measurements are of ΔC channels to have a mixture of conductive and inactivated selectivity filters. K^+ ion binding to E71C-ΔC mutant channel in 100 mM NaCl has an apparent K_D = 0.10 mM (**Figure 23B**). The $K_D(K^+)$ was determined by measuring the apparent K^+ affinity at different Na^+ concentrations in the ITC chamber, to yield a dissociation constant of 83 μM (**Figure 23D**). The $K_D(K^+)$ was similar for R64A-ΔC with a value of 54 μM (**Figure 23H**).

Channel	$\tau_{inactivation}$, ms	I / I_o
WT	2,100 ± 550 (4)	0.12 ± 0.04 (4)
E71C	8,200 ± 4,600 (5)	0.58 ± 0.13 (5)
R64A	3,800 ± 1,300 (10)	0.57 ± 0.12 (10)

Table 5. Electrophysiology parameters for wild-type and mutant channels. I / I_o: the ratio of current at the end of the pH pulse to the peak current

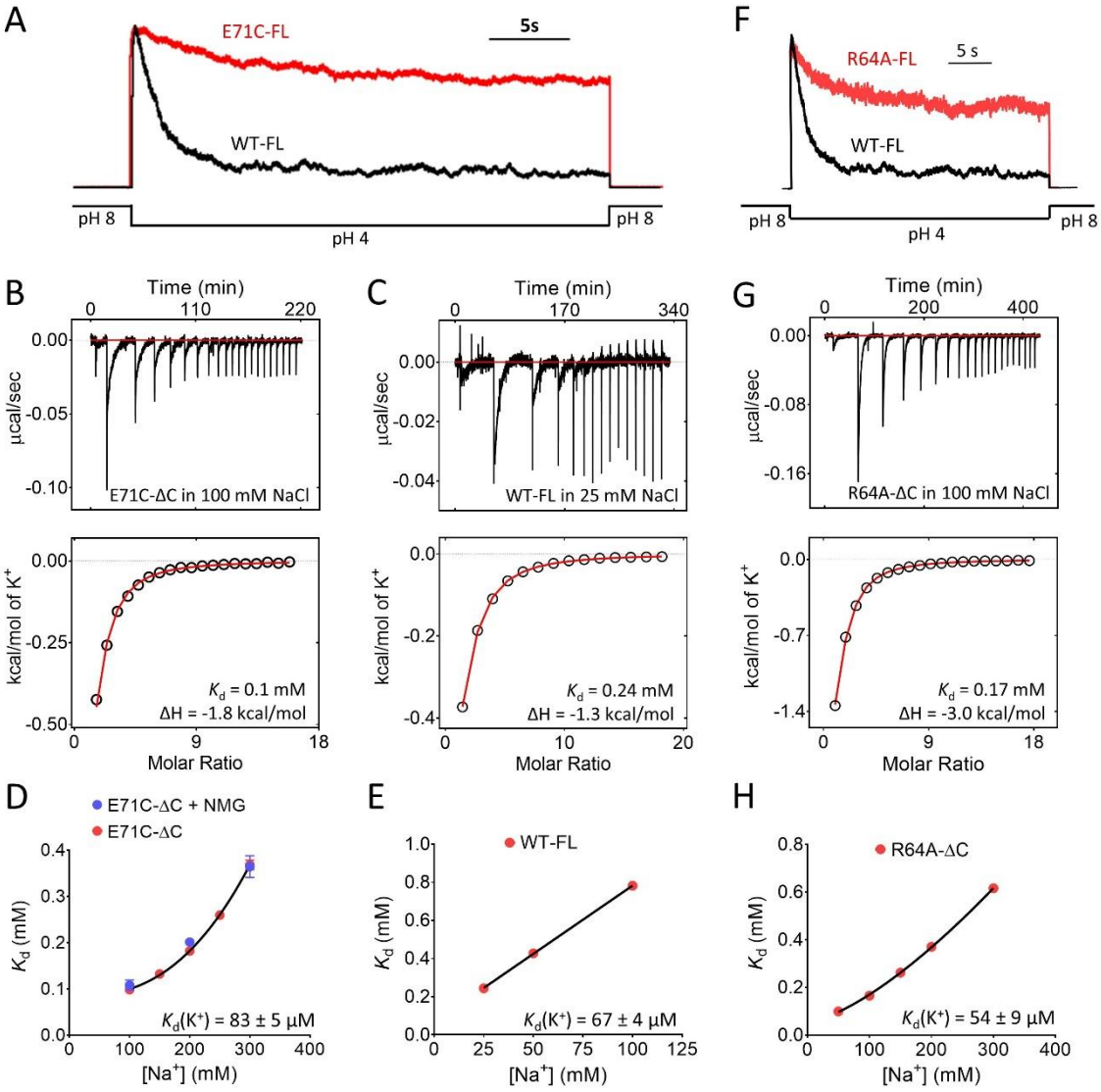

Figure 23. Ion binding to KcsA channels in their conductive conformation. (A and F) Macroscopic currents of WT, E71C and R64A mutant KcsA obtained by a pH jump from pH 8 to pH 4 reveal different degrees of inactivation. The current traces were normalized to the peak current. (B, C and G) (top) Thermogram of E71C-ΔC, WT-FL and R64A-ΔC with KCl in the presence of 100 mM NaCl at pH 8. (bottom) The integrated heat from each injection is fit to single ion-binding function to obtain the apparent binding affinity. (D, E and H) The apparent affinities determined from isotherms are plotted as a function of Na^+ concentration, which are fit to a competition function to obtain $K_D(K^+)$. The mean and s.d. of three or more experiments are shown. The effect of ionic strength on K^+ binding to E71C-ΔC is evaluated by adding NMG^+ to maintain a total ionic strength ([NaCl] + [NMGCl]) of 300 mM. The mean of three or more experiments and their s.d. are shown.

The second approach that was used to obtain channels in their conductive conformation is predicated on the EPR result (**Figure 22**) that full-length KcsA in lipid membranes and detergent are both closed at pH 8. Because crystal structures of closed KcsA have a conductive filter in K^+ solutions, the selectivity filter of the full-length KcsA in detergent should also be in its conductive conformation [51, 53, 192]. K^+ ion binding to full-length KcsA at various concentrations of Na^+ ions in solution yielded a dissociation constant of 67 μM (**Figure 23E**), close to the E71C-ΔC and R64A-ΔC mutant channels' K^+ affinities. Using these two approaches, I find that KcsA channels with a conductive or partially conductive filters have $K_D(K^+)$s that are very similar to one another (**Table 5**).

Ion binding to mutant channels with constricted filters

I next compared the K^+ ion-binding properties of the constricted filter which was previously proposed to be the structure of an inactivated filter. Two approaches were used to trap and quantify K^+ dissociation constant of a constricted filter. First, I determined the $K_D(K^+)$ of the M96V-ΔC mutant channel that was shown to remain in the constricted conformation even at high $[K^+]$ in the crystal (**Figure 24D**) [111]. The apparent K_D for ion binding to the M96V-ΔC channel is much higher than other channels under the same conditions, so the concentration of competing NaCl was lowered to reliably capture ion binding. The apparent K_D values were fit to a competition equation to reveal a 350 μM affinity, which is significantly lower than the inactivated wild type channel **(Figure 24A&E**).

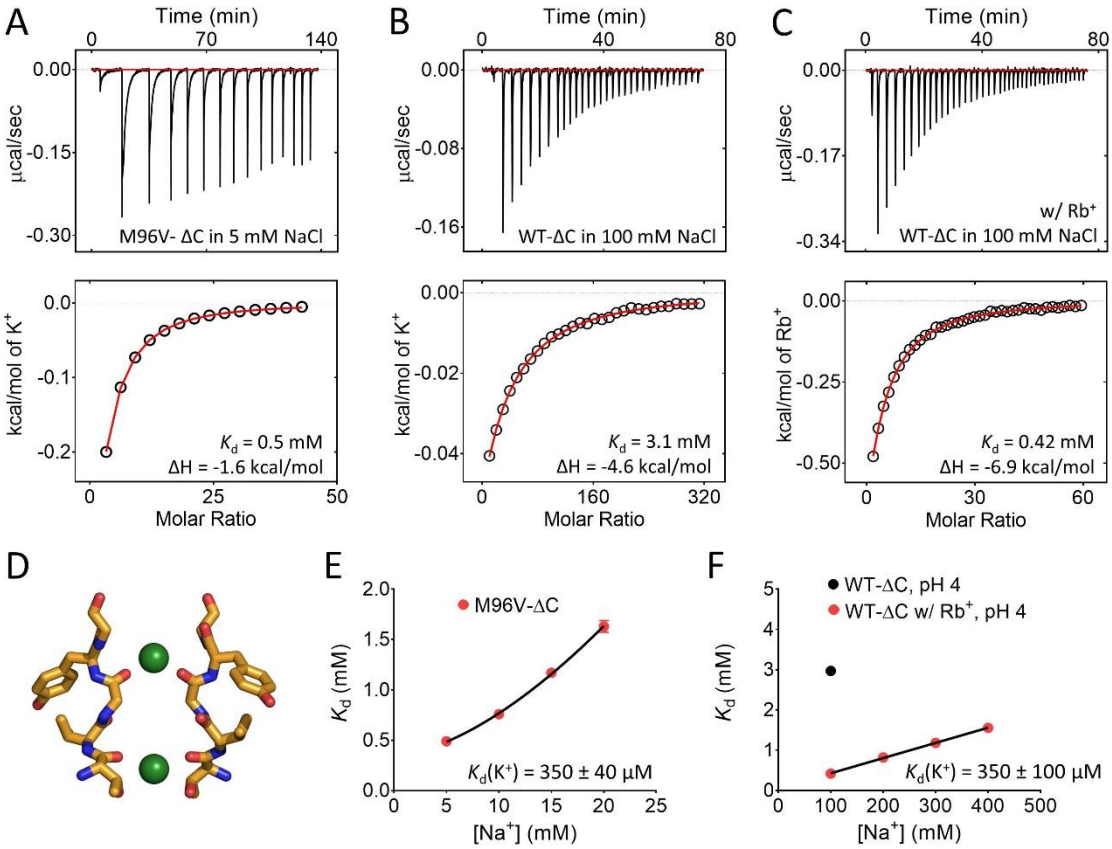

Figure 24. Ion binding to KcsA channels with a constricted filter. (A, B and C) (top) Thermogram of M96V-ΔC titrated with KCl in the presence of 5 mM NaCl at pH 8, WT-ΔC titrated with KCl or RCl in presence of 100 mM NaCl at pH 4. (bottom) The integrated heat from each injection is fit to single ion-binding function to obtain the apparent binding affinity. (D) The selectivity filter of the M96V mutant KcsA channel in a constricted conformation (pdb2NLJ). (E and F) The apparent ion affinities determined from isotherms are plotted as a function of Na^+ concentration, which are fit to a competition function to obtain $K_D(K^+)$ and $K_D(Rb^+)$. The mean and s.d. of three or more experiments are shown.

Second, the K^+ affinity was measured in WT-ΔC channels at pH 4, where channels are in their constricted conformation [121, 122, 204]. A fit to the integrated heat from the thermogram reveals an apparent K_D = 3.1 mM in 100 mM NaCl, which is

significantly lower than the apparent K^+ affinity of WT-ΔC at pH 8 (K_D = 0.15 mM) (**Figure 24B, C&E**). However, the low affinity of this reaction reduced the reliability of the apparent K_Ds determined at higher Na^+ concentrations used to determine the $K_D(K^+)$. Therefore, I took an alternative approach to obtain $K_D(Na^+)$, which could then be used to calculate $K_D(K^+)$ from the apparent $K_D(K^+)$. Rb^+ ions are similar to K^+ ions in size, charge density, occupancy in KcsA's selectivity filter and permeability through KcsA K^+ channels . I found that Rb^+ binds to KcsA at pH 4 with a higher affinity (K_D = 0.42 mM) than K^+ ions (**Figure 24C**), allowing us to obtain $K_D(Rb^+)$ and $K_D(Na^+)$ by measuring the apparent affinity over a range of concentration of Na^+ ions (**Figure 24E**). Since both the K^+ binding and the Rb^+ binding reactions begin from the same Na^+ bound protein, the value of $K_D(Na^+)$ was used to calculate $K_D(K^+)$ = 350 ± 100 μM from the apparent K^+ dissociation constant of 3.1 mM measured in 100 mM NaCl.

The significant difference in the K+ ion-binding properties of the constricted filter determined using two different approaches and the filter of inactivated WT-ΔC channels suggest that the conformations of the selectivity filters of these channels are distinct from one another. By comparison, the K^+ affinity ($K_D(K^+)$) for channels in the inactivated and conductive conformations are similar to one another (**Figure 25** and **Table 4)**.

Discussion

C-type inactivation in voltage-dependent K^+ channels and desensitization in ligand-dependent channels are important physiological processes that arrest the flow of

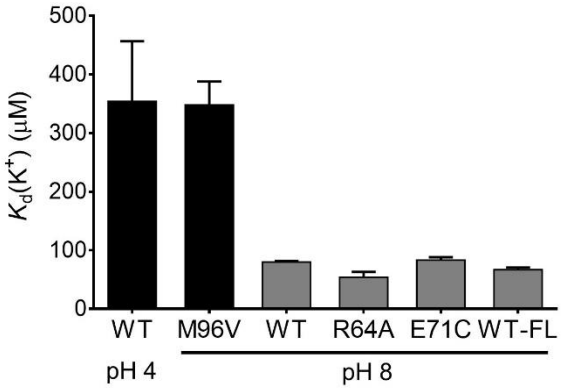

Figure 25. Comparison of $K_D(K^+)$ obtained from KcsA channels in detergent micelles. The channels are grouped by the likely conformation of their selectivity filter based on a combination of crystal structures of the channel, the functional state of the channel in electrophysiology experiments, and EPR measurements of the intracellular gate. Black bars are channels with a constricted filter, and gray bars are channels with either a conductive or inactivated filter. Channels are C-terminally truncated, except WT-FL.

ions while the channel gate is open. The KcsA K^+ channel inactivates with many of the characteristics of C-type inactivation in K_V channels, and so it has become a model system to study this process [194]. While many different approaches have been employed to trap and characterize the structure of the selectivity filter of an inactivated channel, there is still considerable debate on whether the constricted filter first observed in low $[K^+]$ is the structure of an inactivated filter characterized by electrophysiology [53, 121, 122, 205, 207, 208, 247]. Here, I measured the ion-binding properties of open KcsA channels with their selectivity filters either in the conductive, constricted, or inactivated states to ask which conformations, from a thermodynamic point-of-view, are most similar to one another (**Figure 20** and **Figure 25**).

Although several structures of conductive and constricted filters are known, the conformation of an inactivated filter is still unknown. The equilibrium K^+ binding

constants reported here can be classified into two groups (**Figure 25**). The first group has high K_D values and is likely in a constricted conformation based on crystal structures. Channels in the second group have either a conductive filter (WT-FL), an inactivated filter (WT-ΔC) or are a combination of both (E71A-ΔC and R64A-ΔC). A structural interpretation of the different binding constants is challenging because of both the classic issue with interpreting mechanisms from thermodynamic data and the binding isotherms fitting well to a single-ion process when the selectivity filter is a known multiple ion-queue. This discrepancy suggests that either one ion binding event in the selectivity filter has a very low K_D, such that I am primarily observing this signal in our measurements, or that multiple ion binding sites have similar affinities across the filter that are not discrete events at the resolution of our experiments. The similar K^+ binding constant between the inactivated and conductive filters suggest that there are either no structural or energetic change in the highest affinity K^+ binding site or that the change is significantly small that the average binding constants across the filter is similar. By contrast, the different K^+ K_D from the two groups suggest that one or more K^+ ion binding sites in the constricted and inactivated filters are significantly different, from which I conclude that the constricted and inactivated filters are structurally not the same.

Previously published structural and functional data support our conclusion that the constricted conformation of the selectivity filter in KcsA is not the inactivated conformation. First, the selectivity filter in structures of open K^+ channels (K_VAP, MthK, K_V1.2 and $K_V$chimera) are all found in their conductive conformation, but should be in an inactivated conformation given the state of their intracellular gate [57-59, 214].

Second, if the constricted conformation in KcsA is the inactivated state, then structures of other K^+ channels in Na^+ should adopt a constricted conformation. The high-resolution structure of MthK in Na^+ alone is in a conductive conformation, which superimposes well onto the K^+ bound structure [90]. Finally, the D-alanine mutation at G77 in KcsA prevents the channel from adopting a constricted conformation, but this channel has the same inactivation properties as wild-type channels [207].

However, the constricted conformation is observed in crystal structures of open KcsA channels obtained through deep truncations. The crystallography and spectroscopy measurements suggest a correlation between the magnitude of channel opening and the conformation of the selectivity filter [204, 247]. The largest opening corresponds to a constricted conformation, while a less open channel (but one open enough to pass ions) corresponds to the conductive conformation. KcsA in detergent is able to open more than KcsA in lipid bilayers, suggesting that the gating-induced constricted filter may lie outside of the spectrum of conformations adopted during typical electrophysiology experiments including channel inactivation [247].

If the constricted conformation is not the inactivated structure, as our data suggest, then the structure of an inactivated channel is still not known. Elucidating the structural changes in the selectivity filter during inactivation may be challenging. Inactivation could involve an asymmetric conformational change in the selectivity filter, whose signal might be averaged out in crystallographic and spectroscopic studies. Additionally, small changes in the selectivity filter may be sufficient to erect a barrier for

ions rapidly crossing the membrane. These changes may be difficult to discern even in high-resolution crystal structures.

During the course of this study, I discovered that WT-ΔC is open at pH 8 in detergent but closed in lipid vesicles. The expectation from crystal structures and electrophysiology experiments was that the channel would be closed, leading us to conclude that crystallization conditions or the presence of the lipid bilayer can shift the equilibrium of the intracellular gate. The influence of the lipid bilayer is not unexpected, since lipids are known to be critical in the purification, crystallization and function of some membrane proteins, presumably by stabilizing specific conformations of the protein [58, 251, 254-258]. However, crystal structure of KcsA were all solved in detergent, so why were the channels not in an open conformation? One possible explanation is that the crystal contacts inhibited their ability to open [252]. The crystal structure of the deep truncations eliminated direct contacts with neighboring molecules, resulting in some open channels [205]. This study further highlights the need to compare the functional and structural properties of membrane proteins in detergent and lipid membranes to understand how a protein's local environment influences its function.

CHAPTER V

CONCLUSIONS

Summary

The goal of this work was to investigate two important properties of K^+ channels: K^+/Na^+ selectivity and C-type inactivation. K^+ channels are known for their highly selective conduction during action potentials in excitable tissues, so a reduction or loss of selectivity affects the propagation of electrical signals and may lead to death. Many years of research have gone into understanding how K^+ channels achieve the ion selectivity. Two decades ago, it was found that the highly conserved sequence, TVGYG, forms a selectivity filter, from which the K^+/Na^+ discrimination originates [42, 43]. A prevailing model based on the anomalous mole fraction effect from several types of K^+ channels suggests that the conduction selectivity stems from two or more K^+-selective sites in the pore domain [85-91, 259]. Consistent with this functional observation, crystal structures of K^+ channels revealed a queue of four K^+ sites inside the selectivity filter [51, 53, 55, 57-60, 62, 63, 68, 214]. Therefore, it had been assumed that achieving conduction selectivity requires multiple K^+-selective sites inside the filter. However, this widely accepted model was challenged by a recent study that showed CNG mimic channels contain three K^+ binding sites, but lacked ion selectivity during conduction [150].

C-type inactivation is the second functional property of K^+ channels investigated in my dissertation. The structure of a C-type inactivated channel has remained

enigmatic. Initially, several lines of evidence suggested that the C-type inactivation involves a conformational change at the outer mouth of the pore domain [161, 162]. Interestingly, the crystal structures of the closed KcsA channels illustrated a K^+ occupancy dependent conformational change of the selectivity filter, while the same change was found to be coupled with gating in a series of open KcsA structures [53, 204, 205]. It was therefore hypothesized that the constricted conformation of the selectivity filter corresponds to the inactivated state during ion conduction. Recently, this idea was challenged by a study that showed a chemically engineered channel prohibits the constricted conformation due to the steric effect, but it is still able to inactivate like the wild-type channel [201]. Immediately, the old question was raised again: What does the inactivated conformation look like?

In order to tackle both problems, the primary approach utilized in this work was to obtain the thermodynamic properties of ion binding to channels, since both the ion selectivity and inactivation occur at the filter. Specifically, isothermal titration calorimetry (ITC) was applied to measure the heat change from ion binding, where ΔH and K are obtained. There were several advantages to using ITC. First, it does not require labeling or secondary molecules that other approaches do. Second, it captures protein properties in aqueous solutions at desired temperatures, which is usually compromised in many other approaches. Third, due to the small sample volume used in the iTC200 machine, the experiment becomes less constrained by the protein yield compared to NMR spectroscopy. Finally, using the apparent binding affinities, I have been able to extrapolate the $K_D(K^+)$ and $K_D(Na^+)$ to the empty channels, so the ion

selectivity in the ratio of $K_D(K^+)$ and $K_D(Na^+)$ can be easily calculated. These affinities can also report the states of the channel with certain ions associated.

ITC was useful in the examination of the origin of ion conduction selectivity. It was recently found that the K^+ channel-mimic, NaK2K, is selective for K^+ ions during conduction, probably because the overall architecture of its selectivity filter resembles that of a K^+ channel with a queue of four K^+ binding sites. However, eliminating either the outermost site or innermost site renders a complete loss of NaK2K's selectivity during conduction [150]. In past studies, the fact that K^+ channels preferentially conduct K^+ ions over Na^+ ions is explained by their high equilibrium selectivity, so non-selective conduction would mean a loss of equilibrium selectivity as well. Another possibility is that only the four-site filter can provide a blocking effect or flux coupling (See Chaptor Four) required for K^+ channels to achieve selective conduction, which is abolished in three-site despite each site being K^+ selective at equilibrium. To test the two possibilities, the equilibrium selectivity of channels with different binding sites was obtained using ITC, and all showed high selectivity for K^+ ions. The fact that the equilibrium selectivity does not correlate with the conduction selectivity shows that the flux coupling is a critical factor indeed for selective conduction.

Clues of the fluxing coupling were discovered long before any structures of K^+ channels were solved. As mentioned, the anomalous mole fraction effect implies that the pore of a K^+ channel comprises multiple interacting K^+-selective sites, which ties in with all the known characteristics of K^+ channels. Using this kinetic model based on flux coupling, it is not hard to imagine that the kinetic interaction exists only if a residing K^+

ion blocks its adjacent site so that another K^+ ion, rather than Na^+ ion, will be preferentially bound based on its equilibrium preference (**Figure 19**). In other words, if K^+ ions leave the filter at diffusion-limited rates, the blocking effect will disappear. It should be noted that although usually described as diffusion limited, the conductance of K^+ channels is a voltage- and concentration- dependent term that varies in a large range, suggesting that the conduction selectivity is not constant for any given channels. Interestingly, the conductance of BK channels is able to approach the theoretical ceiling, the rate of diffusion of an ion to the entrance of the channel, so whether BK channels have compromised selectivity at their maximum conduction still needs to be tested (see future direction).

My approach using ITC was also advantageous toward differentiating states of the KcsA K^+ channel. As introduced earlier, one of the unsettled problems in studying K^+ channels has been identifying the inactivated conformation of the selectivity filter. A recent study showed that inactivation does not rely on the constricted conformation to occur; hence, indicating filter constriction is not relevant to the inactivated state of K^+ channels [194, 195, 204, 205]. An different model suggests that inactivation results in a dilated selectivity filter, where partially hydrated ions are not able to flux across the hydrophobic barrier [208]. The dilation model implies a conformational change at the outer mouth of the pore domain, seemingly consistent with all existing data, but no directly supportive evidence of the dilation has been found thus far. Regardless of the status of the channel, either constriction or dilation, a conformational change of the filter could be reflected in the K^+ binding affinities. I parsed the problem by determining the

$K_D(K^+)$ of channels that are trapped in three different states, the constricted, the inactivated and the conductive conformations. Based on the results, it is apparent that the thermodynamic property of the inactivated channels are more similar to the conductive than that of the constricted conformation, so I propose that the inactivated state may resemble the conductive state of the filter.

In fact, several lines of evidence support my hypothesis. First, the conductive conformation has been observed in K^+ channel structures that should have been inactivated. For example, Kv1.2/2.1 inactivates in lipid bilayer at zero millivolts, while under the same condition its crystal structure shows four well-coordinated sites in its filter, which is identical to the conductive conformation observed from KcsA [59]. Second, the NMR spectroscopy characterization of the truncated KcsA channels in detergent DM showed two distinct chemical shifts of the valine residue inside the selectivity filter between Na^+ and K^+ bound states [260]. The truncated KcsA is normally regarded as being closed at neutral pH, whereas I showed in this study that under the same condition it is open like the full-length KcsA in lipid vesicles. Thus, when this open KcsA is saturated with K^+ ions, its chemical shift actually should correspond to the inactivated conformation. Consistent with my hypothesis, this chemical shift is more closely resembles that of the conductive conformation than the Na^+-bound constricted conformation.

There may be more than one conformation corresponding to the inactivated state of K^+ channels. Although KcsA has been a model system to investigate the inactivation mechanism, K^+ channels may have evolved multiple means to modulate their

inactivation processes. Different channels also feel the effects of mutations differently. For example, mutating the glutamate 71 residue has been shown to change the inactivation rate in KcsA, but the same effect was marginally replicated in Kv1.2 with equivalent mutations [195]. Another example is the hydrogen network surrounding the selectivity filter, which has profound effects on modulating the inactivation rate. The W67F mutation in the network renders KcsA unable to inactivate, but the equivalent mutation induces a very fast inactivation in Kv1.2 [196]. A recent study also illustrated that the inactivation rate in KcsA can be altered by the ion occupancy of each site inside the filter [201]. Furthermore, the inactivation of Kv1.5 channels comprises of a fast phase and a slow phase, where the fast phase has been shown to correlate with the conformational change of the turrets on the pore domain [261]. Finally, protonation at the outer side of the pore domain can also affect the inactivation in a few types of K^+ channels [169-171]. In summary, C-type inactivation could involve in a subtle conformational rearrangement around the selectivity filter.

Discussion

Functional implications of ion selectivity and C-type inactivation in K^+ channels

Ion selectivity and C-type inactivation are two important properties in K^+ channels that regulate cell responses via electrical signals. Although both properties affect the redistribution of ions across lipid membranes, they play distinctly different roles. The K^+/Na^+ selectivity ensures a solely K^+-dependent membrane potential change that prevents Na^+ ions entering the cell, while C-type inactivation is a gating process that

spatiotemporally controls K^+ channel's activity. Due to the essentiality of K^+ channels in higher organisms, even a minor dysfunction to either property could lead to severe physiological consequences, and eventually cause death. For the same reason, there has been very few natural mutations discovered to this date that result in either loss of selectivity or alteration of C-type inactivation, so biophysical understandings of these two properties are often inferred to their functions *in vivo*.

C-type inactivation or desensitization is commonly found in K^+ channels, and it is very critical to voltage-gated K^+ channels in neurological systems, since ceasing K^+ efflux determines both the speed and degree of repolarization during action potential. If C-type inactivation takes place too fast, K^+ ions will not have enough time to leave the cell so as to repolarize the cell membrane. As a result, the axon will not be able to send another wave of signal until the membrane potential is reset by Na^+/K^+ ATPase. On the contrary, if the rate of C-type inactivation is too small, the excessive amount of K^+ influx could also lead to an impeded electrical firing in the axon. The KcsA K^+ channel has many features similar to the Kv channels, so it has been utilized as a model system to understand the molecular mechanism of C-type inactivation. Previously, the Na^+ bound constricted conformation was proposed to be the inactivated conformation in the KcsA K^+ channels [204, 205]; however, K^+/Na^+ exchange in my ITC experiments showed the inactivated state of KcsA is more similar to the conductive rather than the constricted conformation. Therefore, the C-type inactivation likely stems from a subtle conformational change in the selectivity filter, whereas the constricted conformation may be an experimental artifact.

Ion selectivity has a broad impact to all types of K^+ channels. In voltage-gated K^+ channels, a loss of selectivity renders both K^+ and Na^+ able to flux across the membrane, so the repolarization during action potential will fail to reach potassium's Nernst potential. In non-excitable cells, K^+ or Na^+ distribution does not undergo a large and quick change to propagate electrical signals, but K^+ channels are still involved in maintaining the membrane potential. For instance, inwardly rectifying K^+ channels keep a low membrane potential to ensure voltage-gated Ca^{2+} channels remain closed [262]. A loss of selectivity from mutations in these channels elevates the resting membrane potential, causing the opening of Ca^{2+} channels. As a second messenger, Ca^{2+} influx could trigger insulin over release in pancreatic cells [263], upregulate aldosterone biosynthesis [104-107], and affect many other downstream reactions.

Ion selection in CNG channels

In contrast to the detrimental consequences caused by loss of selectivity in K^+ channels, some cellular functions relying on non-selective channels, such as cyclic-nucleotide gated (CNG) ion channels. CNG channels were initially discovered in rod cells in the retina, and they are a class of tetrameric channels closely related to K^+ channels in phylogenetic tree [209]. In response to light, cyclic nucleotides are produced in rod cells, which subsequentially activate CNG channels. Under other physiological conditions, the opening of CNG channels either depolarizes or hyperpolarizes the membrane potential to regulate downstream processes such as the excitability of photoreceptors, rhythmicity in heart, etc. Recently, several high resolution structures of

CNG mimic channels revealed that K^+ ions in their filters are coordinated in the same way as in K^+ channels', but there are only three rather than four sites inside the filter, and the anomalous mole fraction effect is not as clear as in K^+ channels [150-152, 236]. These comparisons between K^+ channels and CNG channels illustrate that the ion interaction inside a four-site filter attributes to the highly selective conduction of K^+ channels [236, 248]. However, it is currently unknown how the cell physiology will change if the filter of a CNG channel is mutated into four-site like a K^+ channel's filter.

Future direction

My study indicates that the flux coupling creates a blocking effect to determine a K^+ channel's conduction selectivity, and that the equilibrium selectivity is the foundation of such effect. In the future, more examinations could be carried out to understand the interplay between the flux coupling and other processes of K^+ channels. There are three aspects that have not yet been explored in great detail.

Firstly, it is intriguing how ion occupancy affects the conduction selectivity of K^+ channels. It has been extensively shown that the highly conserved sequence, TVGYG, ensures four K^+-selective sites inside the filter so that the flux coupling can be preserved. However, rare exceptions have been found with channels that contain four K^+-binding sites but lack conduction selectivity. One example is the NaK2K(Y55F) channel, whose high resolution structure manifests four K^+ binding sites, but the protein is unable to distinguish K^+ ions with Na^+ ions during conduction [152]. According to my model, there has to be at least two selective sites that create a blocking effect in order to achieve

selective conduction, meaning it is possible that only one selective site exists in NaK2K(Y55F). To test this hypothesis, a crystallographic titration can be applied by detecting the electron density change of the K^+ ions inside the filter. If there indeed is only one highly selective site in NaK2K(Y55F), it explains why this channel does not preferentially conduct K^+ ions over Na^+ ion; otherwise, other mechanisms may be involved.

On the other hand, if comprising four K^+ sites is a prerequisite for selective conduction, then how does evolution convert a non-selective channel like NaK2K(Y55F) into a K^+ channel? Rather than pursuing random mutagenesis and selection to mimic evolution, I could artificially lower the ion occupancy at site 2 or site 3, which increases the energy barrier in the middle of the filter. In other words, the energy barrier will implement a blocking effect to mimic naturally selective channels. Conveniently, an approach of introducing non-natural amino acids into protein has been developed, which requires feeding *E.coli* cells with the desired amino acid that will be incorporated into the tRNA targeting the amber stop codon [201, 264]. By engineering the amber stop codon into the protein of interest, I can replace any amino acid of interests in the protein sequence. This approach has been successfully used to replace the tyrosine residue in the selectivity filter of several K^+ channels; furthermore, the site 2 occupancy in KcsA was greatly diminished by incorporating an ester bond with a tyrosine derivative [207]. I may apply the same approach to NaK2K(Y55F) and verify the disappearance of the electron density at site 2 via crystallography. Electrophysiology will be applied to test whether NaK2K(Y55F)(ester) can be converted into a K^+ channel.

Secondly, I could examine how three-site channels retain their conduction selectivity. In spite of the conservation of four binding sites in the selectivity filter, eliminating site 4 does not uniformly convert K^+ channels into non-selective ion channels. It was found that the *shaker* K^+ channel are able to retain its selectivity upon site 4 mutations [37], so I propose that the structural dynamics of C-type inactivating channels renders more constraints on the selectivity filter, and, therefore, contributes to the resistance to site 4 deletions. To test that, I would compare the conduction selectivity of the double mutation that eliminates both the inactivation and site 4 occupancy with the corresponding single mutants. For example, the site 4 mutation (T75A) will be applied to the non-inactivating mutant, KcsA(E71A), and the conduction selectivity will be measured and compared between two single mutants and the double mutant. Crystal structures of channels harboring T75G could be obtained to verify the elimination of site 4. Similar comparison may be repeated in other C-type inactivating channels. Conversely, I may convert non-inactivating channels, such as MthK, to be inactivating, and characterize whether their site-4 deleted mutants can retain the ion selectivity during conduction. For the three-site channels that are non-selective during conduction, I hypothesize that creating an energy barrier between site 1 and site 3 could restore their ion selectivity. Essentially, the same approach using non-natural mutation, which has been described earlier, will be employed again.

Finally, the relation between ion selectivity and conductance will be explored. My kinetic model supports the hypothesis that the equilibrium selectivity sets the conduction selectivity of K^+ channels; however, this model holds true only if the

conductance is smaller than diffusion of ions. In other words, if the conductance is equal to or exceeding the rate of diffusion, the movement of conducted ions does not meet major energy barriers inside the filter, and the ion selectivity will be primarily the ratio of the association rates between two competing ions. This would indicate the ion selectivity of a fast conducting channel is largely compromised, since the ion association rate is assumed to be similar between Na^+ and K^+. The conductance of most K^+ channels do not approach the rate of diffusion, but BK channels are the exception. Besides being exceptionally large, the conductance of BK channels also shows a hyperbolic and saturable behavior as a function of ion concentration. The properties of BK channels meet the theoretical one-ion channel model, whereas their structures manifest four K^+ binding sites like all other known K^+ channels; thus, the energy barrier from flux coupling may not apply to BK channels. In order to investigate whether the conduction selectivity of BK channels is compromised at their maximum conductance, I would examine the anomalous mole fraction effect in a lower range of voltages. If the mole fraction corresponding to the lowest conductance is shifted to the right or disappears when the voltage is raised, my model will correctly predict the relationship between conduction selectivity and conductance. Otherwise, there might be other mechanisms in K^+ channels to occlude Na^+ ions, which may be investigated using a combination of techniques including crystallography, NMR spectroscopy, etc.

REFERENCES

1. Ringer, S., *Concerning the influence exerted by each of the constituents of the blood on the contraction of the ventricle.* J Physiol, 1882. **3**(5-6): p. 380-93.
2. Ringer, S., *A third contribution regarding the influence of the inorganic constituents of the blood on the ventricular contraction.* J Physiol, 1883. **4**(2-3): p. 222-5.
3. Ringer, S., *A further contribution regarding the influence of the different constituents of the blood on the contraction of the heart.* J Physiol, 1883. **4**(1): p. 29-42 3.
4. Nernst, W., *Zur kinetik der in lösung befindlichen körper. I. Theorie der Diffusion.* Z. Phys. Chem., 1988. **4**: p. 129-181.
5. Bernstein, J., *Untersuchungen zur thermodynamik der bioelektrischen Ströme.* Pflügers Arch, 1902. **92**: p. 521-562.
6. Bernstein, J., *Elektrobiologie. die lehre von den elektrischen vorgängen im organismus auf moderner grundlage dargestellt.* 1912: Vieweg & Sohn, Braunschweig.
7. Cole, K.S. and H.J. Curtis, *Electric impedance of the squid giant axon during activity.* J Gen Physiol, 1939. **22**(5): p. 649-70.
8. Hodgkin, A.L., *Evidence for electrical transmission in nerve: Part II.* J Physiol, 1937. **90**(2): p. 211-32.

9. Hodgkin, A.L., *Evidence for electrical transmission in nerve: Part I.* J Physiol, 1937. **90**(2): p. 183-210.

10. Hodgkin, A.L.a.H., A.F., *Action potentials recorded from inside a nerve fibre.* Nature, 1939. **144**: p. 710-711.

11. Hodgkin, A.L. and B. Katz, *The effect of sodium ions on the electrical activity of giant axon of the squid.* J Physiol, 1949. **108**(1): p. 37-77.

12. Neher, E. and B. Sakmann, *Single-channel currents recorded from membrane of denervated frog muscle fibres.* Nature, 1976. **260**(5554): p. 799-802.

13. Sakmann, B., J. Patlak, and E. Neher, *Single acetylcholine-activated channels show burst-kinetics in presence of desensitizing concentrations of agonist.* Nature, 1980. **286**(5768): p. 71-3.

14. Sigworth, F.J. and E. Neher, *Single Na+ channel currents observed in cultured rat muscle cells.* Nature, 1980. **287**(5781): p. 447-9.

15. Colquhoun, D., et al., *Inward current channels activated by intracellular Ca in cultured cardiac cells.* Nature, 1981. **294**(5843): p. 752-4.

16. Conti, F. and E. Neher, *Single channel recordings of K+ currents in squid axons.* Nature, 1980. **285**(5761): p. 140-3.

17. Hamill, O.P., et al., *Improved patch-clamp techniques for high-resolution current recording from cells and cell-free membrane patches.* Pflugers Arch, 1981. **391**(2): p. 85-100.

18. Novitski, E., *Drosophila infopmation service* 1949. **23**: p. 61.

19. Salkoff, L., *Genetic and voltage-clamp analysis of a Drosophila potassium channel*. Cold Spring Harb Symp Quant Biol, 1983. **48 Pt 1**: p. 221-31.

20. Timpe, L.C. and L.Y. Jan, *Gene dosage and complementation analysis of the Shaker locus in Drosophila*. J Neurosci, 1987. **7**(5): p. 1307-17.

21. Wu, C.F. and F.N. Haugland, *Voltage clamp analysis of membrane currents in larval muscle fibers of Drosophila: alteration of potassium currents in Shaker mutants*. J Neurosci, 1985. **5**(10): p. 2626-40.

22. Papazian, D.M., et al., *Cloning of genomic and complementary DNA from Shaker, a putative potassium channel gene from Drosophila*. Science, 1987. **237**(4816): p. 749-53.

23. Tempel, B.L., et al., *Sequence of a probable potassium channel component encoded at Shaker locus of Drosophila*. Science, 1987. **237**(4816): p. 770-5.

24. Gundersen, C.B., R. Miledi, and I. Parker, *Voltage-operated channels induced by foreign messenger RNA in Xenopus oocytes*. Proc R Soc Lond B Biol Sci, 1983. **220**(1218): p. 131-40.

25. Miledi, R., I. Parker, and K. Sumikawa, *Recording of single gamma-aminobutyrate- and acetylcholine-activated receptor channels translated by exogenous mRNA in Xenopus oocytes*. Proc R Soc Lond B Biol Sci, 1983. **218**(1213): p. 481-4.

26. Iverson, L.E., et al., *A-type potassium channels expressed from Shaker locus cDNA*. Proc Natl Acad Sci U S A, 1988. **85**(15): p. 5723-7.

27. Rudy, B., et al., *At least two mRNA species contribute to the properties of rat brain A-type potassium channels expressed in Xenopus oocytes.* Neuron, 1988. **1**(8): p. 649-58.

28. Bargmann, C.I., *Neurobiology of the Caenorhabditis elegans genome.* Science, 1998. **282**(5396): p. 2028-33.

29. Littleton, J.T. and B. Ganetzky, *Ion channels and synaptic organization: analysis of the Drosophila genome.* Neuron, 2000. **26**(1): p. 35-43.

30. Gutman, G.A., et al., *International union of pharmacology. XLI. Compendium of voltage-gated ion channels: potassium channels.* Pharmacol Rev, 2003. **55**(4): p. 583-6.

31. MacKinnon, R., *Determination of the subunit stoichiometry of a voltage-activated potassium channel.* Nature, 1991. **350**(6315): p. 232-5.

32. Yellen, G., et al., *Mutations affecting internal TEA blockade identify the probable pore-forming region of a K+ channel.* Science, 1991. **251**(4996): p. 939-42.

33. Hartmann, H.A., et al., *Exchange of conduction pathways between two related K+ channels.* Science, 1991. **251**(4996): p. 942-4.

34. MacKinnon, R. and G. Yellen, *Mutations affecting TEA blockade and ion permeation in voltage-activated K+ channels.* Science, 1990. **250**(4978): p. 276-9.

35. Ketchum, K.A., et al., *A new family of outwardly rectifying potassium channel proteins with two pore domains in tandem.* Nature, 1995. **376**(6542): p. 690-5.

36. Heginbotham, L., T. Abramson, and R. MacKinnon, *A functional connection between the pores of distantly related ion channels as revealed by mutant K+ channels*. Science, 1992. **258**(5085): p. 1152-5.

37. Heginbotham, L., et al., *Mutations in the K+ channel signature sequence*. Biophys J, 1994. **66**(4): p. 1061-7.

38. Kirsch, G.E., et al., *A single nonpolar residue in the deep pore of related K+ channels acts as a K+:Rb+ conductance switch*. Biophys J, 1992. **62**(1): p. 136-43; discussion 143-4.

39. Yool, A.J. and T.L. Schwarz, *Alteration of ionic selectivity of a K+ channel by mutation of the H5 region*. Nature, 1991. **349**(6311): p. 700-4.

40. Stocker, M. and C. Miller, *Electrostatic distance geometry in a K+ channel vestibule*. Proc Natl Acad Sci U S A, 1994. **91**(20): p. 9509-13.

41. Hidalgo, P. and R. MacKinnon, *Revealing the architecture of a K+ channel pore through mutant cycles with a peptide inhibitor*. Science, 1995. **268**(5208): p. 307-10.

42. Ranganathan, R., J.H. Lewis, and R. MacKinnon, *Spatial localization of the K+ channel selectivity filter by mutant cycle-based structure analysis*. Neuron, 1996. **16**(1): p. 131-9.

43. Lipkind, G.M., D.A. Hanck, and H.A. Fozzard, *A structural motif for the voltage-gated potassium channel pore*. Proc Natl Acad Sci U S A, 1995. **92**(20): p. 9215-9.

44. Schrempf, H., et al., *A prokaryotic potassium ion channel with two predicted transmembrane segments from Streptomyces lividans*. EMBO J, 1995. **14**(21): p. 5170-8.

45. Cortes, D.M. and E. Perozo, *Structural dynamics of the Streptomyces lividans K+ channel (SKC1): oligomeric stoichiometry and stability*. Biochemistry, 1997. **36**(33): p. 10343-52.

46. Heginbotham, L., E. Odessey, and C. Miller, *Tetrameric stoichiometry of a prokaryotic K+ channel*. Biochemistry, 1997. **36**(33): p. 10335-42.

47. Heginbotham, L., L. Kolmakova-Partensky, and C. Miller, *Functional reconstitution of a prokaryotic K+ channel*. J Gen Physiol, 1998. **111**(6): p. 741-9.

48. Cuello, L.G., et al., *pH-dependent gating in the Streptomyces lividans K+ channel*. Biochemistry, 1998. **37**(10): p. 3229-36.

49. LeMasurier, M., L. Heginbotham, and C. Miller, *KcsA: it's a potassium channel*. J Gen Physiol, 2001. **118**(3): p. 303-14.

50. MacKinnon, R., et al., *Structural conservation in prokaryotic and eukaryotic potassium channels*. Science, 1998. **280**(5360): p. 106-9.

51. Doyle, D.A., et al., *The structure of the potassium channel: molecular basis of K+ conduction and selectivity*. Science, 1998. **280**(5360): p. 69-77.

52. Jiang, Y. and R. MacKinnon, *The barium site in a potassium channel by x-ray crystallography*. J Gen Physiol, 2000. **115**(3): p. 269-72.

53. Zhou, Y., et al., *Chemistry of ion coordination and hydration revealed by a K+ channel-Fab complex at 2.0 A resolution.* Nature, 2001. **414**(6859): p. 43-8.

54. Morais-Cabral, J.H., Y. Zhou, and R. MacKinnon, *Energetic optimization of ion conduction rate by the K+ selectivity filter*. Nature, 2001. **414**(6859): p. 37-42.

55. Zhou, Y. and R. MacKinnon, *The occupancy of ions in the K+ selectivity filter: charge balance and coupling of ion binding to a protein conformational change underlie high conduction rates.* J Mol Biol, 2003. **333**(5): p. 965-75.

56. Gouaux, E. and R. Mackinnon, *Principles of selective ion transport in channels and pumps.* Science, 2005. **310**(5753): p. 1461-5.

57. Jiang, Y., et al., *X-ray structure of a voltage-dependent K+ channel*. Nature, 2003. **423**(6935): p. 33-41.

58. Long, S.B., E.B. Campbell, and R. Mackinnon, *Crystal structure of a mammalian voltage-dependent Shaker family K+ channel.* Science, 2005. **309**(5736): p. 897-903.

59. Long, S.B., et al., *Atomic structure of a voltage-dependent K+ channel in a lipid membrane-like environment*. Nature, 2007. **450**(7168): p. 376-82.

60. Yuan, P., et al., *Structure of the human BK channel Ca2+-activation apparatus at 3.0 A resolution.* Science, 2010. **329**(5988): p. 182-6.

61. Yuan, P., et al., *Open structure of the Ca2+ gating ring in the high-conductance Ca2+-activated K+ channel*. Nature, 2012. **481**(7379): p. 94-7.

62. Nishida, M., et al., *Crystal structure of a Kir3.1-prokaryotic Kir channel chimera.* EMBO J, 2007. **26**(17): p. 4005-15.

63. Tao, X., et al., *Crystal structure of the eukaryotic strong inward-rectifier K+ channel Kir2.2 at 3.1 A resolution.* Science, 2009. **326**(5960): p. 1668-74.

64. Hansen, S.B., X. Tao, and R. MacKinnon, *Structural basis of PIP2 activation of the classical inward rectifier K+ channel Kir2.2.* Nature, 2011. **477**(7365): p. 495-8.

65. Whorton, M.R. and R. MacKinnon, *X-ray structure of the mammalian GIRK2-betagamma G-protein complex.* Nature, 2013. **498**(7453): p. 190-7.

66. Whorton, M.R. and R. MacKinnon, *Crystal structure of the mammalian GIRK2 K+ channel and gating regulation by G proteins, PIP2, and sodium.* Cell, 2011. **147**(1): p. 199-208.

67. Brohawn, S.G., E.B. Campbell, and R. MacKinnon, *Physical mechanism for gating and mechanosensitivity of the human TRAAK K+ channel.* Nature, 2014. **516**(7529): p. 126-30.

68. Brohawn, S.G., J. del Marmol, and R. MacKinnon, *Crystal structure of the human K2P TRAAK, a lipid- and mechano-sensitive K+ ion channel.* Science, 2012. **335**(6067): p. 436-41.

69. Miller, A.N. and S.B. Long, *Crystal structure of the human two-pore domain potassium channel K2P1.* Science, 2012. **335**(6067): p. 432-6.

70. Hille, B., *Pharmacological modifications of the sodium channels of frog nerve.* J Gen Physiol, 1968. **51**(2): p. 199-219.

71. Moore, J.W.a.R.G.P., *Kinetics and mechanism, 3rd Ed*. Vol. 455. 1981, New York: Wiley.

72. Diebler, H., M. Eigen, G. Ilgenfritz, G. Maas and R. Wrinkler, *Kinetics and mechanism of reactions of main group metal ions with biologcial carriers.* Pure Appl. Chem., 1969. **20**: p. 93-115.

73. Latorre, R. and C. Miller, *Conduction and selectivity in potassium channels.* J Membr Biol, 1983. **71**(1-2): p. 11-30.

74. Hodgkin, A.L. and A.F. Huxley, *Currents carried by sodium and potassium ions through the membrane of the giant axon of Loligo.* J Physiol, 1952. **116**(4): p. 449-72.

75. Hodgkin, A.L. and R.D. Keynes, *The potassium permeability of a giant nerve fibre.* J Physiol, 1955. **128**(1): p. 61-88.

76. Ussing, H.H., *The distinction by means of tracers between active transport and diffusion - the transfer of iodide across the isolated frog skin.* Acta Physiologica Scandinavica, 1949. **19**(1): p. 43-56.

77. Heckmann, K., *Zur theorie der single file -diffusion I.* Zeitschrift Fur Physikalische Chemie-Frankfurt, 1965. **44**(3-4): p. 184-&.

78. Heckmann, K., *Zur theorie der single file -diffusion .2.* Zeitschrift Fur Physikalische Chemie-Frankfurt, 1965. **46**(1-2): p. 1-&.

79. Heckmann, K., *Theory of single file diffusion .3. sigmoidal concentration dependence of unidirectional flow in single file diffusion.* Zeitschrift Fur Physikalische Chemie-Frankfurt, 1968. **58**(1-4): p. 206-&.

80. Heckmann, K., *Single file diffusion.* Biomembranes, 1972. **3**: p. 127-53.

81. Hille, B. and W. Schwarz, *Potassium channels as multi-ion single-file pores.* J Gen Physiol, 1978. **72**(4): p. 409-42.

82. Begenisich, T. and P. De Weer, *Potassium flux ratio in voltage-clamped squid giant axons.* J Gen Physiol, 1980. **76**(1): p. 83-98.

83. Horowicz, P., P.W. Gage, and R.S. Eisenberg, *The role of the electrochemical gradient in determining potassium fluxes in frog striated muscle.* J Gen Physiol, 1968. **51**(5): p. 193-203.

84. Vestergaard-Bogind, B., P. Stampe, and P. Christophersen, *Single-file diffusion through the Ca2+-activated K+ channel of human red cells.* J Membr Biol, 1985. **88**(1): p. 67-75.

85. Hagiwara, S., et al., *Anomalous permeabilities of the egg cell membrane of a starfish in K+-Tl+ mixtures.* J Gen Physiol, 1977. **70**(3): p. 269-81.

86. Korn, S.J. and S.R. Ikeda, *Permeation selectivity by competition in a delayed rectifier potassium channel.* Science, 1995. **269**(5222): p. 410-2.

87. Stampe, P. and T. Begenisich, *Unidirectional K+ fluxes through recombinant Shaker potassium channels expressed in single Xenopus oocytes.* J Gen Physiol, 1996. **107**(4): p. 449-57.

88. Stampe, P., et al., *Nonindependent K+ movement through the pore in IRK1 potassium channels.* J Gen Physiol, 1998. **112**(4): p. 475-84.

89. Kiss, L., et al., *The interaction of Na+ and K+ in voltage-gated potassium channels. Evidence for cation binding sites of different affinity.* J Gen Physiol, 1998. **111**(2): p. 195-206.

90. Ye, S., Y. Li, and Y. Jiang, *Novel insights into K+ selectivity from high-resolution structures of an open K+ channel pore.* Nat Struct Mol Biol, 2010. **17**(8): p. 1019-23.

91. Heginbotham, L. and R. MacKinnon, *Conduction properties of the cloned Shaker K+ channel.* Biophys J, 1993. **65**(5): p. 2089-96.

92. Berneche, S. and B. Roux, *Energetics of ion conduction through the K+ channel.* Nature, 2001. **414**(6859): p. 73-7.

93. Lees-Miller, J.P., et al., *Novel gain-of-function mechanism in K(+) channel-related long-QT syndrome: altered gating and selectivity in the HERG1 N629D mutant.* Circ Res, 2000. **86**(5): p. 507-13.

94. Satler, C.A., et al., *Multiple different missense mutations in the pore region of HERG in patients with long QT syndrome.* Hum Genet, 1998. **102**(3): p. 265-72.

95. Teng, G.Q., et al., *Homozygous missense N629D hERG (KCNH2) potassium channel mutation causes developmental defects in the right ventricle and its outflow tract and embryonic lethality.* Circ Res, 2008. **103**(12): p. 1483-91.

96. Patil, N., et al., *A potassium channel mutation in weaver mice implicates membrane excitability in granule cell differentiation.* Nat Genet, 1995. **11**(2): p. 126-9.

97. Reeves, R.H., et al., *The mouse neurological mutant weaver maps within the region of chromosome 16 that is homologous to human chromosome 21.* Genomics, 1989. **5**(3): p. 522-6.

98. Navarro, B., et al., *Nonselective and G betagamma-insensitive weaver K+ channels.* Science, 1996. **272**(5270): p. 1950-3.

99. Slesinger, P.A., et al., *Functional effects of the mouse weaver mutation on G protein-gated inwardly rectifying K+ channels.* Neuron, 1996. **16**(2): p. 321-31.

100. Kofuji, P., et al., *Functional analysis of the weaver mutant GIRK2 K+ channel and rescue of weaver granule cells.* Neuron, 1996. **16**(5): p. 941-52.

101. Silverman, S.K., et al., *A regenerative link in the ionic fluxes through the weaver potassium channel underlies the pathophysiology of the mutation.* Proc Natl Acad Sci U S A, 1996. **93**(26): p. 15429-34.

102. Rossi, P., et al., *The weaver mutation causes a loss of inward rectifier current regulation in premigratory granule cells of the mouse cerebellum.* J Neurosci, 1998. **18**(10): p. 3537-47.

103. Surmeier, D.J., P.G. Mermelstein, and D. Goldowitz, *The weaver mutation of GIRK2 results in a loss of inwardly rectifying K+ current in cerebellar granule cells.* Proc Natl Acad Sci U S A, 1996. **93**(20): p. 11191-5.

104. Choi, M., et al., *K+ channel mutations in adrenal aldosterone-producing adenomas and hereditary hypertension.* Science, 2011. **331**(6018): p. 768-72.

105. Kuppusamy, M., et al., *A Novel KCNJ5-insT149 somatic mutation close to, but outside, the selectivity filter causes resistant hypertension by loss of selectivity for potassium.* Journal of Clinical Endocrinology & Metabolism, 2014. **99**(9): p. E1765-E1773.

106. Monticone, S., et al., *A novel Y152C KCNJ5 mutation responsible for familial hyperaldosteronism type III*. Journal of Clinical Endocrinology & Metabolism, 2013. **98**(11): p. E1861-E1865.

107. Scholl, U.I., et al., *Hypertension with or without adrenal hyperplasia due to different inherited mutations in the potassium channel KCNJ5*. Proceedings of the National Academy of Sciences of the United States of America, 2012. **109**(7): p. 2533-2538.

108. Goldman, D.E., *Potential, impedance, and rectification in membranes*. J Gen Physiol, 1943. **27**(1): p. 37-60.

109. Bezanilla, F. and C.M. Armstrong, *Negative conductance caused by entry of sodium and cesium ions into the potassium channels of squid axons*. J Gen Physiol, 1972. **60**(5): p. 588-608.

110. Hille, B., *Potassium channels in myelinated nerve. Selective permeability to small cations*. J Gen Physiol, 1973. **61**(6): p. 669-86.

111. Lockless, S.W., M. Zhou, and R. MacKinnon, *Structural and thermodynamic properties of selective ion binding in a K+ channel*. PLoS Biol, 2007. **5**(5): p. e121.

112. Almers, W. and E.W. McCleskey, *Non-selective conductance in calcium channels of frog muscle: calcium selectivity in a single-file pore*. J Physiol, 1984. **353**: p. 585-608.

113. Friel, D.D. and R.W. Tsien, *Voltage-gated calcium channels: direct observation of the anomalous mole fraction effect at the single-channel level.* Proc Natl Acad Sci U S A, 1989. **86**(13): p. 5207-11.

114. Hess, P. and R.W. Tsien, *Mechanism of ion permeation through calcium channels.* Nature, 1984. **309**(5967): p. 453-6.

115. Urban, B.W. and S.B. Hladky, *Ion transport in the simplest single file pore.* Biochim Biophys Acta, 1979. **554**(2): p. 410-29.

116. Corry, B., et al., *Mechanisms of permeation and selectivity in calcium channels.* Biophys J, 2001. **80**(1): p. 195-214.

117. Nonner, W., L. Catacuzzeno, and B. Eisenberg, *Binding and selectivity in L-type calcium channels: a mean spherical approximation.* Biophys J, 2000. **79**(4): p. 1976-92.

118. Nonner, W. and B. Eisenberg, *Ion permeation and glutamate residues linked by Poisson-Nernst-Planck theory in L-type calcium channels.* Biophys J, 1998. **75**(3): p. 1287-305.

119. Schumaker, M.F. and R. MacKinnon, *A simple model for multi-ion permeation. Single-vacancy conduction in a simple pore model.* Biophys J, 1990. **58**(4): p. 975-84.

120. Bhate, M.P., et al., *Conformational dynamics in the selectivity filter of KcsA in response to potassium ion concentration.* J Mol Biol, 2010. **401**(2): p. 155-66.

121. Imai, S., et al., *Structural basis underlying the dual gate properties of KcsA.* Proc Natl Acad Sci U S A, 2010. **107**(14): p. 6216-21.

122. Bhate, M.P. and A.E. McDermott, *Protonation state of E71 in KcsA and its role for channel collapse and inactivation.* Proc Natl Acad Sci U S A, 2012. **109**(38): p. 15265-70.

123. Ader, C., et al., *Coupling of activation and inactivation gate in a K+-channel: potassium and ligand sensitivity.* EMBO J, 2009. **28**(18): p. 2825-34.

124. Allen, T.W., O.S. Andersen, and B. Roux, *On the importance of atomic fluctuations, protein flexibility, and solvent in ion permeation.* J Gen Physiol, 2004. **124**(6): p. 679-90.

125. Berneche, S. and B. Roux, *Molecular dynamics of the KcsA K(+) channel in a bilayer membrane.* Biophys J, 2000. **78**(6): p. 2900-17.

126. Luzhkov, V.B. and J. Aqvist, *K(+)/Na(+) selectivity of the KcsA potassium channel from microscopic free energy perturbation calculations.* Biochim Biophys Acta, 2001. **1548**(2): p. 194-202.

127. Noskov, S.Y., S. Berneche, and B. Roux, *Control of ion selectivity in potassium channels by electrostatic and dynamic properties of carbonyl ligands.* Nature, 2004. **431**(7010): p. 830-4.

128. Bostick, D.L. and C.L. Brooks, 3rd, *Selectivity in K+ channels is due to topological control of the permeant ion's coordinated state.* Proc Natl Acad Sci U S A, 2007. **104**(22): p. 9260-5.

129. Thomas, M., D. Jayatilaka, and B. Corry, *The predominant role of coordination number in potassium channel selectivity.* Biophys J, 2007. **93**(8): p. 2635-43.

130. Varma, S. and S.B. Rempe, *Tuning ion coordination architectures to enable selective partitioning.* Biophys J, 2007. **93**(4): p. 1093-9.

131. Noskov, S.Y. and B. Roux, *Ion selectivity in potassium channels.* Biophys Chem, 2006. **124**(3): p. 279-91.

132. Baukrowitz, T. and G. Yellen, *Use-dependent blockers and exit rate of the last ion from the multi-ion pore of a K+ channel.* Science, 1996. **271**(5249): p. 653-6.

133. Neyton, J. and C. Miller, *Discrete Ba2+ block as a probe of ion occupancy and pore structure in the high-conductance Ca2+ -activated K+ channel.* J Gen Physiol, 1988. **92**(5): p. 569-86.

134. Neyton, J. and C. Miller, *Potassium blocks barium permeation through a calcium-activated potassium channel.* J Gen Physiol, 1988. **92**(5): p. 549-67.

135. Piasta, K.N., D.L. Theobald, and C. Miller, *Potassium-selective block of barium permeation through single KcsA channels.* J Gen Physiol, 2011. **138**(4): p. 421-36.

136. Vergara, C., O. Alvarez, and R. Latorre, *Localization of the K+ lock-In and the Ba2+ binding sites in a voltage-gated calcium-modulated channel. Implications for survival of K+ permeability.* J Gen Physiol, 1999. **114**(3): p. 365-76.

137. Allen, T.W., S. Kuyucak, and S.H. Chung, *Molecular dynamics study of the KcsA potassium channel.* Biophys J, 1999. **77**(5): p. 2502-16.

138. Allen, T.W. and S.H. Chung, *Brownian dynamics study of an open-state KcsA potassium channel.* Biochim Biophys Acta, 2001. **1515**(2): p. 83-91.

139. Chung, S.H., et al., *Permeation of ions across the potassium channel: Brownian dynamics studies.* Biophys J, 1999. **77**(5): p. 2517-33.

140. Thompson, A.N., et al., *Mechanism of potassium-channel selectivity revealed by Na(+) and Li(+) binding sites within the KcsA pore.* Nat Struct Mol Biol, 2009. **16**(12): p. 1317-24.

141. Bucher, D., et al., *Coordination numbers of K(+) and Na(+) Ions inside the selectivity filter of the KcsA potassium channel: insights from first principles molecular dynamics.* Biophys J, 2010. **98**(10): p. L47-9.

142. Burykin, A., M. Kato, and A. Warshel, *Exploring the origin of the ion selectivity of the KcsA potassium channel.* Proteins, 2003. **52**(3): p. 412-26.

143. Kim, I. and T.W. Allen, *On the selective ion binding hypothesis for potassium channels.* Proc Natl Acad Sci U S A, 2011. **108**(44): p. 17963-8.

144. Adelman, W.J., Jr. and R.J. French, *Blocking of the squid axon potassium channel by external caesium ions.* J Physiol, 1978. **276**: p. 13-25.

145. Yellen, G., *Relief of Na+ block of Ca2+-activated K+ channels by external cations.* J Gen Physiol, 1984. **84**(2): p. 187-99.

146. Heginbotham, L., et al., *Single streptomyces lividans K(+) channels: functional asymmetries and sidedness of proton activation.* J Gen Physiol, 1999. **114**(4): p. 551-60.

147. Nimigean, C.M. and C. Miller, *Na+ block and permeation in a K+ channel of known structure.* J Gen Physiol, 2002. **120**(3): p. 323-35.

148. Alam, A. and Y. Jiang, *High-resolution structure of the open NaK channel.* Nat Struct Mol Biol, 2009. **16**(1): p. 30-4.

149. Shi, N., et al., *Atomic structure of a Na+- and K+-conducting channel.* Nature, 2006. **440**(7083): p. 570-4.

150. Derebe, M.G., et al., *Tuning the ion selectivity of tetrameric cation channels by changing the number of ion binding sites.* Proc Natl Acad Sci U S A, 2011. **108**(2): p. 598-602.

151. Derebe, M.G., et al., *Structural studies of ion permeation and Ca2+ blockage of a bacterial channel mimicking the cyclic nucleotide-gated channel pore.* Proc Natl Acad Sci U S A, 2011. **108**(2): p. 592-7.

152. Sauer, D.B., et al., *Protein interactions central to stabilizing the K+ channel selectivity filter in a four-sited configuration for selective K+ permeation.* Proc Natl Acad Sci U S A, 2011. **108**(40): p. 16634-9.

153. Chakrapani, S., J.F. Cordero-Morales, and E. Perozo, *A quantitative description of KcsA gating I: macroscopic currents.* J Gen Physiol, 2007. **130**(5): p. 465-78.

154. Perozo, E., D.M. Cortes, and L.G. Cuello, *Three-dimensional architecture and gating mechanism of a K+ channel studied by EPR spectroscopy.* Nat Struct Biol, 1998. **5**(6): p. 459-69.

155. Perozo, E., D.M. Cortes, and L.G. Cuello, *Structural rearrangements underlying K+-channel activation gating.* Science, 1999. **285**(5424): p. 73-8.

156. Jiang, Y., et al., *The open pore conformation of potassium channels.* Nature, 2002. **417**(6888): p. 523-6.

157. Jiang, Q.X., D.N. Wang, and R. MacKinnon, *Electron microscopic analysis of KvAP voltage-dependent K+ channels in an open conformation.* Nature, 2004. **430**(7001): p. 806-10.

158. Hoshi, T., W.N. Zagotta, and R.W. Aldrich, *Biophysical and molecular mechanisms of Shaker potassium channel inactivation.* Science, 1990. **250**(4980): p. 533-8.

159. MacKinnon, R., R.W. Aldrich, and A.W. Lee, *Functional stoichiometry of Shaker potassium channel inactivation.* Science, 1993. **262**(5134): p. 757-9.

160. Zhou, M., et al., *Potassium channel receptor site for the inactivation gate and quaternary amine inhibitors.* Nature, 2001. **411**(6838): p. 657-61.

161. Liu, Y., M.E. Jurman, and G. Yellen, *Dynamic rearrangement of the outer mouth of a K+ channel during gating.* Neuron, 1996. **16**(4): p. 859-67.

162. Yellen, G., et al., *An engineered cysteine in the external mouth of a K+ channel allows inactivation to be modulated by metal binding.* Biophys J, 1994. **66**(4): p. 1068-75.

163. Fedida, D., N.D. Maruoka, and S. Lin, *Modulation of slow inactivation in human cardiac Kv1.5 channels by extra- and intracellular permeant cations.* J Physiol, 1999. **515 (Pt 2)**: p. 315-29.

164. Lopez-Barneo, J., et al., *Effects of external cations and mutations in the pore region on C-type inactivation of Shaker potassium channels.* Receptors Channels, 1993. **1**(1): p. 61-71.

165. Rasmusson, R.L., et al., *C-type inactivation controls recovery in a fast inactivating cardiac K+ channel (Kv1.4) expressed in Xenopus oocytes*. J Physiol, 1995. **489 (Pt 3)**: p. 709-21.

166. Kaulin, Y.A., et al., *Mechanism of the modulation of Kv4:KChIP-1 channels by external K+*. Biophys J, 2008. **94**(4): p. 1241-51.

167. Baukrowitz, T. and G. Yellen, *Modulation of K+ current by frequency and external [K+]: a tale of two inactivation mechanisms.* Neuron, 1995. **15**(4): p. 951-60.

168. Levy, D.I. and C. Deutsch, *Recovery from C-type inactivation is modulated by extracellular potassium.* Biophys J, 1996. **70**(2): p. 798-805.

169. Claydon, T.W., et al., *K+ activation of kir3.1/kir3.4 and kv1.4 K+ channels is regulated by extracellular charges.* Biophys J, 2004. **87**(4): p. 2407-18.

170. Kehl, S.J., et al., *Molecular determinants of the inhibition of human Kv1.5 potassium currents by external protons and Zn(2+).* J Physiol, 2002. **541**(Pt 1): p. 9-24.

171. Li, X., et al., *Regulation of N- and C-type inactivation of Kv1.4 by pHo and K+: evidence for transmembrane communication.* Am J Physiol Heart Circ Physiol, 2003. **284**(1): p. H71-80.

172. Panyi, G. and C. Deutsch, *Cross talk between activation and slow inactivation gates of Shaker potassium channels.* J Gen Physiol, 2006. **128**(5): p. 547-59.

173. Ray, E.C. and C. Deutsch, *A trapped intracellular cation modulates K+ channel recovery from slow inactivation.* J Gen Physiol, 2006. **128**(2): p. 203-17.

174. Panyi, G. and C. Deutsch, *Probing the cavity of the slow inactivated conformation of shaker potassium channels.* J Gen Physiol, 2007. **129**(5): p. 403-18.

175. Kuo, M.M., et al., *The desensitization gating of the MthK K+ channel is governed by its cytoplasmic amino terminus.* PLoS Biol, 2008. **6**(10): p. e223.

176. Thomson, A.S., et al., *Initial steps of inactivation at the K+ channel selectivity filter.* Proc Natl Acad Sci U S A, 2014. **111**(17): p. E1713-22.

177. Starkus, J.G., et al., *Ion conduction through C-type inactivated Shaker channels.* J Gen Physiol, 1997. **110**(5): p. 539-50.

178. Wang, Z., J.C. Hesketh, and D. Fedida, *A high-Na(+) conduction state during recovery from inactivation in the K(+) channel Kv1.5.* Biophys J, 2000. **79**(5): p. 2416-33.

179. Wang, Z., X. Zhang, and D. Fedida, *Regulation of transient Na+ conductance by intra- and extracellular K+ in the human delayed rectifier K+ channel Kv1.5.* J Physiol, 2000. **523 Pt 3**: p. 575-91.

180. Kiss, L. and S.J. Korn, *Modulation of C-type inactivation by K+ at the potassium channel selectivity filter.* Biophys J, 1998. **74**(4): p. 1840-9.

181. Swenson, R.P., Jr. and C.M. Armstrong, *K+ channels close more slowly in the presence of external K+ and Rb+.* Nature, 1981. **291**(5814): p. 427-9.

182. Spruce, A.E., N.B. Standen, and P.R. Stanfield, *Rubidium ions and the gating of delayed rectifier potassium channels of frog skeletal muscle.* J Physiol, 1989. **411**: p. 597-610.

183. Shapiro, M.S. and T.E. DeCoursey, *Permeant ion effects on the gating kinetics of the type L potassium channel in mouse lymphocytes.* J Gen Physiol, 1991. **97**(6): p. 1251-78.

184. Demo, S.D. and G. Yellen, *Ion effects on gating of the Ca(2+)-activated K+ channel correlate with occupancy of the pore.* Biophys J, 1992. **61**(3): p. 639-48.

185. Starkus, J.G., et al., *Macroscopic Na+ currents in the "Nonconducting" Shaker potassium channel mutant W434F.* J Gen Physiol, 1998. **112**(1): p. 85-93.

186. Harris, R.E., H.P. Larsson, and E.Y. Isacoff, *A permanent ion binding site located between two gates of the Shaker K+ channel.* Biophys J, 1998. **74**(4): p. 1808-20.

187. Ogielska, E.M. and R.W. Aldrich, *Functional consequences of a decreased potassium affinity in a potassium channel pore. Ion interactions and C-type inactivation.* J Gen Physiol, 1999. **113**(2): p. 347-58.

188. Yellen, G., *The moving parts of voltage-gated ion channels.* Q Rev Biophys, 1998. **31**(3): p. 239-95.

189. Guidoni, L., V. Torre, and P. Carloni, *Potassium and sodium binding to the outer mouth of the K+ channel.* Biochemistry, 1999. **38**(27): p. 8599-604.

190. Shrivastava, I.H. and M.S. Sansom, *Simulations of ion permeation through a potassium channel: molecular dynamics of KcsA in a phospholipid bilayer.* Biophys J, 2000. **78**(2): p. 557-70.

191. Tatulian, S.A., D.M. Cortes, and E. Perozo, *Structural dynamics of the Streptomyces lividans K+ channel (SKC1): secondary structure characterization from FTIR spectroscopy*. FEBS Lett, 1998. **423**(2): p. 205-12.

192. Liu, Y.S., P. Sompornpisut, and E. Perozo, *Structure of the KcsA channel intracellular gate in the open state*. Nat Struct Biol, 2001. **8**(10): p. 883-7.

193. Gao, L., et al., *Activation-coupled inactivation in the bacterial potassium channel KcsA*. Proc Natl Acad Sci U S A, 2005. **102**(49): p. 17630-5.

194. Cordero-Morales, J.F., et al., *Molecular determinants of gating at the potassium-channel selectivity filter*. Nat Struct Mol Biol, 2006. **13**(4): p. 311-8.

195. Cordero-Morales, J.F., et al., *Molecular driving forces determining potassium channel slow inactivation*. Nat Struct Mol Biol, 2007. **14**(11): p. 1062-9.

196. Cordero-Morales, J.F., et al., *A multipoint hydrogen-bond network underlying KcsA C-type inactivation*. Biophys J, 2011. **100**(10): p. 2387-93.

197. Chakrapani, S., et al., *On the structural basis of modal gating behavior in K(+) channels*. Nat Struct Mol Biol, 2011. **18**(1): p. 67-74.

198. Yifrach, O. and R. MacKinnon, *Energetics of pore opening in a voltage-gated K(+) channel*. Cell, 2002. **111**(2): p. 231-9.

199. Larsson, H.P. and F. Elinder, *A conserved glutamate is important for slow inactivation in K+ channels*. Neuron, 2000. **27**(3): p. 573-83.

200. Pless, S.A., et al., *Hydrogen bonds as molecular timers for slow inactivation in voltage-gated potassium channels*. Elife, 2013. **2**: p. e01289.

201. Matulef, K., et al., *Using protein backbone mutagenesis to dissect the link between ion occupancy and C-type inactivation in K+ channels.* Proc Natl Acad Sci U S A, 2013. **110**(44): p. 17886-91.

202. Yellen, G., *Keeping K+ completely comfortable.* Nat Struct Biol, 2001. **8**(12): p. 1011-3.

203. Yellen, G., *The voltage-gated potassium channels and their relatives.* Nature, 2002. **419**(6902): p. 35-42.

204. Cuello, L.G., et al., *Structural basis for the coupling between activation and inactivation gates in K(+) channels.* Nature, 2010. **466**(7303): p. 272-5.

205. Cuello, L.G., et al., *Structural mechanism of C-type inactivation in K(+) channels.* Nature, 2010. **466**(7303): p. 203-8.

206. Tao, X. and R. MacKinnon, *Functional analysis of Kv1.2 and paddle chimera Kv channels in planar lipid bilayers.* J Mol Biol, 2008. **382**(1): p. 24-33.

207. Devaraneni, P.K., et al., *Semisynthetic K+ channels show that the constricted conformation of the selectivity filter is not the C-type inactivated state.* Proc Natl Acad Sci U S A, 2013. **110**(39): p. 15698-703.

208. Hoshi, T. and C.M. Armstrong, *C-type inactivation of voltage-gated K+ channels: pore constriction or dilation?* J Gen Physiol, 2013. **141**(2): p. 151-60.

209. Hille, B., *Ion channels of excitable membrane, 3rd Ed*. 2001, Sunderland, MS, USA: Sinauer Associates, Inc.

210. Luzhkov, V.B. and J. Aqvist, *A computational study of ion binding and protonation states in the KcsA potassium channel.* Biochim Biophys Acta, 2000. **1481**(2): p. 360-70.

211. Andersen, O.S., *Perspectives on: ion selectivity.* J Gen Physiol, 2011. **137**(5): p. 393-5.

212. Krishnan, M.N., et al., *Functional role and affinity of inorganic cations in stabilizing the tetrameric structure of the KcsA K+ channel.* J Gen Physiol, 2005. **126**(3): p. 271-83.

213. Renart, M.L., et al., *Ion binding to KcsA: implications in ion selectivity and channel gating.* Biochemistry, 2010. **49**(44): p. 9480-7.

214. Jiang, Y., et al., *Crystal structure and mechanism of a calcium-gated potassium channel*. Nature, 2002. **417**(6888): p. 515-22.

215. Freiburger, L.A., K. Auclair, and A.K. Mittermaier, *Elucidating protein binding mechanisms by variable-c ITC.* Chembiochem : a European journal of chemical biology, 2009. **10**(18): p. 2871-3.

216. Tellinghuisen, J., *Statistical error in isothermal titration calorimetry: variance function estimation from generalized least squares.* Analytical biochemistry, 2005. **343**(1): p. 106-15.

217. Chill, J.H., et al., *NMR study of the tetrameric KcsA potassium channel in detergent micelles.* Protein Sci, 2006. **15**(4): p. 684-98.

218. Kuo, A., et al., *Crystal structure of the potassium channel KirBac1.1 in the closed state.* Science, 2003. **300**(5627): p. 1922-6.

219. Valiyaveetil, F.I., et al., *Ion selectivity in a semisynthetic K+ channel locked in the conductive conformation.* Science, 2006. **314**(5801): p. 1004-7.

220. Freiburger, L.A., K. Auclair, and A.K. Mittermaier, *Elucidating protein binding mechanisms by variable-c ITC.* Chembiochem, 2009. **10**(18): p. 2871-3.

221. Krishnamoorthy, J. and S. Mohanty, *Open-ITC: an alternate computational approach to analyze the isothermal titration calorimetry data of complex binding mechanisms.* J Mol Recognit, 2011. **24**(6): p. 1056-66.

222. Jensen, M.O., et al., *Principles of conduction and hydrophobic gating in K+ channels.* Proc Natl Acad Sci U S A, 2010. **107**(13): p. 5833-8.

223. Parsegian, A., *Energy of an ion crossing a low dielectric membrane: solutions to four relevant electrostatic problems.* Nature, 1969. **221**(5183): p. 844-6.

224. Eisenman, G., R. Latorre, and C. Miller, *Multi-ion conduction and selectivity in the high-conductance Ca++-activated K+ channel from skeletal muscle.* Biophys J, 1986. **50**(6): p. 1025-34.

225. Ogielska, E.M. and R.W. Aldrich, *A mutation in S6 of Shaker potassium channels decreases the K+ affinity of an ion binding site revealing ion-ion interactions in the pore.* J Gen Physiol, 1998. **112**(2): p. 243-57.

226. Page, M.J. and E. Di Cera, *Role of Na+ and K+ in enzyme function.* Physiol Rev, 2006. **86**(4): p. 1049-92.

227. Dietrich, B., *Coordination chemistry of alkali and alkaline-earth cations with macrocyclic ligands.* Journal of Chemical Education, 1985. **62**(11): p. 954-964.

228. Ban, F., P. Kusalik, and D.F. Weaver, *Density functional theory investigations on the chemical basis of the selectivity filter in the K+ channel protein.* J Am Chem Soc, 2004. **126**(14): p. 4711-6.

229. Egwolf, B. and B. Roux, *Ion selectivity of the KcsA channel: a perspective from multi-ion free energy landscapes.* J Mol Biol, 2010. **401**(5): p. 831-42.

230. Aqvist, J. and V. Luzhkov, *Ion permeation mechanism of the potassium channel.* Nature, 2000. **404**(6780): p. 881-4.

231. Varma, S., et al., *Perspectives on: ion selectivity: design principles for K+ selectivity in membrane transport.* J Gen Physiol, 2011. **137**(6): p. 479-88.

232. Renart, M.L., et al., *Contribution of ion binding affinity to ion selectivity and permeation in KcsA, a model potassium channel.* Biochemistry, 2012. **51**(18): p. 3891-900.

233. Krishnan, M.N., P. Trombley, and E.G. Moczydlowski, *Thermal stability of the K+ channel tetramer: cation interactions and the conserved threonine residue at the innermost site (S4) of the KcsA selectivity filter.* Biochemistry, 2008. **47**(19): p. 5354-67.

234. Liu, S., X. Bian, and S.W. Lockless, *Preferential binding of K+ ions in the selectivity filter at equilibrium explains high selectivity of K+ channels.* J Gen Physiol, 2012. **140**(6): p. 671-9.

235. Picollo, A., et al., *Basis of substrate binding and conservation of selectivity in the CLC family of channels and transporters.* Nat Struct Mol Biol, 2009. **16**(12): p. 1294-301.

236. Sauer, D.B., et al., *Sodium and potassium competition in potassium-selective and non-selective channels.* Nat Commun, 2013. **4**: p. 2721.

237. Alam, A., N. Shi, and Y. Jiang, *Structural insight into Ca2+ specificity in tetrameric cation channels.* Proc Natl Acad Sci U S A, 2007. **104**(39): p. 15334-9.

238. Grabe, M., et al., *K+ channel selectivity depends on kinetic as well as thermodynamic factors.* Proc Natl Acad Sci U S A, 2006. **103**(39): p. 14361-6.

239. Hille, B., *Ionic selectivity, saturation, and block in sodium channels. A four-barrier model.* J Gen Physiol, 1975. **66**(5): p. 535-60.

240. Baker, K.A., et al., *Conformational dynamics of the KcsA potassium channel governs gating properties.* Nat Struct Mol Biol, 2007. **14**(11): p. 1089-95.

241. Loots, E. and E.Y. Isacoff, *Protein rearrangements underlying slow inactivation of the Shaker K+ channel.* J Gen Physiol, 1998. **112**(4): p. 377-89.

242. Choi, K.L., R.W. Aldrich, and G. Yellen, *Tetraethylammonium blockade distinguishes two inactivation mechanisms in voltage-activated K+ channels.* Proc Natl Acad Sci U S A, 1991. **88**(12): p. 5092-5.

243. Levy, D.I. and C. Deutsch, *A voltage-dependent role for K+ in recovery from C-type inactivation.* Biophys J, 1996. **71**(6): p. 3157-66.

244. Hoshi, T., W.N. Zagotta, and R.W. Aldrich, *Two types of inactivation in Shaker K+ channels: effects of alterations in the carboxy-terminal region.* Neuron, 1991. **7**(4): p. 547-56.

245. Yang, Y., Y. Yan, and F.J. Sigworth, *How does the W434F mutation block current in Shaker potassium channels?* J Gen Physiol, 1997. **109**(6): p. 779-89.

246. Kiss, L., J. LoTurco, and S.J. Korn, *Contribution of the selectivity filter to inactivation in potassium channels.* Biophys J, 1999. **76**(1 Pt 1): p. 253-63.

247. Hulse, R.E., et al., *Conformational dynamics at the inner gate of KcsA during activation.* Biochemistry, 2014. **53**(16): p. 2557-9.

248. Liu, S. and S.W. Lockless, *Equilibrium selectivity alone does not create K+-selective ion conduction in K+ channels.* Nat Commun, 2013. **4**: p. 2746.

249. Tellinghuisen, J., *Isothermal titration calorimetry at very low c.* Anal Biochem, 2008. **373**(2): p. 395-7.

250. Cao, E., et al., *TRPV1 channels are intrinsically heat sensitive and negatively regulated by phosphoinositide lipids.* Neuron, 2013. **77**(4): p. 667-79.

251. Valiyaveetil, F.I., Y. Zhou, and R. MacKinnon, *Lipids in the structure, folding, and function of the KcsA K+ channel.* Biochemistry, 2002. **41**(35): p. 10771-7.

252. Cuello, L.G., et al., *Design and characterization of a constitutively open KcsA.* FEBS Lett, 2010. **584**(6): p. 1133-8.

253. Thompson, A.N., et al., *Molecular mechanism of pH sensing in KcsA potassium channels.* Proc Natl Acad Sci U S A, 2008. **105**(19): p. 6900-5.

254. Nussberger, S., et al., *Lipid-protein interactions in crystals of plant light-harvesting complex.* J Mol Biol, 1993. **234**(2): p. 347-56.

255. Dart, C., *Lipid microdomains and the regulation of ion channel function.* J Physiol, 2010. **588**(Pt 17): p. 3169-78.

256. Marius, P., et al., *The interfacial lipid binding site on the potassium channel KcsA is specific for anionic phospholipids*. Biophys J, 2005. **89**(6): p. 4081-9.

257. Oliver, D., et al., *Functional conversion between A-type and delayed rectifier K+ channels by membrane lipids*. Science, 2004. **304**(5668): p. 265-70.

258. Schmidt, D., Q.X. Jiang, and R. MacKinnon, *Phospholipids and the origin of cationic gating charges in voltage sensors*. Nature, 2006. **444**(7120): p. 775-9.

259. Hagiwara, S. and K. Takahashi, *The anomalous rectification and cation selectivity of the membrane of a starfish egg cell*. J Membr Biol, 1974. **18**(1): p. 61-80.

260. Imai, S., et al., *Functional equilibrium of the KcsA structure revealed by NMR*. J Biol Chem, 2012. **287**(47): p. 39634-41.

261. Eduljee, C., et al., *SCAM analysis reveals a discrete region of the pore turret that modulates slow inactivation in Kv1.5*. Am J Physiol Cell Physiol, 2007. **292**(3): p. C1041-52.

262. Koyrakh, L., et al., *Molecular and cellular diversity of neuronal G-protein-gated potassium channels*. J Neurosci, 2005. **25**(49): p. 11468-78.

263. Ashcroft, F.M. and P. Rorsman, *K(ATP) channels and islet hormone secretion: new insights and controversies*. Nat Rev Endocrinol, 2013. **9**(11): p. 660-9.

264. Guo, J., et al., *Evolution of amber suppressor tRNAs for efficient bacterial production of proteins containing nonnatural amino acids*. Angew Chem Int Ed Engl, 2009. **48**(48): p. 9148-51.

265. Alam, A. and Y. Jiang, *Structural analysis of ion selectivity in the NaK channel.* Nat Struct Mol Biol, 2009. **16**(1): p. 35-41.

266. Noskov, S.Y. and B. Roux, *Importance of hydration and dynamics on the selectivity of the KcsA and NaK channels.* J Gen Physiol, 2007. **129**(2): p. 135-43.

267. Vora, T., D. Bisset, and S.H. Chung, *Conduction of Na+ and K+ through the NaK channel: molecular and Brownian dynamics studies.* Biophys J, 2008. **95**(4): p. 1600-11.

268. Tang, L., et al., *Structural basis for Ca2+ selectivity of a voltage-gated calcium channel.* Nature, 2014. **505**(7481): p. 56-61.

269. Shen, R. and W. Guo, *Ion binding properties and structure stability of the NaK channel.* Biochim Biophys Acta, 2009. **1788**(5): p. 1024-32.

270. Choe, H., H. Sackin, and L.G. Palmer, *Permeation properties of inward-rectifier potassium channels and their molecular determinants.* J Gen Physiol, 2000. **115**(4): p. 391-404.

271. Furini, S. and C. Domene, *Gating at the selectivity filter of ion channels that conduct Na+ and K+ ions.* Biophys J, 2011. **101**(7): p. 1623-31.

272. Cordero-Morales, J.F., L.G. Cuello, and E. Perozo, *Voltage-dependent gating at the KcsA selectivity filter.* Nat Struct Mol Biol, 2006. **13**(4): p. 319-22.

273. Varga, K., L. Tian, and A.E. McDermott, *Solid-state NMR study and assignments of the KcsA potassium ion channel of S. lividans.* Biochim Biophys Acta, 2007. **1774**(12): p. 1604-13.

APPENDIX I

EXPLORING THE EQUILIBRIUM PREFERENCE OF NAK CHANNEL TO K^+ IONS AND THE KINETIC MODELING OF ION CONDUCTION SELECTIVITY

Introduction

Ion channels are ubiquitous membrane proteins that play important roles in setting the membrane potential, cell signaling and other cellular processes. Among a huge variety of ion channels, some of the most selective ones are tetrameric channels, such as K^+ channels. However, even within the superfamily of tetrameric channels, ion selectivity varies from one to another. For example, NaK channel is a non-selective ion channel discovered from *Bacillus cereus*, which is remarkably similar to the pore domain of K^+ channel except that its filter sequence is TVGDG rather than TVGYG [149] (**Figure 26A**). Mutating the aspartic acid into tyrosine converts the non-selective NaK into a K^+ selective channel, NaK2K [150] (**Figure 26B**), demonstrating the close relation between NaK channel and K^+ channels during evolution. Thus, studying the selectivity of NaK channel is a great opportunity to understand the ion selection mechanism in tetrameric ion channels.

The crystal structure of NaK illustrates an unusual arrangement of the filter structure and associated ions. First, the side chain of the aspartic acid interacts with a nitrogen atom from the filter that makes the backbone re-orientate locally [149, 237]. The rotation consequentially leaves a relatively large pocket in the filter, equivalent to

A

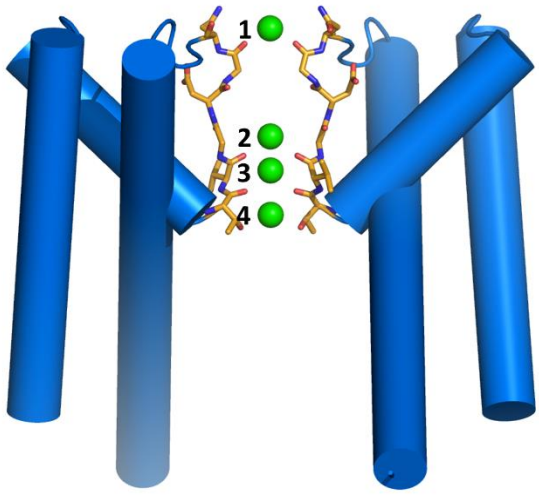

B

```
NaK       PIDALYFSVVTLTTVGDGNFSPQTDFGKIFTILYIFIG
NaK2K     PIDALYFSVVTLTTVGYGDFSPQTDFGKIFTILYIFIG
```

Figure 26. The structural model of the NaK channel and sequences of NaK and NaK2K channels. (A) A cartoon diagram of the NaK channel. The front and back subunits are taken from the tetramer for clarity. The filters are shown in sticks and K^+ binding sites in green spheres. (B) Sequence comparison between NaK and NaK2K channels. Their selectivity filter regions are highlighted in yellow.

destroying site 1 and 2 from K^+ channels (**Figure 18**). Although monovalent ions are able to reside in the pocket, the ion occupancy is considerably lower [265]. Four water molecules were found in the pocket to assist ion coordination in a high resolution structure [265]. Second, on the extracellular side of the filter, asparagine residues form an extra K^+ binding site. This site was found to prefer divalent ion association, which explains why NaK can be blocked by Ca^{2+} ions during conduction [265]. Compared to a K^+ channel, only two intact sites were site 3 and 4 on the intracellular side. Although

overall comprising the same number of sites in the filter, it failed to preferentially permeate K^+ as opposite to K^+ channels [148-150].

The lack of conduction selectivity is attributed to the unique feature of NaK's filter. Taking the structural dynamics into account, the free energy perturbation molecular simulation revealed that ions are more hydrated in the NaK than K^+ channels [266]. The access to water molecules for site one and site two significantly reduced the constraints from the filter backbone, thereby lowering ions' relative free energy [266, 267]. Interestingly, partial ion hydration was proposed to explain the ion selectivity in a few other types of tetrameric ion channels such as Na^+ and Ca^{2+} channels [268], so other factors must be attribute to the non-selective behavior of the NaK channel. In addition, Na^+ ions tend to bind to an oxygen plane created by carbonyl groups, which have also been observed in the non-selective CNG mimic channels [265, 267, 269]. Due to a less constrained ion binding queue, site 3 was found to be the most K^+ selective site [269].

When an ion channel conducts ions, the binding properties obtained from thermodynamic equilibrium do not necessarily predict its conduction selectivity. The difference is that conduction selectivity (as quantified by permeability ratio) is the ratio of the numbers of two competing ions that flux through at a steady state, whereas affinity captures ion association preference at equilibrium. Several hypotheses were raised to explain conduction selectivity by emphasizing either the on rates or binding affinities of permeant ions, i.e., the kinetic versus the thermodynamic perspective. Recent studies using NaK mutants illustrated that a filter with four K^+ binding sites ensures the selective conduction; reducing the number of binding sites could abolish the

conduction selectivity but not the equilibrium preference for K^+ ions, suggesting equilibrium preference is insufficient to explain the conduction selectivity [236, 248]. In this study, I applied isothermal titration calorimetry (ITC) to characterize the ion preference of the NaK channel at equilibrium. Although the K^+ and Na^+ affinities to the empty NaK channel were not obtained due to insufficient fitting constraints, my results still qualitatively demonstrated an equilibrium selectivity for K^+ ions. Furthermore, kinetic models to calculate ion selectivity of both the single-ion and two-ion channels were created.

Materials and methods

Protein expression and purification

The NaK channel without the first 19 residues was cloned in pQE60 expression vector, which was chemically transformed into M19[pREP4] *Escherichia coli* competent cells. After growing overnight on LB plates containing 100 μg/ml ampicillin and 50 μg/ml kanamycin, the colonies were inoculated into LB broth media and grown at 37 °C. When OD_{600} = 0.8, 0.4 mM IPTG was added to induce the expression of the NaK channel for 18 hours at 25 °C. After 18 hours, the cells were spun down at 5,000 rpm (JA-10 rotor, Beckmann Coulter) and collected. The cell pellets were stored at -80 °C before use. For purification, the cell pellets were re-suspended in 50 mM Tris (pH 8.0), 150 mM KCl, 1 mM PMSF, 2 μg/ml DNase, 10 μg/ml lysozyme and 2 μg/ml leupeptin and lysed by sonication. The lysate was mixed with *n*-Decyl-β-D-maltoside (DM) to the final 40 mM concentration, followed by incubation at room temperature for 2 hours until

cell membrane was solubilized. The lysate was spun at 12,000 rpm (JA-20 rotor, Beckmann Coulter) for 20 min. The supernatant was applied to Co^{2+} resin (Clontech), which had been pre-equilibrated with 50 mM Tris (pH 8.0), 150 mM KCl, 5 mM DM. After washed with buffer containing 15 mM imidazole, the protein was eluted in 300 mM imidazole. The C-terminal His tag was cleaved by addition of thrombin at 0.5 U/mg of channel protein and incubated for 5 hours at room temperature. The digestion was stopped by 1 mM PMSF. The protein was further purified through a Superdex 200 (GE Healthcare) size exclusion column in 50 mM Tris (pH 8), 100 mM NaCl and 5 mM DM.

Ion binding to NaK using ITC

The purified NaK protein was dialyzed against 50 mM Tris (pH 8.0), 50-150 mM NaCl, 5 mM DM. To test the effect of divalent ions on blocking K^+ binding, $CaCl_2$ was added at the desired concentrations with 150 mM NMG (*N*-methyl-D-glucamine; Sigma-Aldrich). Ion binding was quantified using either iTC200 or VP-ITC (GE Healthcare) at 25 °C and 1,000-rpm spinning speed. The chamber was filled with protein solution and titrated with a 20-80 mM KCl solution in the same buffer from the chamber. In the thermogram shows the real time plot of the signal from heat change in the chamber with each deflection representing one injection. The area under the curve comes from the heat change of binding and the heat of diluting concentrated ligand. Control experiments (not shown) were done to ensure the heat of dilution is a constant value throughout the entire titrations to allow for a constant background subtraction. Integrating the heat of each injection creates a binding isotherm, which was fit to either a sequential two-binding

function or a two independent-binding function. The results from fitting to the sequential function was justified in the main text and were chosen for interpretation. Two apparent association constants (*K*) and enthalpy (*H*) were obtained from the best fit with the lowest χ^2. The apparent dissociation constant K_D (1/*K*) is reported in the text. The Na^+ and K^+ affinities to the empty channel were determined using the following competition function.

$$1/K_D = \frac{1/K_D^{K^+}}{1 + [Na^+]^n \cdot 1/K_D^{Na^+}}$$

where K_D is the fit apparent dissociation constant, $K_D^{K^+}$ and $K_D^{Na^+}$ are dissociation constants for K^+ and Na^+ to the empty channel, and n is a Hill coefficient. $K_D^{K^+}$, $K_D^{Na^+}$ and n were fit using Prism (GraphPad Software). The equilibrium selectivity of the channel is the ratio $K_D^{Na^+} / K_D^{K^+}$.

Global fitting ITC data

Due to the degenerate solutions of fitting data to the sequential-binding function, the titration at 50 mM Tris (pH 8.0), 50-150 mM NaCl, 5 mM DM, 100 mM NaCl and 150 mM NMG was performed six times and investigated using global fitting. The Mittermaier lab kindly provided the initial MATLAB script. Three different schemes of linking parameters in the global fitting was tested. The first scheme linked K_1 and K_2 of two binding events, respectively. In addition to that, the second scheme added a factor of α between ΔH_1 and ΔH_2 to link the enthalpies from two different binding events. The third scheme applied an additional linkage of ΔH_1 and ΔH_2, respectively, so four

parameters are linked among datasets. By systematically fixing K_1 and K_2 to a series of values, the χ^2 of global fits were plotted in heat maps in a red, yellow and blue color palette, from the high to low values.

Results

NaK ion binding and competition

I first examined K^+ binding to NaK in the presence of 100 mM NaCl. After several trials, it became apparent that a one-site function was inadequate to fit the binding isotherm. A similar isotherm was seen in a previous study in the lab when analyzing the titration of the MthK K^+ Channel [234]. The thermogram displays a "hook" at a low molar ratio, indicative of two separate ion binding events (**Figure 27A**). Fitting the data to either sequential-binding function with the second binding dependent on the first or two-site function with two independent binding shows that two apparent affinities are similar to each other. To obtain the K^+ affinities in the absence of Na^+, Na^+ concentration was varied, and the data were fit to a competition function (**Figure 27B**). The two-site function generated ambiguous values that can be seen as large standard deviation in the titrations at 150mM Na^+. Ion binding to a queue of sites in NaK should be a highly coupled process such that the second binding affinity is dependent of the first ion binding event, so I hypothesized that the sequential-binding function would better capture this process.

The K^+ affinities obtained from the competition function are similar for both binding events, but the Na^+ affinities are different from each other (**Figure 27B**). The

first Na^+ affinity is high enough that it only manifests 7-fold selectivity for K^+ over Na^+, whereas the second binding event is 140-fold. Why does the first binding event have such a low selectivity but show a higher apparent K^+ affinity? The answer to this question lies in the competition function. As shown in **Figure 27B**, the Hill coefficient of the first binding event is approximately 2, which when interpreted literally means that

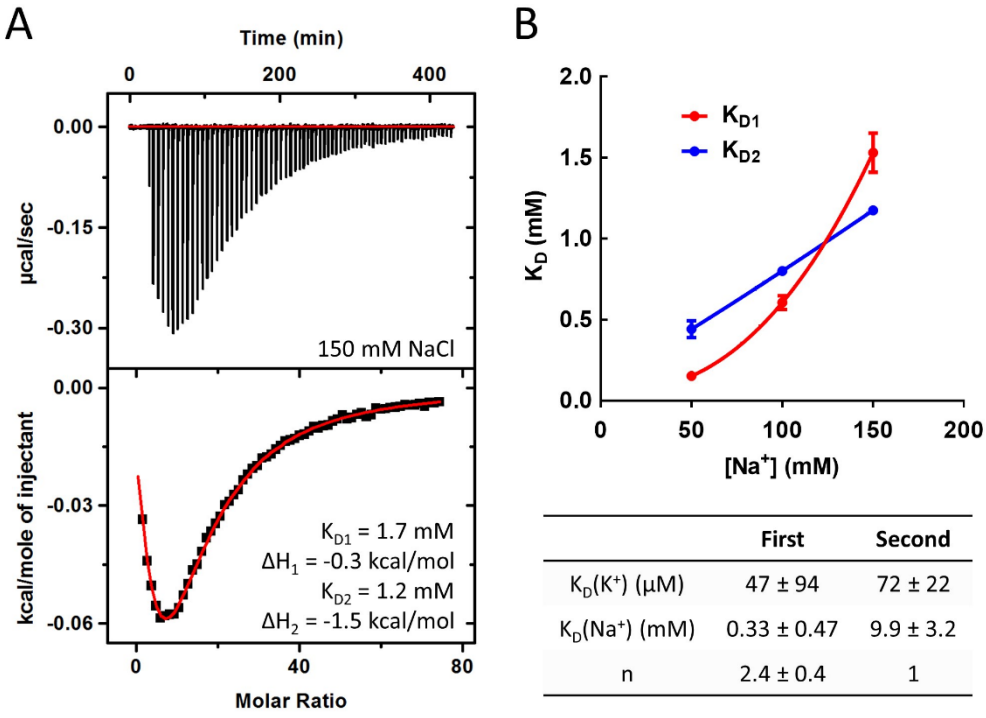

	First	Second
$K_D(K^+)$ (µM)	47 ± 94	72 ± 22
$K_D(Na^+)$ (mM)	0.33 ± 0.47	9.9 ± 3.2
n	2.4 ± 0.4	1

Figure 27. K^+ binding and competition with Na^+ ions. (A) Thermogram of NaK titrated with K^+ in the presence of 150 mM NaCl (Top). The heat exchange of ion binding was integrated in the isotherm and fit to a sequential-binding function (Bottom). (B) The apparent affinity of K^+ ions to NaK as a function of Na^+ concentration, which is fit to a competition function to obtain $K_D(K^+)$ and $K_D(Na^+)$. The mean of three or more experiments and their standard deviation are plotted. The results are summarized in the table.

one K^+ ion replaces at least two Na^+ ions. Therefore, the $K_D(Na^+)$ in the competition function is an apparent value, which should be the product of two actual Na^+ affinities. If assuming the two Na^+ affinities of empty channels were identical, then each would be equaled to the square root of $K_D(Na^+)$. This would yield ~350 fold selectivity for the one-to-one ion competition. However, simple as it is, this assumption is not well supported. First, unlike hemoglobin where ligand binds to four identical monomers, NaK has several ion binding sites that are all different from one another (**Figure 27A**). Second, from a practical point of view, the competition curve does not contain enough information to constrain the term $(K_D(Na^+))^n$.

As shown in the table of **Figure 27**, the first binding curve is not well constrained with a large standard deviation. Repeating ITC experiments at another Na^+ concentration will not likely fix this problem. The thermodynamic properties of K^+/Na^+ competition to NaK sets a few limitations. At lower Na^+ concentrations, the enthalpy of the first binding event is too low to capture the "hook" without tremendously increasing protein concentration, which is not experimentally feasible. At higher Na^+ concentrations, the affinity of the first binding event is largely reduced so that it is completely masked by the second event.

The structural origins of two binding events

K^+/Na^+ exchange in NaK channel did not yield a well-constrained result but qualitatively showed a K^+-selective binding that likely occurs in the filter. However, based solely on the binding affinities, it is improbable to tell which site each binding

event corresponds to. The crystal structures of NaK channel provide some hints on how to distinguish these binding events. One hint is that site 1 and 2 in the filter are more hydrated than site 3 and 4 [265], so their selectivity is more likely affected by different ionic strengths in the solution. The other hind is that site 1 has been shown to preferentially associate divalent ions. With the help of structural information, three different approaches were employed to map the two binding events onto the NaK structures.

First, to test the effect of ionic strength on K^+ binding, I added a non-permeant ion, NMG, to increase the ionic strength of the solution. At 100 mM NaCl + 150 mM NMG, both affinities have marginally changed (**Figure 28A**), making it impossible to distinguish their corresponding sites.

Second, D66N is a mutant channel where the divalent site or site 1 has been abolished completely [237], so repeating the titration with D66N could potentially help identify the binding sites. My previous results showed D66N has only one binding event as expected, but its apparent affinity is similar to both affinities of the NaK channel (**Figure 18**) [248].

The results from first two approaches are inconclusive, so I applied a third one to dissect the binding properties of NaK channel. Both experimental and computational studies show that site 1 is a selective site for divalent ions [131, 237, 269]. Based on this, I hypothesize that by adding divalent ions in the buffer, the first site in NaK's filter is not accessible for K^+ ions. For instance, calcium ions are shown to associate at site 1 with significantly higher affinity than other three sites, and crystallographic titration reveals a

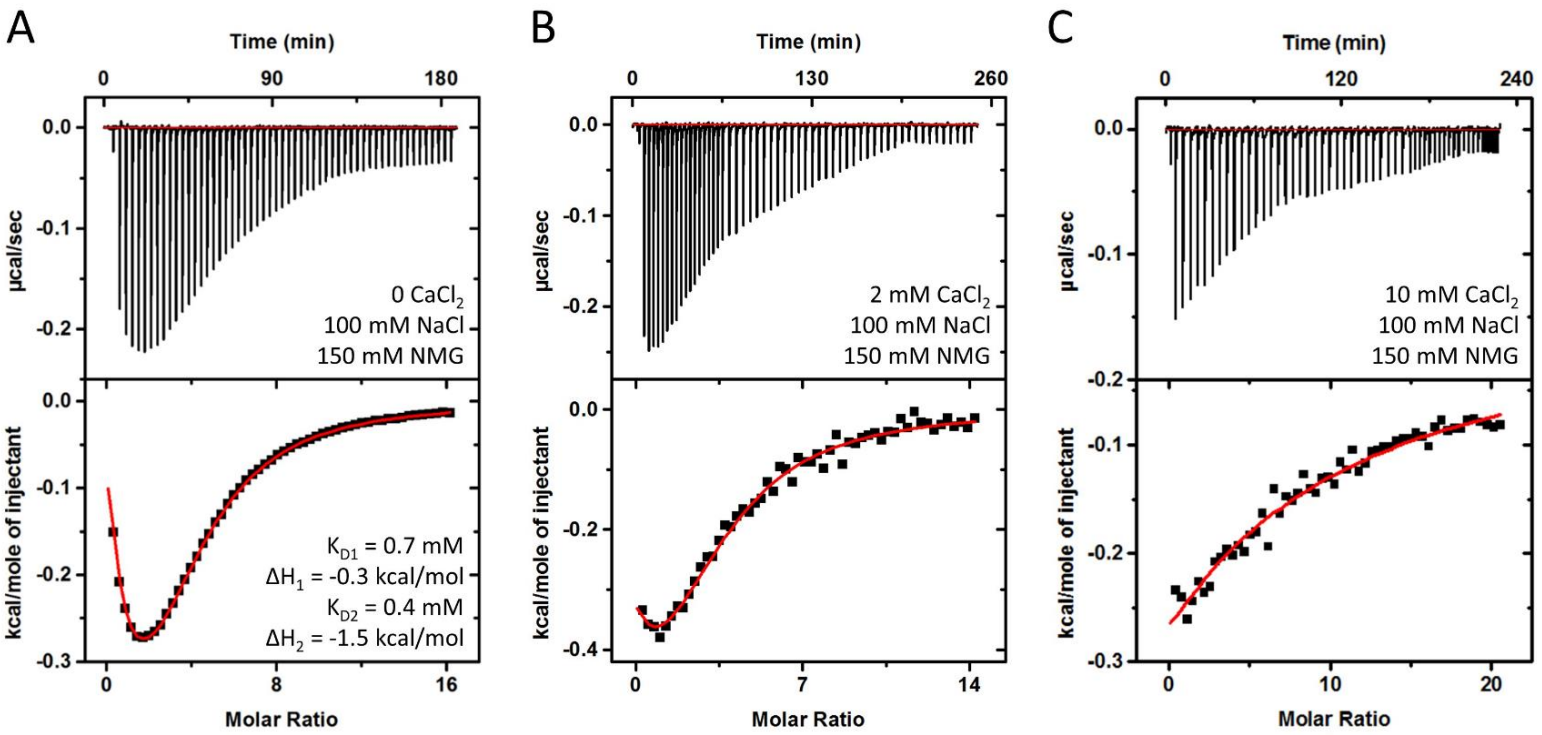

Figure 28. K^+ binding in the presence of divalent ion Ca^{2+}. Thermograms of NaK titrated by K^+ with 0, 2 and 10 mM (C) $CaCl_2$ pre-incubated (Top). The heat exchange of ion binding was integrated in the isotherm (Bottom). The isotherm obtained without adding Ca^{2+} is fit to a competition function (A). The trendlines in isotherms obtained with 2 mM (B) and 10 mM Ca^{2+} (C) are not well constrained, so the fits are not shown in the figure.

K_D of 2 mM in the presence of 100 mM NaCl at site 1 [265]. After Ca^{2+} is added into the ITC buffer, the affected ion binding event then suggest its signal originates from site 1. Indeed, as the Ca^{2+} concentration is raised from 2 mM to 10 mM, the first binding event has almost vanished (**Figure 28**). According to these results, I propose that site 1 at least partially corresponds to the first K^+ binding event, while site 3 and 4 correspond to the second binding event. However, further analyses may be required to investigate the structural origins of these two binding events.

Global fitting of the ITC data

As stated earlier, both two-site function and sequential-binding function insufficiently constrain the ITC thermogram because parameters involved in these functions are strongly dependent of one another, and multiple solutions yield the same minimum χ^2.

I explored whether the global fitting could add enough constraints to the fitting process. The MATLAB program used for this purpose was generously provided by Dr. L. A Freiburger [220], and adapted (when necessary) to constrain parameters as described below. In the global fitting function, I linked parameters across six replicates in three different ways. First, K_1 and K_2 are linked across datasets, respectively. Second, besides the linkage of Ks, ΔH_1 and ΔH_2 are linked by a factor of α within each dataset, assuming the signal from two binding events are correlated. Third, two Ks and two ΔHs are linked across datasets, respectively. By systemically varying K_1 and K_2, the minimum χ^2 was calculated in each way individually and plotted in the heat maps (**Figure 29**). Although

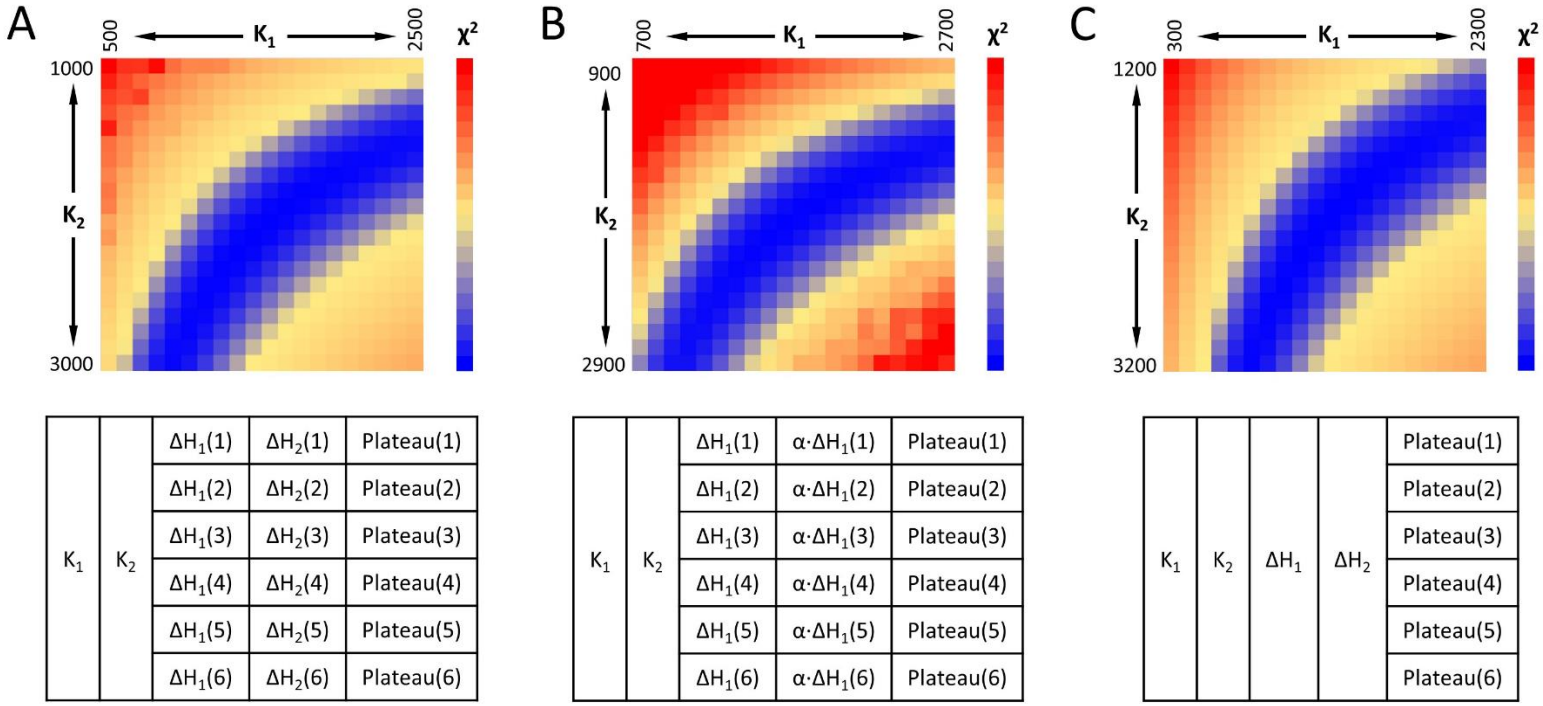

K_1	K_2	$\Delta H_1(1)$	$\Delta H_2(1)$	Plateau(1)
		$\Delta H_1(2)$	$\Delta H_2(2)$	Plateau(2)
		$\Delta H_1(3)$	$\Delta H_2(3)$	Plateau(3)
		$\Delta H_1(4)$	$\Delta H_2(4)$	Plateau(4)
		$\Delta H_1(5)$	$\Delta H_2(5)$	Plateau(5)
		$\Delta H_1(6)$	$\Delta H_2(6)$	Plateau(6)

K_1	K_2	$\Delta H_1(1)$	$\alpha \cdot \Delta H_1(1)$	Plateau(1)
		$\Delta H_1(2)$	$\alpha \cdot \Delta H_1(2)$	Plateau(2)
		$\Delta H_1(3)$	$\alpha \cdot \Delta H_1(3)$	Plateau(3)
		$\Delta H_1(4)$	$\alpha \cdot \Delta H_1(4)$	Plateau(4)
		$\Delta H_1(5)$	$\alpha \cdot \Delta H_1(5)$	Plateau(5)
		$\Delta H_1(6)$	$\alpha \cdot \Delta H_1(6)$	Plateau(6)

K_1	K_2	ΔH_1	ΔH_2	Plateau(1)
				Plateau(2)
				Plateau(3)
				Plateau(4)
				Plateau(5)
				Plateau(6)

Figure 29. Global fitting ITC data with six experimental repeats. K_1 and K_2 values are systematically fixed to 10 values, respectively, in the global fit to the sequential-binding function. Parameters in the sequential-binding function are linked in three different ways as shown in A, B and C. The Heat maps of χ^2 are plotted in a red (highest), to yellow (medium) and to blue (lowest) color palette above their corresponding fitting schemes.

the constraints are increasingly stringent from the first to the third modification, all three heat maps generated multiple equivalent solutions shown in red. A possible cause is that the fits are very sensitive to the background from the heat of dilution, which varies slightly from one ITC experiment to another. Perhaps varying other experimental conditions, such as employing the van't Hoff's equation, could help in constraining the global fit, but NaK is such a complicated system that it may not be achievable to deconvolve different effects in the end.

Mathematic models of conduction selectivity

Previously, my work on NaK channel derivatives revealed that the number of K-selective sites inside the filter determines the ion selectivity during conduction (Chapter three) [248]. Creating mathematical models to investigate the origin of ion selectivity is an alternative means to understand how selectivity is achieved, and molecular dynamic simulations have already been a useful tool to assess conduction selectivity to several channels [143]. In this study, two simplistic models are used to represent K^+ channels and non-selective tetrameric ion channels, respectively. Because K^+ channels only have on average two ions bound at any time, they are represented as the two-ion channel, whereas non-selective channels were modeled as a one-ion channel (**Figure 30**).

For simplicity, ion concentration is as the sole driving force, and the channel is in a lipid bilayer in a bi-ionic solution with equal concentration of Na^+ and K^+ on two sides of the membrane. For the one-ion channel, Na^+ and K^+ ions compete according to their on rates and ion concentrations. Imagining one ion molecule has entered the channel,

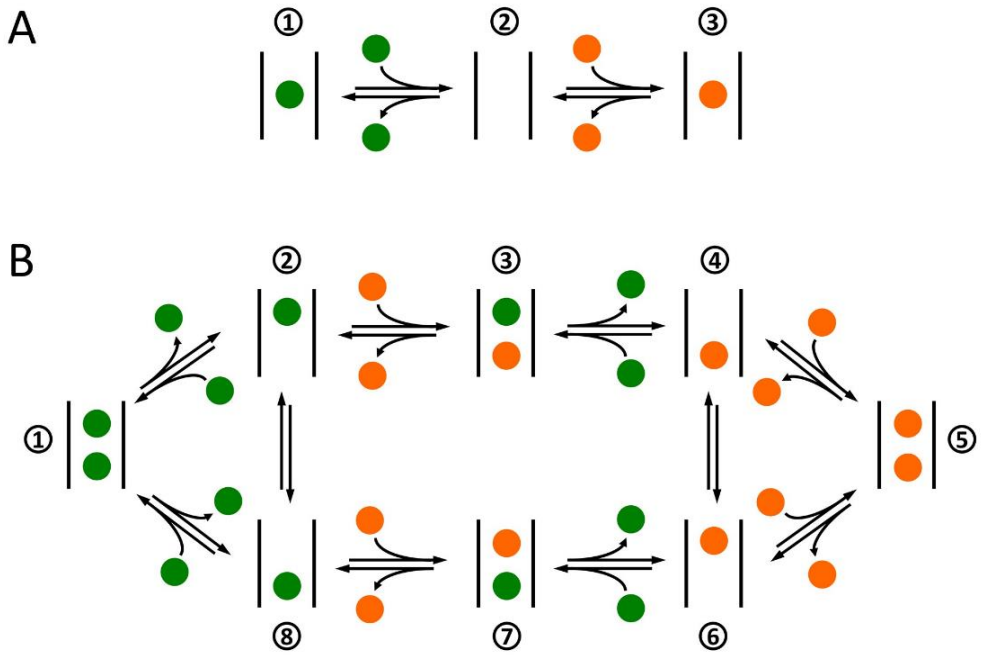

Figure 30. Models of the ion competition during conduction in one-ion (A) and two-ion (B) channels, respectively. Possible kinetic states with different ion occupancies and binding species are identified in both models. The K^+ and Na^+ ions are represented in green and orange spheres, respectively. The channels are modeled in a bi-ionic condition with K^+ solution on one side and Na^+ solution on the other side of the membrane.

there is no barrier for it to move to either side of the membrane, so it will dissociate back to the solution immediately, which is diffusion limited process. Therefore, the conduction selectivity of this channel is simply the ion occupancy ratio between two competing ions. Ion occupancy, however, is determined by the product of on rate and concentration of a certain ion. Since ion concentrations are equal to K^+ and Na^+ ions, the on rate becomes the only determinant of conduction selectivity. Because two ions have similar on rates to enter the channel, if their concentrations are the same, the permeability ratio of two ion is simply 1:1. However, the two-ion channel is more

complicated as eight possible states were identified with different binding ion species and occupancies (**Figure 30**). The state without ions in the filter was excluded from the system, because it is the least probable state to occur and does not affect the qualitative result.

During conduction, the channel shifts from one state to the next, and the total number of channels is not changing at any given time. Therefore, the probability (P_i) of each state should be constant for any given channel. A process like this can be mathematically described by flux equations. In this case, each state is given by a flux equation. For instance, the first state can be expressed by:

$$\frac{dP_1}{dt} = -k_{off}^{K^+} \cdot P_1 + k_{on}^{K^+} \cdot [K^+] \cdot P_2 - k_{off}^{K^+} \cdot P_1 = 0$$

where $k_{on}^{K^+}$ and $k_{off}^{K^+}$ are the on and off rate of K^+ to the channel, respectively. Similarly,

$$\frac{dP_2}{dt} = -k_{on}^{K^+} \cdot [K^+] \cdot P_2 + k_{off}^{K^+} \cdot P_1 - k_{on}^{Na^+} \cdot [Na^+] \cdot P_2 + k_{off}^{Na^+} \cdot P_3 - k_t^{K+} \cdot P_2 + k_t^{K+} \cdot P_8 = 0$$

$$\frac{dP_3}{dt} = -k_{off}^{Na^+} \cdot P_3 + k_{on}^{Na^+} \cdot [Na^+] \cdot P_2 - k_{off}^{K^+} \cdot P_3 = 0$$

$$\frac{dP_4}{dt} = k_{off}^{K^+} \cdot P_3 + k_{off}^{Na^+} \cdot P_5 - k_t^{Na+} \cdot P_4 + k_t^{Na+} \cdot P_6 = 0$$

$$\frac{dP_5}{dt} = -k_{off}^{Ka^+} \cdot P_5 - k_{off}^{Na^+} \cdot P_5 + k_{on}^{Na^+} \cdot [Na^+] \cdot P_6 = 0$$

$$\frac{dP_6}{dt} = -k_{on}^{K^+} \cdot [K^+] \cdot P_6 + k_{off}^{K^+} \cdot P_7 - k_{on}^{Na^+} \cdot [Na^+] \cdot P_6 + k_{off}^{Na^+} \cdot P_5 - k_t^{Na+} \cdot P_6 + k_t^{Na+} \cdot P_4 = 0$$

$$\frac{dP_7}{dt} = -k_{off}^{Na^+} \cdot P_7 - k_{off}^{K^+} \cdot P_7 + k_{on}^{K^+} \cdot [K^+] \cdot P_6 = 0$$

$$\frac{dP_8}{dt} = k_{off}^{K^+} \cdot P_1 + k_{off}^{Na^+} \cdot P_7 - k_t^{K+} \cdot P_8 + k_t^{K+} \cdot P_2 = 0$$

where $k_{on}^{Na^+}$ and $k_{off}^{Na^+}$ are the on rate and off rate of Na^+, and k_t^{K+} and k_t^{Na+} are the transition rates for K^+ and Na^+ between the two sites, respectively. Finally,

$$\sum P_i = 1$$

combining all the equations into a matrix, P_i can be numerically solved. Then, the permeability ratio or the conduction selectivity is simply the flux ratio of K^+ over Na^+, given by:

$$\frac{J_{K^+}}{J_{Na^+}} = \frac{k_{off}^{K^+} \cdot P_1 - k_{on}^{K^+} \cdot [K^+] \cdot P_8 + k_{off}^{K^+} \cdot P_3 - k_{on}^{K^+} \cdot [K^+] \cdot P_4}{k_{off}^{Na^+} \cdot P_5 - k_{on}^{Na^+} \cdot [Na^+] \cdot P_4 + k_{off}^{Na^+} \cdot P_7 - k_{on}^{Na^+} \cdot [Na^+] \cdot P_8}$$

By varying the on rate and off rate values that are suggested from experimental data, this mathematical model can serve as a platform to systematically investigate the conduction selectivity under different scenarios, such as when electrical driving force is added, when two ion binding sites are not identical. A similar modeling method has been applied to understand the selectivity of IRK channels [270].

Discussion

In this study, I examined the equilibrium K^+ binding properties of NaK channel. The structure of NaK is unique in that half of its filter is fully coordinated by the amino acids, whereas the other half requires water molecules. Although there are four total K^+ binding sites in the filter like a K^+ channel, NaK is not selective during conduction.

Unexpectedly, two high affinity K^+ binding events were resolved in the titrations even in the presence of 150 mM NaCl. Inhibited by the Ca^{2+} ions, the first binding event was mapped onto site 1 of the filter, while the second binding event likely come from a combination of site 3 and 4. The fitting results indicated that the first binding event has high K^+ affinity with marginal selectivity for K^+ ion, whereas the second event showed both high K^+ affinity and selectivity. The contradictory characteristics of the first binding event may mathematically stem from the fact that multiple Na^+ ions are displaced by one K^+ ion.

If NaK indeed has two K^+ selective sites, then why does it not select K^+ ions during conduction? As mentioned above, the competition results provide some clues. Since more than one Na^+ ion is displaced by one K^+ ion in the first binding event, the effective equilibrium selectivity is much lower than one-to-one competition. This means in NaK's filter there might be more Na^+ bound at any given time. Even when the blocking effect existed with two highly selective K^+ sites, the conduction of K^+ ions could always carry one or more Na^+ ions through concurrently.

It is also possible that ion binding does not reflect the functional state of the filter. As shown by a previous study, the narrowest section of NaK's filter is between site 1 and the pocket site, which is built by four hydrophobic carbon atoms; thus, neither K^+ nor Na^+ conduction is permissible [271]. The single channel recordings of NaK were extremely spiky and unstable [150], supporting the idea that it does not prefer staying in a high conductive state. Perhaps, the conductive conformation is a transient state where the site 1 is eliminated so that the channel is left with site 3 and site 4. This scenario

resembles the D66N mutant, which was previously characterized as a non-selective channel [248]. Additionally, the kinetic model of two-ion channels suggests a strong K+ selectivity, so crystal structures of NaK with four sites are unlikely to be the conductive state of the channel.

APPENDIX II

CHARACTERIZATION OF THE ION BINDING KINETICS OF KCSA K^+ CHANNEL

Introduction

Inactivation is a timer mechanism for voltage gated K^+ (Kv) channels to cease ion conduction while a stimulus is still present. There are generally two types of inactivation. The first is N-type inactivation, in which the N-terminal peptide plugs the pore of an ion channel. The second is C-type inactivation that relies on a conformational change at the selectivity filter to block ion flow. The latter has been studied extensively using a bacterial K^+ channel homologue, KcsA. By lowering intracellular pH, the KcsA K^+ channel opens and then the K^+ channel quickly decays to a steady-state level, a process that highly resembles Kv channels [194, 272]. The crystal structure of the closed KcsA revealed a constricted conformation of the selectivity filter in Na^+ or low K^+ conditions, which is different from the conductive conformation in high K^+ conditions [53]. This conformational change was proposed to correlate with the K^+-concentration-sensitive inactivation of Kv channels [158, 163-168]. Finally, my study showed when K^+ ions are bound the inactivated filter is similar to the conductive conformation from an energetic point of view. Surprisingly, the displacement of Na^+ and subsequent binding of K^+ is slow when monitored using ITC, taking up to one hour to complete. NMR titrations also illustrated a slow exchange between two states of the selectivity filter

[120, 122, 273], so the slow binding is likely derived from a slow conformational change. In this study, I investigated the kinetics of the K^+ binding to KcsA using ITC.

Materials and methods

Protein expression and purification

Wild-type KcsA in pET28a expression plasmid was chemically transformed into BL21 *E.coli* competent cells and grown on LB agar plate with 50 μg/ml Kanamycin overnight. The colonies were transferred into LB broth media containing 50 μg/ml Kanamycin and continue to grow at 37 °C until OD_{600} = 0.8. 0.5 mM IPTG was added to the media to induce the expression for 3 hours at 37 °C. Cells were pelleted through spinning at 5,000 rpm (JA-10 rotor, Beckmann Coulter), and the harvested cells were stored at -80 °C before use. Upon purification, the frozen cells were re-suspended in 50 mM Tris (pH 8.0), 150 mM KCl, 1 mM PMSF, 2 μg/ml DNase and 10 μg/ml lysozyme. Cells were lysed through sonication, followed by adding 40 mM *n*-Decyl-β-D-maltoside (DM) to solubilize the KcsA protein. The lysate was incubated for 2 hours before spun down at 12,000 rpm (JA-20 rotor, Beckmann Coulter) for 20 min. The supernatant was applied to the Ni-NTA column (Qiagen) equilibrated with 50 mM Tris (pH 8.0), 150 mM KCl, 5 mM DM. After washed with 15 mM imidazole and eluted with 300 mM imidazole, the full-length protein was dialyzed against buffer without imidazole. 5-10 mg/ml of chymotrypsin (Sigma-Aldrich) was added to remove the intracellular region of KcsA for two hours. The digestion was stopped by 1 mM PMSF. The pore region of KcsA was further purified by a Superdex 200 (GE Healthcare) size exclusion column.

Ion binding to KcsA using ITC

All ITC experiments were done in an iTC200 (Malvern) at 25 °C and 1,000-rpm spinning speed. The chamber was filled with 100 μM KcsA, which was titrated by concentrated KCl or RbCl solution in the same buffer from the injector. Each injection can be seen as change in heat in the thermogram, the area of which includes the heat from ligand binding and dilution. Controls experiments were done to ensure the heat of dilution is constant throughout the titration. Integrating the thermogram generates an isotherm that is fit to the one-site function to obtain the apparent association constant (K) and enthalpy (H) from the best fit when χ^2 is minimized. The apparent dissociation constant K_D ($1/K$) is reported in the text. For the K^+/Rb^+ competition experiments, the protein was dialyzed against buffer containing KCl at desired concentrations. RbCl was added to the injector in the same buffer. The isotherm from the competition experiment was fit to the one-site function, where the best fits were reported and plotted as a function of K^+ concentration. The data were fit to a linear function, and the y-intercept manifests the apparent Rb^+ binding affinity, which is statistically consistent with the affinity determined without KCl bound to the protein. The K^+ binding, Rb^+ binding and K^+/Rb^+ competition titrations were repeated with 100 μM protein, respectively. Based on the apparent ion binding affinity at each K^+ concentration, certain amount of ion ligand was injected to saturate 50% of the channel after the first injection. These signal traces were roughly fit to the one-exponential function so that apparent kinetic rates were obtained and compared.

Results

In this study, chymotrypsin-cut WT KcsA was used for all the experiments. Based on the EPR results from Chapter 4, we believe the channel was in the constricted conformation with the Na^+ bound but in the inactivated conformation with the K^+ bound. I hypothesized that the slow K^+ binding in 100 mM NaCl corresponds to the conformational change from constricted to inactivated conformation of the filter (**Figure 31A**). One prediction is that the slow binding is not particular to K^+ ions. To test that, the titration was repeated by replacing K^+ with Rb^+ ions, since they are very similar in terms of their size, charge, permeability and inactivation rate. As expected, Rb^+ binding showed a similar affinity with a relatively slower kinetics (**Figure 31B**), demonstrating that the slow binding is not solely dependent of K^+ binding.

If the slow binding requires the conformational change in the filter, ion binding to a filter already in the inactivated conformation should be fast. To test this, I used KCl to shift the channel to its inactivated conformation and the measured Rb^+/K^+ exchange. If the conformational change is required, then the exchange will be fast; otherwise, it is a slow reaction. According to the apparent K^+ affinity in the presence of 100 mM competing Na^+, 90% of KcsA is saturated by 1.5 mM KCl. Indeed, with 1.5 mM KCl pre-equilibrated with KcsA, the Rb^+ binding was greatly increased (**Figure 31C**). Importantly, the apparent Rb^+ affinity varied linearly as a function of K^+ concentration, indicating that the competition between two ions is a simple stoichiometry of 1:1 (**Figure 31D**). Collectively, my data suggest the slow ion binding to KcsA derives from shifting the filter from the constricted to the inactivated conformation.

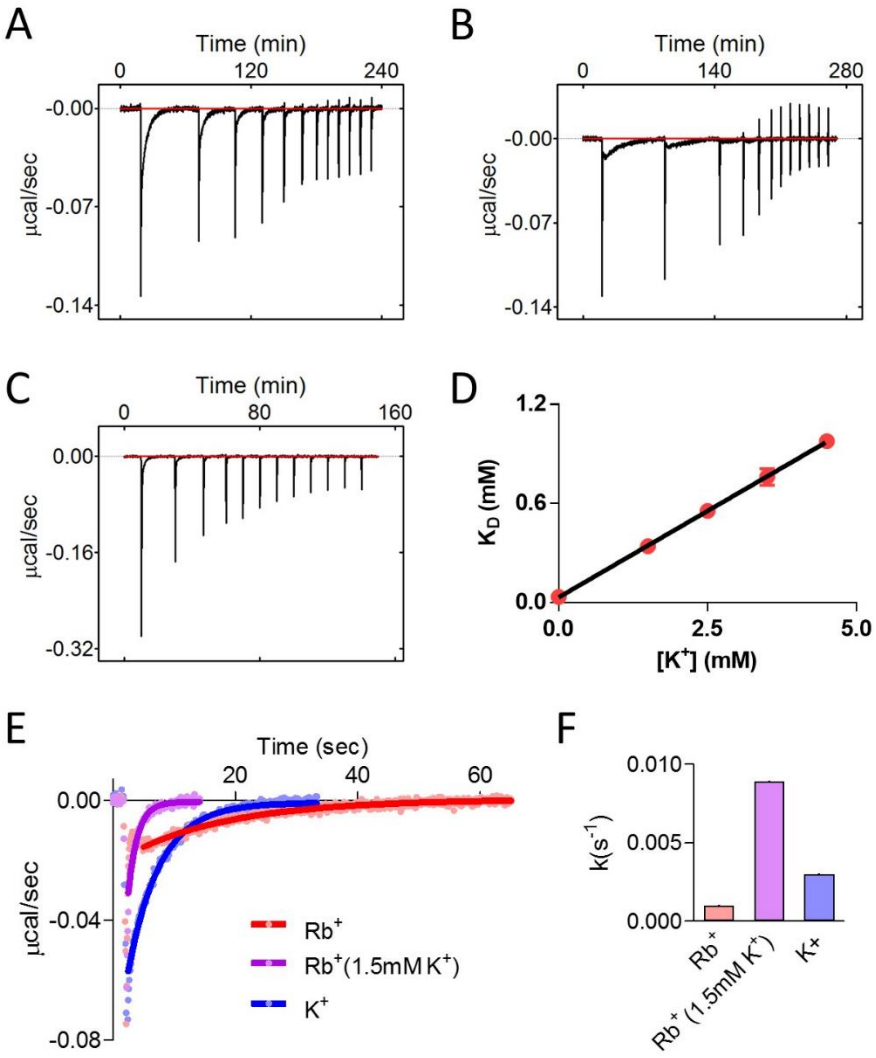

Figure 31. Characterization of the kinetic properties of KcsA binding to K^+ or Rb^+ ions. K^+ (A) or Rb^+ (B) binding to 100 µM KcsA, where 50% of the protein is designed to be bound with the titrant after the first injection. (C) The Rb^+ binding experiment was repeated in the presence of 1.5 mM KCl in the solution. (D) The apparent Rb^+ binding affinities are plotted as a function of Na^+ concentration, and the data are fit to a linear competition function. (E) The traces of the first injections from A, B and C are overlaid and fit to the one-exponential function. The extracted apparent binding rates are plotted and compared (F).

Second, I characterized the apparent binding rates of K^+ binding, Rb^+ binding and K^+/Rb^+ competition reactions. All three experiments were performed by saturating 50% of 100 µM protein after the first injection (**Figure 31E**). The traces were fit to the exponential function so that the apparent reaction rates could be extrapolated and compared. As shown, the K^+ binding is 3-fold slower than Rb^+ binding, while Rb^+ binding in presence of 1.5 mM KCl is almost one-order of magnitude faster than Rb^+ alone (**Figure 31F**). This means Rb^+ binding to a filter that has been shifted to the inactivated conformation is a faster reaction.

Discussion

The rate of C-type inactivation in Kv channels depends on the ion present in the solution. Na^+ solutions have been demonstrated to increase the inactivation rate [86, 89, 177-180]. Similarly, when the prototypic K^+ channel KcsA is bound with Na^+ ions, its selectivity filter adopts a constricted conformation hindering ion conduction [53]. However, in a physiologically relevant condition, the selectivity filter of the KcsA K^+ channel is always saturated by K^+ ions, meaning the constricted conformation may not correlate with the inactivation. Indeed, my previous study (Chapter 4) showed the inactivated state is more similar to the conductive than the constricted state.

In order to investigate whether the slow K^+ binding kinetics correspond to the conformation change, I tested two predictions of the model: 1) similar ions should bind to the channel with similar slow reaction rates, and 2) ion binding to a filter in the inactivated state should be fast. I found Rb^+ as a substitute ion binds KcsA in a similarly

slow fashion to K^+ ion. In addition, the titration between these two ions showed a 1:1 stoichiometry, indicative of a simple competition. More importantly, the K^+/Rb^+ competition is faster than that of either ion binding to KcsA, so it is evident that the slow K^+ binding kinetics between the Na^+-bound constricted state and the K^+ or Rb^+-bound inactivated state derives from a conformational change of the selectivity filter.

Under most physiologically relevant conditions, K^+ channels are constantly in tens-to-hundreds mM of K^+ ions, meaning a constricted conformation of the selectivity filter must not be a dominant state at any given time. However, for the soil bacterial *S.lividans*, the constricted conformation could potentially help cells prevent ion loss from the cytosol, especially when the extracellular K^+ ions are suddenly depleted.

APPENDIX III

MATHEMATICAL FUNCTIONS USED IN FITTING ITC DATA

Isothermal titration calorimetry (ITC) is a technique that detects heat as the indicator of how much a binding reaction has proceeded. The machines I used in this dissertation were VP-ITC and iTC200 (MicroCal) that mainly comprise of two parts, an injector where ligand is loaded into a syringe and a chamber that stores the protein of interest. Throughout the time course of the titration, ligand is injected into the chamber in the same amount (except the first small injection) for multiple times till a plateau is reached. As ligand and protein are mixed by stirring a pedal inside the chamber, two molecules form a complex, from which the heat is either released or absorbed. In all my experiments, each injection in the thermogram is shown as a deflection of signals followed by a recovery period until the baseline is reached. Integrating the area under each deflection generates an isotherm.

Fitting the isotherm extrapolates two parameters, the association constant (K) and the enthalpy of the reaction (ΔH). The dissociation constant can be calculated as $K_D = 1 / K$, and the entropy (ΔS) is obtained through $\Delta G = - RT\ln K = \Delta H - T\Delta S$. When applying the singe-site binding function, I fixed the stoichiometry (N) to 1, since the association constant stays the same with N fixed to various values under the conditions of my experiments. The two fitting functions, one-site binding function and two-site sequential binding function, used in this dissertation are provided below.

One-site binding function

The ITC chamber detects the heat change in a constant volume (V_o), which contains protein at a constant concentration (P_t). The protein may have n binding sites with the same binding constant (K). After ligand is injected into the chamber, the total ligand concentration will be L_t. Since a fraction (θ) of binding sites are occupied, the free concentrations of protein and ligand will be changed to P and L, respectively. Combining two basic equations as shown below

$$\theta = \frac{KL}{1 + KL}$$

$$L_t = L + n\theta P_t$$

yields

$$\theta^2 - \theta\left(1 + \frac{L_t}{nP_t} + \frac{1}{nKP_t}\right) + \frac{L_t}{nP_t} = 0$$

Solving this quadratic equation gives

$$\theta = \frac{\left(1 + \frac{L_t}{nP_t} + \frac{1}{nKP_t}\right) - \sqrt{\left(1 + \frac{L_t}{nP_t} + \frac{1}{nKP_t}\right)^2 - \frac{4L_t}{nP_t}}}{2}$$

Since the amount of heat generated or absorbed is directly proportional to θ, the total heat gives

$$Q = nP_t \Delta H V_o \theta$$

where ΔH is the enthalpy of this binding reaction. However, the thermogram only reports the heat change from each injection rather than the total heat change, so the ΔQ between i^{th} injection and i-1$^{\text{th}}$ injection is given as

$$\Delta Q_i = Q_i - Q_{i-1} + \frac{dV_i}{V_o}\left(\frac{Q_i + Q_{i-1}}{2}\right)$$

where the third term is a correction of the heat being lost from displacing protein at a volume of dV_i in each injection.

Two-site sequential binding function

For ligand binding in a sequential manner, the association constants are redefined as

$$K_1 = \frac{PL}{P \cdot L}$$

$$K_2 = \frac{PL_2}{PL \cdot L}$$

Therefore, the bound fractions, θ_1 andθ_2, in the sequential binding reaction are modified as

$$\theta_1 = \frac{K_1 L}{1 + K_1 L + K_1 K_2 L^2}$$

$$\theta_2 = \frac{K_1 K_2 L^2}{1 + K_1 L + K_1 K_2 L^2}$$

Since the protein of interest has a fraction with one site occupied and a fraction with two sites occupied, this yields

$$L_t = L + P_t(\theta_1 + 2\theta_2)$$

Replacing θ_1 and θ_2 generates a cubic equation, the positive real solution of which gives L. The total heat in the two-site sequential binding reaction then yields,

$$Q = P_t V_o(\theta_1 \Delta H_1 + \theta_2[\Delta H_1 + \Delta H_2])$$

$$= P_t V_o \left(\frac{K_1 L \Delta H_1}{1 + K_1 L + K_1 K_2 L^2} + \frac{K_1 K_2 L^2 [\Delta H_1 + \Delta H_2]}{1 + K_1 L + K_1 K_2 L^2} \right)$$

And, as previously,

$$\Delta Q_i = Q_i - Q_{i-1} + \frac{dV_i}{V_o} \left(\frac{Q_i + Q_{i-1}}{2} \right)$$